Système embarqué autonome en énergie pour objets mobiles communicants

Chiraz Chaabane

THESE EN COTUTELLE

entre

L'Université de Nice Sophia Antipolis

ECOLE DOCTORALE STIC

et

L'École Nationale d'Ingénieurs de Sfax

En vue de l'obtention du

DOCTORAT

Mention *Informatique*

Par

Chiraz CHAABANE

Système embarqué autonome en énergie pour objets mobiles communicants

Soutenu le 30 juin 2014, devant le jury composé de :

M.	**François VERDIER (Professeur des Universités à l'UNS)**	**Président**
M.	**Abderrazek JEMAI (Maître de Conférences à l'INSAT Université de Carthage)**	**Rapporteur**
M.	**François PECHEUX (Professeur à l'UPMC)**	**Rapporteur**
M.	**Alain PEGATOQUET (Maître de Conférences à l'UNS)**	**Examinateur**
M.	**Michel AUGUIN (Directeur de Recherche CNRS)**	**Directeur de Thèse**
M.	**Maher BEN JEMAA (Maître de Conférences à l'ENIS)**	**Directeur de Thèse**

Système embarqué autonome en énergie pour objets mobiles communicants

Chiraz CHAABANE

الخلاصة: ان زيادة عدد الأجهزة المحمولة ذات التواصل اللاسلكي (الهاتف المحمول، المساعد الشخصي الرقمي، الخ) و تعقيد تطبيقاتها يؤدي لزيادة استهلاك الطاقة. من أجل الحد من تأثير التلوث بسبب النفايات المنجرة عن البطاريات المتلفة و انبعاثات ثاني اكسيد الكربون، من المهم أن تتم الاستفادة المثلى من استهلاك الطاقة في أجهزة التواصل. هذه الأطروحة تركز على كفاءة استخدام الطاقة في شبكات الاستشعار اللاسلكي و تقترح مقاربات جديدة للتعامل مع الأجسام المتواصلة و المتحركة. أولا، نقترح هندسة شبكة شاملة للاستشعار و منهج جديد لإدارة تنقل الأجهزة زيجبي/ IEEE802.15.4 بصفة تضمن كفاءة في استخدام الطاقة. نقترح في البداية هندسة شاملة لشبكة الاستشعار ونهج جديدة ذات كفاءة في استخدام الطاقة في إدارة التنقل للأجهزة الطرفية. و تستند هذه المقاربة الجديدة على الرابط مقدر الجودة وتستخدم خوارزمية المضاربة. نقترح و نقيم خوارزميتين مختلفتين اثنتين من المضاربة. ثم، نقوم بدراسة و تقييم كفاءة استخدام الطاقة عند استخدام خوارزمية تكيف معدل البيانات الذي يأخذ بعين الاعتبار ظروف قناة الاتصال. أولا نقترح خوارزمية تكيف معدل البيانات متصلة بعملية إدارة التنقل ونقيم كفاءته حسب تنظيمنا للشبكة. ثم نقترح ونقيم تكيف معدل استنادا إلى خوارزمية مختلطة تقوم على تقدير أكثر دقة لرابط القناة. عمليات المحاكاة التي أجريت على طول هذه الدراسة تظهر لكفاءة استخدام الطاقة في نهجنا المقترحة وتحسين التواصل بين الأجهزة.

Résumé : Le nombre et la complexité croissante des applications qui sont intégrées dans des objets mobiles communicants sans fil (téléphone mobile, PDA, etc.) implique une augmentation de la consommation d'énergie. Afin de limiter l'impact de la pollution due aux déchets des batteries et des émissions de CO2, il est important de procéder à une optimisation de la consommation d'énergie de ces appareils communicants. Cette thèse porte sur l'efficacité énergétique dans les réseaux de capteurs. Dans cette étude, nous proposons de nouvelles approches pour gérer efficacement les objets communicants mobiles. Tout d'abord, nous proposons une architecture globale de réseau de capteurs et une nouvelle approche de gestion de la mobilité économe en énergie pour les appareils terminaux de type IEEE 802.15.4/ZigBee. Cette approche est basée sur l'indicateur de la qualité de lien (LQI) et met en œuvre un algorithme spéculatif pour déterminer le prochain coordinateur. Nous avons ainsi proposé et évalué deux algorithmes spéculatifs différents. Ensuite, nous étudions et évaluons l'efficacité énergétique lors de l'utilisation d'un algorithme d'adaptation de débit prenant en compte les conditions du canal de communication. Nous proposons d'abord une approche mixte combinant un nouvel algorithme d'adaptation de débit et notre approche de gestion de la mobilité. Ensuite, nous proposons et évaluons un algorithme d'adaptation de débit hybride qui repose sur une estimation plus précise du canal de liaison. Les différentes simulations effectuées tout au long de ce travail montrent l'efficacité énergétique des approches proposées ainsi que l'amélioration de la connectivité des nœuds.

Abstract: The increasing number and complexity of applications that are embedded into wireless mobile communicating devices (mobile phone, PDA, etc.) implies an increase of energy consumption. In order to limit the impact of pollution due to battery waste and CO2 emission, it is important to conduct an optimization of the energy consumption of these communicating end devices. This thesis focuses on energy efficiency in sensor networks. It proposes new approaches to handle mobile communicating objects. First, we propose a global sensor network architecture and a new energy-efficient mobility management approach for IEEE 802.15.4/ZigBee end devices. This new approach is based on the link quality estimator (LQI) and uses a speculative algorithm. We propose and evaluate two different speculative algorithms. Then, we study and evaluate the energy efficiency when using a rate adaptation algorithm that takes into account the communication channel conditions. We first propose a mobility-aware rate adaptation algorithm and evaluate its efficiency in our network architecture. Then, we propose and evaluate a hybrid rate adaptation algorithm that relies on more accurate link channel estimation. Simulations conducted all along this study show the energy-efficiency of our proposed approaches and the improvement of the nodes' connectivity.

المفاتيح: IEEE802.15.4؛ زيجبي؛ الطاقة؛ التنقل؛ تقدير جودة القناة؛ تكيف معدل الإرسال.

Mots clés: IEEE 802.15.4; ZigBee; Energie; Mobilité; Estimation de la qualité du canal; Adaptation de débit de transmission

Key-words: IEEE 802.15.4; ZigBee; Energy; Mobility; Link quality estimation; Data rate adaptation

Acknowledgements

It would not have been possible to write this doctoral thesis without the help and support of the kind people around me, to only some of whom it is possible to give particular mention here.

First and foremost, I offer my sincerest gratitude to my advisor, Michel Auguin, who has supported me throughout my thesis with his patience and knowledge. One simply could not wish for a better advisor.

I also offer my deepest gratitude to my second advisor Maher Ben Jemaa for his valuable help, insightful comments and advices.

I am extremely grateful to my co-advisor, Alain Pegatoquet for his valuable help, his availability and his patience. He has guided through the ups and downs of these last few years with good humor and high human qualities.

Besides my advisors, I would like to thank the rest of my thesis committee: François Verdier, Abderrazek Jemai and François Pêcheux for their precious time, their insightful comments and constructive criticism.

I am also grateful to Mohamed Jemaiel my former advisor who has accepted to be my advisor and helped me a lot with the administrative procedures.

I also thank the members of LEAT laboratory and more particularly the MCSOC team for the friendly atmosphere and the good humor. It has been a pleasure knowing you and working with you.

I am thankful to Antoine Fraboulet who had kindly received me for a week in the CITI Laboratory - INSA de Lyon in order to follow quality training with the WSIM-WSNet simulator.

I feel extremely privileged to be accepted for an intership under the supervision of Pr. Mounir Hamdi in the Hong Kong University of Science and Technology (HKUST). Despite his busy schedule, he has always found the time to guide me and help me with my research. I feel lucky to know him and to have worked with him.

I am very grateful to Pr. Khaled beltaief who has welcomed me in HKUST. I am indebted to him for his help with administrative procedures.

I would also like to thank researchers of the Computer Science Engineering Department of HKUST for their kindness and help and more particularly Arafet Ben Makhlouf and Lu Wang.

Finally I would like to thank my parents for their unconditional support. Maman, Papa, I would not have made it without your encouragements.

Abbreviations and Acronyms

AWGN	**A**dditive **W**hite **G**aussian **N**oise
BER	**B**it **E**rror **R**ate
CAP	**C**ontention **A**ccess **P**eriod
CCI	**C**hip **C**orrelation *I*ndicator
CDMA	**C**ode **D**ivision **M**ultiple **A**ccess
CER	**C**hip **E**rror **R**ate
CFP	**C**ontention **F**ree **P**eriod
CSS	**C**hirp **S**pread **S**pectrum
CPU	**C**ontrol **P**rocessing **U**nit
CSMA	**C**arrier **S**ense **M**ultiple **A**ccess
CSMA-CA	**C**arrier **S**ense **M**ultiple **A**ccess with **C**ollision **A**voidance
DAC	**D**igital to **A**nalog **C**onverter
FFD	**F**ull **F**unction **D**evice
FH	**F**requency **H**opping
GSM	**G**lobal **S**ystem for **M**obile communications
GTS	**G**uaranteed **T**ime **S**lot
GPRS	**G**eneral **P**acket **R**adio **S**ervice
ICT	**I**nformation and **C**ommunication **T**echnologies
ISM	**I**ndustrial, **S**cientific and **M**edical radio bands
IoT	**I**nternet **o**f **T**hings
LQI	**L**ink **Q**uality **I**ndicator
MIMO	**M**ultiple-**I**nput **M**ultiple-**O**utput
MAC layer	**M**edia **A**ccess **C**ontrol sublayer

NWK layer	**N**et**w**or**k** layer
PAN	**P**ersonal **A**rea **N**etwork
PDR	**P**acket **D**elivery **R**atio
PHY layer	**Phy**sical layer
PM	**P**ower **M**anager
PRR	**P**acket **R**eception **R**atio
RFD	**R**educed **F**unction **D**evice
RSSI	**R**eceived **S**trength **S**ignal **I**ndicator
SSCS	**S**ervice **S**pecific **C**onvergence **S**ublayer
SNR	**S**ignal to **N**oise **R**atio
SINR	**S**ignal to **I**nterference and **N**oise **R**atio
TDMA	**T**ime **D**ivision **M**ultiple **A**ccess
WPAN	**W**ireless **P**ersonal **A**rea **N**etwork
WSN	**W**ireless **S**ensor **N**etworks

Table of Contents

Chapter 1. Introduction 1
1.1. General context 1
1.2. Short range protocols 2
1.1. Wireless Sensor Networks 5
1.2. Challenges in WSN 6
1.2.1. Energy consumption 6
1.2.2. Channel conditions 7
1.2.3. Medium access 9
1.2.4. Mobility 9
1.3. Contributions and manuscript organization 9
Chapter 2. IEEE802.15.4/ZigBee overview 11
2.1. Introduction 11
2.2. Sensor node architecture 12
2.2.1. The sensing unit 12
2.2.2. The processing unit 13
2.2.3. The transmission unit 13
2.2.4. The power supply unit 13
2.3. IEEE 802.15.4 overview 13
2.3.1. IEEE 802.15.4 versions 13
2.3.2. IEEE 802.15.4 nodes 14
2.3.3. IEEE 802.15.4 topology 14
2.3.4. Physical layer 15
2.3.5. Mac sublayer 20
2.3.6. Logic Link Control (LLC) sublayer 28
2.4. ZigBee protocol [ZigBee] 29
2.4.1. Topology 29

2.4.2. Addressing mode 30
2.4.3. ZigBee routing protocols 31
2.5. Energy consumption in IEEE 802.15.4 WSNs 34
2.5.1. PHY Layer 34
2.5.2. MAC Sublayer 36
2.6. Summary 37
Chapter 3. State of the art 39
3.1. Introduction 39
3.2. Proposed approaches for reducing energy consumption 39
3.2.1. PHY Layer 39
3.2.2. MAC sublayer 40
3.3. Mobility 42
3.3.1. Ad hoc networks 42
3.3.2. Mobility in cellular networks: different solutions 43
3.3.3. Mobility in IEEE 802.15.4 47
3.3.4. Mobility models 52
3.4. Link Quality Estimation 53
3.4.1. Considered parameters 53
3.4.2. Overview of link quality estimators 55
3.5. Rate adaptation in IEEE 802.15.4 60
3.5.1. Available rates in IEEE 802.15.4 61
3.5.2. Overview of proposed rate adaptation algorithms for IEEE 802.15.4 62
3.6. Summary 64
Chapter 4. An Enhanced Mobility Management Approach for IEEE 802.15.4 protocol 66
4.1. Introduction 66
4.2. Proposed network architecture 67
4.2.1. Network topology 67

4.2.2. Addressing and routing 69
4.3. Simulation tools and general simulation setup 69
4.4. Energy consumption in the standard procedure 72
4.5. Handover procedure 74
4.6. Efficiency of using LQI in mobility management 75
4.6.1. Network architecture and initialization 75
4.6.2. Selection of the new coordinator 77
4.6.3. Simulation use cases 77
4.6.4. Gain in energy and delay for both scenarios 80
4.7. An $LQI_{threshold}$ formula for mobility management 82
4.7.1. $LQI_{threshold}$ formula 83
4.7.2. Impact of β parameter 84
4.8. Same-road speculative algorithm 86
4.8.1. Simulation setup 88
4.8.2. Evaluation of the proposed approach 89
4.9. Probabilistic speculative algorithm 95
4.9.1. Description of the Probabilistic Algorithm 96
4.9.2. Gains in energy and delay of the probabilistic algorithm 98
4.10. Summary 99
Chapter 5. Rate adaptation algorithm 101
5.1. Introduction 101
5.2. A Mobility-aware Rate Adaptation Algorithm 102
5.2.1. Rate selection algorithm 102
5.2.2. Evaluation of the Approach 103
5.3. An adaptive rate adaptation algorithm 109
5.3.1. Link Quality Estimation Metrics based on chip error rate 110
5.3.2. Rate Selection Algorithm 112

5.3.3. Scenario description and simulation setup 117
5.3.4. PDR evaluation and mobility impact 121
5.3.5. Energy efficiency 122
5.4. Summary 124
Chapter 6. Conclusion and perspectives 126
6.1. Conclusion 126
6.1.1. Mobility management 127
6.1.2. Rate adaptation 127
6.2. Perspectives 128
6.2.1. A more efficient dynamic $LQI_{threshold}$ management 128
6.2.2. Enhancement of the speculative algorithm 128
6.2.3. Accurate IEEE 802.15.4 protocol stack modeling 129
6.2.4. Harvesting energy 129
6.2.5. Impact of α and β on the rate adaptation algorithm 130
6.2.6. A reverse mobility approach in order to reduce energy consumption 130
6.2.7. Interoperability of mobile devices and security issues 131
References 133
Personal Publications 146
Annex A. Some MAC attributes and constants [IEEE TG 15.4 2006] 148
Annex B. CSMA-CA algorithm 150
Annex C. Box-Muller Method [Box 1958] 151
Annex D. Frames Fields [IEEE TG 15.4 2006] [ZigBee] 153

List of Figures

Figure 1. ZigBee robustness [Freescale] 3
Figure 2. IEEE 802.15.4/ZigBee layers 11
Figure 3. System architecture of a typical wireless sensor node [Bharathidasan 2002] 12
Figure 4. Modulation and spreading functions for the O-QPSK PHYs 17
Figure 5. IEEE 802.15.4 Beacon-enabled Superframe 22
Figure 6. GTS and Backoff slots in IEEE 802.15.4 Beacon-enabled Superframe 23
Figure 7. CSMA-CA Algorithm in the slotted mode 25
Figure 8. Unslotted IEEE 802.15.4 CSMA-CA 27
Figure 9. Interframe spacing 27
Figure 10. ZigBee topologies 30
Figure 11. Example of hierarchical addresses attribution 33
Figure 12. Attachment and detachment procedures in GSM. 45
Figure 13. Handover in IEEE 802.11f 47
Figure 14. Mobility management in 802.15.4 standard 48
Figure 15. Association procedure in IEEE 802.15.4 standard protocol 49
Figure 16. Manhattan mobility model 52
Figure 17. Conditional probability [Srinivasan 2008] 56
Figure 18. Network Organization 68
Figure 19. Proposed network topology 68
Figure 20. Changing cell procedure 74
Figure 21. A multi-road network 76
Figure 22. Single road use case for different $LQI_{threshold}$ 79
Figure 23. Success rate vs. $LQI_{threshold}$ and speed 79
Figure 24. Success rate vs. $LQI_{threshold}$ and speed 80
Figure 25. Energy gain for the Single-road and the Multi-road use cases in comparison to the standard 82
Figure 26. Energy gain for the Single-road and the Multi-road use cases in comparison to the standard 82
Figure 27. LQI value during node movement through a cell 83
Figure 28. Coordinators in the grid architecture 85
Figure 29. Energy spent in cell reselection procedures for different β values 86
Figure 30. Success rate Vs. Velocity of node for different β values 86

Figure 31. Average energy and average dalay during cell reselection procedures..... 89
Figure 32. Gain in average energy and average delay using 3 different mobility models..... 90
Figure 33. Average energy spent in cell reselection procedures (MHT model)..... 91
Figure 34. Gain in energy (MHT model) 91
Figure 35. Gain in delay (MHT model) 92
Figure 36. Remaining energy of node M vs. number of end devices..... 93
Figure 37. Number of received beacons by node M vs. Number of end devices..... 93
Figure 38. Average energy and average delay during cell reselection procedures..... 95
Figure 39. Gain in average energy and average delay using 3 different mobility models..... 95
Figure 40. Grid architecture 97
Figure 41. Gain in energy of the probabilistic speculative algorithm in comparison with same-road algorithm..... 99
Figure 42. Gain in delay of the probabilistic speculative algorithm in comparison with same-road algorithm 99
Figure 43. Average number of received beacons 105
Figure 44. Average remaining energy 105
Figure 45. Number of received beacons for communicating nodes..... 107
Figure 46. Remaining energy of communicating nodes..... 107
Figure 47. Packet delivery ratio 107
Figure 48. Remaining energy of communicating nodes Vs. CBR interval..... 108
Figure 49. Number of received beacon of communicating nodes Vs. CBR interval..... 109
Figure 50. Packet delivery ratio of communicating nodes Vs. CBR interval 109
Figure 51. Data rate adaptation during packet exchange 113
Figure 52. State machine of the unslotted CSMA-CA algorithm in WSNet simulator..... 120
Figure 53. Modified state machine of the unslotted CSMA-CA algorithm in WSNet 121
Figure 54. Packet delivery ratio (PDR) at the MAC sublayer vs. network nodes' number for static (Stc) and mobile (Mob) scenarios..... 122
Figure 55. CBR Packet delivery ratio (PDR) vs. network nodes' number for static (Stc) and mobile (Mob) scenarios..... 122
Figure 56. Energy consumption in both scenarios vs. network nodes' number for static (Stc) and mobile (Mob) scenarios..... 123
Figure 57. Gain in energy in comparison to the standard for static (Stc) and mobile (Mob) scenarios..... 123
Figure 58. Network energy efficiency…….124

Figure 59 CSMA-CA Algorithm [IEEE TG 15.4 2006] 150

List of Tables

Table 1. Overview of short range protocols [Lee 2007] 4
Table 2. A Comparison of WSN technologies [Cao 2009] 6
Table 3. Frequency band of the IEEE 802.15.4 16
Table 4 Topologies characteristics 51
Table 5. Overview of link quality estimators 60
Table 6 Available rates 61
Table 7. Network simulators 70
Table 8 CC2420 energy consumption values [CC2420] 72
Table 9 Common simulation setup for the mobility management approach 72
Table 10 Energy consumption Evaluation of the standard procedure 72
Table 11 Simulation setup 88
Table 12. Simulation setup for noisy environment 94
Table 13. Zones of a coordinator 97
Table 14. Rotation Table to determine the next zone 98
Table 15. Coordinates of the next coordinator 98
Table 16. Simulation setup in mobility-aware rate adaptation algorithm evaluation 104
Table 17. Simulation setup for the adaptive data rate adaptation algorithm 117
Table 18. Parameters of the rate adaptation metrics and thresholds 119

Chapter 1. **Introduction**

1.1. General context

Energy consumption resulting in global CO2 emission and battery waste caused by data communication and networking devices is increasing exponentially. Information and communication technology (ICT) is responsible for about two percent of the global CO2 emissions. However, ICT includes Internet of things (IoT) technologies and applications that have a direct effect on lowering CO2 emissions by increasing energy efficiency, reducing power consumption, and achieving efficient waste recycling. IoT has, therefore, an interesting dual role in CO2 emission [CarbonRoom] [Vermesan 2011] since its developments show that we will have 16 billion connected devices by the year 2020 (i.e. average out to six devices per person on earth and to many more per person in digital societies) [Vermesan 2011]. A recent report by the Carbon War Room [CarbonRoom] estimates that the incorporation of machine-to-machine communication in the energy, transportation, and agriculture sectors could reduce global greenhouse gas emissions by 9.1 gigatons of CO2 equivalent annually. Nowadays there is a need to develop applications that are environmentally friendly. In this context, the GRECO project (GREen wireless Communicating Objects) proposed to study the design of autonomous communicating objects. This means that, within a given time period, the power consumption is lower than or equivalent to the energy the object can harvest from its environment. The approach developed in GRECO aims at reaching a global power optimization for a communicating object.

This thesis is conducted as part of the GRECO project and as a joint guardianship with the National Engineering School of Sfax (Tunisia) and the LEAT from the University of Nice Sophia Antipolis. In this context, I conceived a new mobility management approach for mobile IEEE 802.15.4/ZigBee end device. The new approach reduces the energy consumption of the devices and it also increases their synchronization time.

During a semester internship in the computer science engineering department of the Hong Kong University of Science and Technology, I have focused on the rate adaptation feature for IEEE 802.15.4 protocol. An efficient rate adaptation algorithm has been proposed. Then a joint rate adaptation and mobility management approach have been conceived.

In the next subsection, we will introduce and compare the main short range wireless protocols.

1.2. Short range protocols

Wireless protocols were first proposed to replace wires that were not suitable to all environments. They progressively gained a bigger place in the market mainly thanks to the diversity of their use and the easiness of their deployment. The diversity of applications offered by wireless protocols led to the emergence of new protocol standards, each one is usually dedicated to a specific use and thus, it better fits some applications among others. Nowadays, one of the most challenging constraints in wireless communication is the energy consumption. This constraint is even more important in the personal area networks (PAN) given that PAN nodes have to operate autonomously over a long period of time (e.g. order of years for wireless sensors). Reducing the energy consumption can affect the communication range. In fact, the higher the range, the higher the signal power; and thus, the higher the energy consumption is.

Four main protocol standards for short range wireless communication with low energy consumption have recently gained a big interest in research: Bluetooth (over IEEE 802.15.1), ultra-wideband (UWB, over IEEE 802.15.3), ZigBee (over IEEE 802.15.4) [IEEE TG 15.4 2006] [ZigBee], and Wi-Fi (over IEEE 802.11). In [Lee 2007], a comparative study of short range communication protocols was proposed. The comparison was based on many criteria such as the radio channels, the network size, the maximum signal rate and the basic cell architecture. Table 1 summarizes the different characteristics of each protocol: the frequency band, the modulation technique, the maximum signal rate, the basic cell architecture, the complex structures that can be built from the basic cell, etc. Bluetooth, ZigBee and Wi-Fi protocols have spread spectrum techniques in the 2.4 GHz band, which is unlicensed in most countries and known as the industrial, scientific, and medical (ISM) band. Protocols use the spread spectrum technique indoors to be more resistant to interferences and noise. Bluetooth uses frequency hopping (FHSS) with 79 channels and 1 MHz bandwidth. ZigBee uses direct sequence spread spectrum (DSSS) with 16 channels and a maximum bandwidth of 2 MHz.

Wi-Fi uses DSSS (802.11), complementary code keying (CCK, 802.1lb) or OFDM modulation (802.1 1a/g) with 14 RF channels (11 available in US, 13 in Europe, and just 1 in Japan) and 22 MHz bandwidth. UWB uses the 3.1-10.6 GHz band, with an unapproved and jammed 802.15.3a standard, in which two spreading techniques are available: direct sequence-UWB (DS-UWB) and multi-band orthogonal frequency division multiplexing (MB-OFDM). The range of IEEE 802.15.4 can reach 100 meters. It is longer than Bluetooth (10 meters), but less than WLAN technologies.

It is important to point out that thanks to the robustness of the physical layer, the range of IEEE 802.15.4 transceiver is comparable to that of a IEEE 802.11 transceiver, but with a lower transmission power: from Figure 1 we can see that at an equal level of signal to noise ratio (SNR), 802.15.4 has a better BER compared to other wireless technologies.

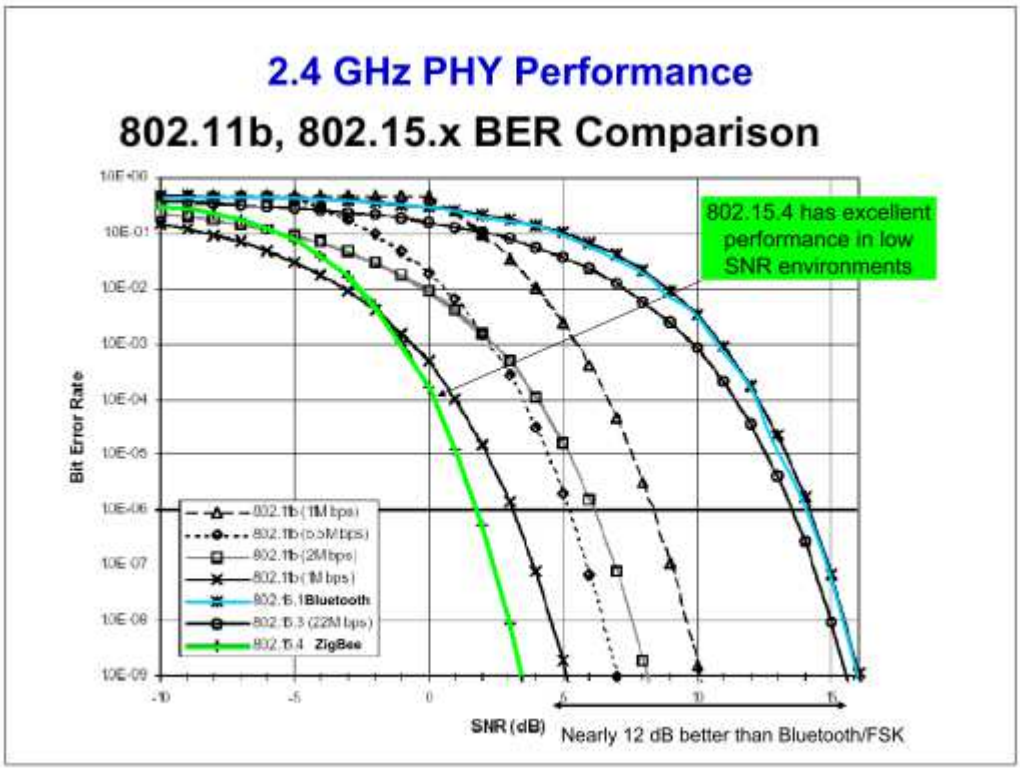

Figure 1. ZigBee robustness [Freescale]

Bluetooth considered a new protocol dedicated to energy-constrained systems: Bluetooth Smart (low energy) (BLE). However, BLE constitutes a single-hop solution applicable to a different space of use cases in areas such as healthcare, consumer electronics, smart energy and security [Gomez 2012]. Besides, a BLE device used for continuous data transfer would

not have lower power consumption than a comparable Bluetooth device transmitting the same amount of data. It would likely use more power, since the protocol is dedicated to applications that need to transmit data over short communication burst before quickly tearing down the connection. Thus, BLE is only optimized for small bursts [Bluetooth].

Table 1. Overview of short range protocols [Lee 2007]

Standard	Bluetooth	UWB	ZigBee	Wi-Fi
IEEE spec.	802.15.1	802.15.3a	802.15.4	802.11a/b/g
Frequency band	2.4 Ghz	3.1-10.6 Ghz	868/915 Mhz ; 2.4 Ghz	2.4 Ghz ; 5Ghz
Max signal rate	1 Mb/s	110 Mb/s	250 kb/s	54 Mb/s
Nominal range	10 m	10 m	10 - 100 m	100 m
Nominal TX power	0 - 10 dBm	-41.3 dBm/MHz	(-25) - 0 dBm	15 – 20 dBm
Number of RF channels	79	(1 – 15)	1/10 ; 16	14 (2.4 GHz)
Channel bandwidth	1 MHz	500 MHz – 7.5 GHz	0.3/0.6 MHz ; 2 MHz	22 MHz
Modulation type	GFSK	BPSK, QPSK	BPSK(+ASK), O-QPSK	BPSK, QPSK, COFDM, CCK, M-QAM
Spreading	FHSS	DS-UWB, MB-OFDM	DSSS	DSSS, CCK, OFDM
Coexistence mechanism	Adaptive freq. hopping	Adaptive freq. hopping	Adaptive freq. hopping	Dynamic freq. Selection; Transmit power control (802.11h)
Basic cell	Piconet	Piconet	Star	BSS
Extension of the basic cell	Scatternet	Peer-to-peer	Cluster tree, Mesh	ESS
Max number of cell nodes	8	8	65536	2007

As it has been mentioned earlier, each protocol is more suitable depending on the application targeted. For instance, Bluetooth is used to connect cordless peripheral such as mouse, keyboard, and hands-free headset. UWB is oriented to multimedia applications requiring high-bandwidth. ZigBee is designed for reliable wirelessly networked monitoring and control networks. Wi-Fi is directed at computer-to-computer connections as an extension or substitution of cabled networks [Lee 2007].

1.1. Wireless Sensor Networks

Wireless sensor networks (WSN) are dedicated to short range wireless communications with low energy consumption. They are designed to handle a small amount of transmitted data generally corresponding to battery-operated sensors measurements (e.g. temperature, pressure, security cameras, controllers for water sprinklers, etc.). They have limited memory and computational capacity. Their use has become widespread in industrial environment, in home automation systems and in military systems [Garcia 2007]. Standardized protocols and proprietary protocols have been proposed. Based on the comparison given in Table 1, the ZigBee protocol has proved to be simpler than the Bluetooth, UWB, and Wi-Fi, which makes it very suitable for sensor networking applications. Other proprietary protocols have been used in sensor networks. However, for the sake of the interoperability between devices, a standardized protocol is preferable. Table 2 was given in [Cao 2009] and it compares some of these proprietary technologies (the Z-wave, Insteon, ANT, etc.) in addition to the ZigBee protocol based on the most common parameters such as the frequency band, the data rate, the corresponding network topology. Almost all protocols use the 2.4 GHz ISM band. This common characteristic can be considered as a first level of standardization. Therefore, it should also be mentioned that even a proprietary protocol has to be in compliance with a number of rules and meet some compatibility requirements such as the national authorities' regulation for radio transmission.

As it is detailed in subsection 1.2, many constraints are considered when designing and deploying sensor networks. The main constraints are related to the energy consumption, the production cost, the hardware limitation, the operating environment, the network topology, the range, the transmission medium and the throughput. This is the reason that makes compromises in term of data rate essential. Depending on the application, additional constraints are added such as mobility management, energy management, etc. Some of these constraints (low consumption, high throughput and large range) are so contradictory that it will never be a unique standard since different solutions can be considered. This gives space to researchers to propose different approaches. Low consumption, high throughput and large range are important factors and are usually used as guidelines to develop algorithms and protocols used in sensor networks. They are also considered as metrics for comparing performance between different solutions in this field.

Table 2. A Comparison of WSN technologies [Cao 2009]

Technology	Frequency band	Data rate (b/s)	Multiple access method	Coverage area (meter)	Network topology
Bluetooth Low Energy	2.4 GHz ISM	1 M	FH + TDMA	10	Star
UWB (ECMA – 368)	3.1 – 10.6 GHz	480 M	CSMA/ TDMA	<10	Star
Bluetooth 3.0 + High Speed	2.4 GHz ISM	3 – 24 M	FH + TDMA/CSMA (WiFi)	10	Star
ZigBee (IEEE 802.15.4)	ISM	250 K	CSMA	30-100	Star/ mesh
Insteon	131.65 KHz (powerline) 902 – 924 MHz	13 K	Unknown	Home area	Mesh
Z- wave	900 MHz ISM	9.6 K	Unknown	30	Mesh
ANT	2.4 GHz ISM	1 M	TDMA	Local area	Star/ mesh
RuBee (IEEE 1902.1)	131 KHz	9.6 K	Unknown	30	Peer-to-peer
RFID (ISO/IEC 18000-6)	860-960 MHz	10-100 K	Slotted- Aloha/ binary tree	1-100	Peer-to-peer
FH: Frequency hopping TDMA: Time division multiple access CSMA: Carrier sense multiple access					

1.2. Challenges in WSN

Communication between sensor nodes faces more challenges than communication in other wireless networks. The constraints imposed by sensor architecture makes it hard to ensure a high quality of service (QoS). Besides, the low signal power used to transmit data makes the signal very vulnerable to channel disturbance. The main challenges to which sensor networks are confronted are mainly the low energy budget, the channel conditions, the collisions that may occur during the packet transmission and the mobility which has to be ensured in many WSN applications. All these features are detailed below.

1.2.1. ***Energy consumption***

Each single execution within electronic devices needs energy. This is why energy consumption optimization is a matter raised at every level from the sensor architecture design

phase to the phase of WSN protocol applications' conception. Besides, WSN nodes are supposed to work autonomously for a long period of time, a low energy budget will impose in certain cases adjustments in the system functionalities in order to reduce the energy consumption [Shah 2002]. The energy budget is, then, both an evaluation metric that gives information about some algorithms performance and a decision metric used by protocol algorithms.

The transmission unit consumes the biggest part of the energy [Raghunathan 2002]. Indeed, datasheets of commercial sensor nodes show that the energy cost of receiving or transmitting a single bit of information is approximately the same as that required by the processing unit for executing a thousand operations [Crossbow] [Tmote]. To overcome this shortcoming, the sleep and the idle modes are used in sensor nodes. In the sleep mode, significant parts of the transceiver are switched off. The node is not able to immediately receive data and needs a recovery time to leave the sleep state (energy consumed during the startup can be significant). In the idle mode, the node is ready to receive, but it is not doing so. Some functions in the hardware can be switched off, thus, reducing the energy consumption. The use of sleep and idle modes raises a new problem which is the synchronization of network nodes. Devices need to know when to switch between the different states: receive, transmit, idle and sleep modes. Moreover, a clock drift may occur [Ganeriwal 2005]. In this case, control packets have to be transmitted to resynchronize the network, which increases the energy consumption.

The major goal when designing WSN applications is to ensure the optimal throughput with a low energy budget according to the targeted application requirements [Chandrakasan 1999].

1.2.2. ***Channel conditions***

Signal distortion during the packet transmission can be caused by predictable and quantifiable phenomena (at least when the transmission environment is well known) and by unpredictable events. The main predictable phenomena are the propagation which consists in the attenuation of the transmitted signals with the distance (path loss), the blocking of signals caused by large obstacles (shadowing), and the reception of multiple copies of the same transmitted signal (multipath fading). These variations can be roughly divided into two types [Tse 2005]:

- Large-scale fading, due to path loss of signal as a function of distance and shadowing by large objects such as buildings and hills. This occurs as the mobile moves through a

distance of the order of the cell size (cellular system), and is typically frequency independent.

- Small-scale fading, due to the constructive and the destructive interference of the multiple signal paths (multipath fading) between the transmitter and receiver. This occurs at the spatial scale of the order of the carrier wavelength, and it is frequency dependent.

Large-scale fading is more relevant to issues such as cell-site planning. Small-scale multipath fading is more relevant to the design of reliable and efficient communication systems.

Unpredictable events happen randomly and are completely unknown by the device. The corresponding effects are the thermal noise and interferences. The thermal noise is introduced by the receiver electronics and is usually modeled as Additive White Gaussian Noise (AWGN). If the medium is not shared with any other RF sources, the signal propagation of simulated transmitters and AWGN can describe the entire channel. However, when several nodes transmit at the same time on the channel, interferences may happen and have to be taken into account in the channel modeling.

In WSN, the transmission power is relatively low, which makes the signal very sensitive to noise. In addition, since the antennas used by the nodes are very close to the ground, the loss of the signal transmitted between them can be very high.

In [Tse 2005], it was highlighted that interference I from neighboring cell is random due to two reasons. One of them is small-scale fading and the other is the physical location of the user in the other cell that is reusing the same channel. The mean of I represents the average interference caused, averaged over all locations from which it could originate and the channel variations. However, due to the fact that the interfering user can be at a wide range of locations, the variance of I is quite high. Therefore, it was noticed in [Tse 2005] that the signal to interference plus noise ratio (SINR) is a random parameter leading to an undesirably poor performance. There is an appreciably high probability of unreliable transmission of even a small and fixed data rate in the frame.

In this work, we only focus on orthogonal interferences: Only interferences that happen in the same channel are considered.

1.2.3. ***Medium access***

WSN have to handle the interconnection between a large number of devices. These devices usually use the same frequency (especially in Ad Hoc networks) to communicate. As a consequence, collisions may occur very often. Bad channel conditions may cause either delay and trigger a backoff period before sending data or the failure of the packet reception. Low network performance that is caused by the medium access mode is, therefore, closely related to the channel conditions and the physical layer design [Miluzzo 2008]. It is also interesting to mention that, given the large scale of sensor networks, the randomness of transmission time makes it difficult to analytically evaluate protocol performance. This is why simulation is an interesting alternative to study and evaluate sensor network protocols.

1.2.4. ***Mobility***

The most important feature in the mobility management is maintaining the synchronization of mobile nodes. When nodes move, the routes of transmitted packets may change. The route change must be quickly handled in order to avoid high transmission delays. Even if the routing protocol differs from a network configuration to another [Norouzi 2012], route discovery always requires additional network overhead (control packets). In addition to delay increase, the packet reception rate may decrease because of the synchronization loss.

One of the direct effects of mobility during the transmission is the Doppler effect that occurs when the source and the receiver are in motion relative to each other. The wave frequency increases when the source and receiver approach each other and decreases when they move apart. The motion of the source causes a real shift in frequency of the wave, while the motion of the receiver produces only an apparent shift in frequency. The computation limitations of sensor nodes do not make the use of complex mobility management techniques possible.

1.3. Contributions and manuscript organization

This thesis proposes new approaches to handle self-efficient embedded system for mobile communicating objects. Therefore, we first examine the energy efficiency in IEEE 802.15.4 sensor networks based on the protocol standard and previous research. Our major concern is reducing the energy consumption of mobile sensor nodes. To do so, we proceed in two phases. At the first stage, we propose a global sensor network architecture and a new energy-efficient mobility management approach for IEEE 802.15.4/ZigBee end devices. The new approach is

based on the link quality estimator (LQI) and uses a speculative algorithm. We propose two speculative algorithms. Then, we study and evaluate the energy efficiency when using a rate adaptation algorithm that takes into account the channel conditions. We first propose a mobility-aware rate adaptation algorithm and evaluate its efficiency in our network architecture. Then, we propose and evaluate a second rate adaptation algorithm that relies on a more accurate link channel estimation.

This manuscript is organized as follows. In Chapter 2, we present an overview of the IEEE 802.15.4/ZigBee protocol. Chapter 3 is dedicated to the state of the art related to our work. In Chapter 4, the network architecture and the new mobility management approach as well as its evaluation are given. In Chapter 5, two rate adaptation algorithms are presented and evaluated. The conclusion and perspectives are given in Chapter 6.

Chapter 2. **IEEE802.15.4/ZigBee overview**

2.1. Introduction

ZigBee is a high-level protocol for wireless personal area networks (WPANs) based on the IEEE 802.15.4 standard. As it is shown in Figure 1, IEEE 802.15.4 defines both the data link and the physical layers, respectively called the MAC and PHY layers in the following. ZigBee takes full advantage of the IEEE 802.15.4 specification, and adds the network, security, and application layers.

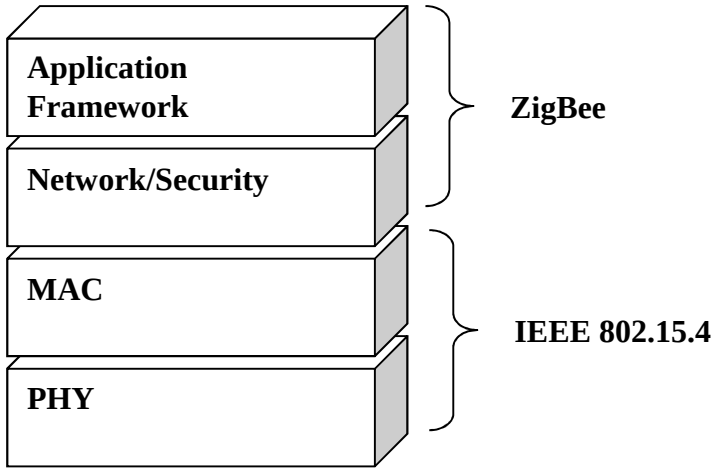

Figure 2. IEEE 802.15.4/ZigBee layers

This section introduces the generic sensor node architecture; then it offers an overview of IEEE802.15.4/ZigBee layers. Finally, it details the energy consumption performance of the IEEE 802.15.4 physical and MAC layers and the ZigBee network layer.

2.2. Sensor node architecture

Sensor nodes are built with respect to some constraints [Bharathidasan 2002] [Raghunathan 2002]. In fact, the sensor nodes have to:

- be small (size)
- consume minimum energy
- operate in a high density (large concentration of operating nodes)
- have a reduced production cost
- be independent and able to operate unattended
- be adaptive to the environment

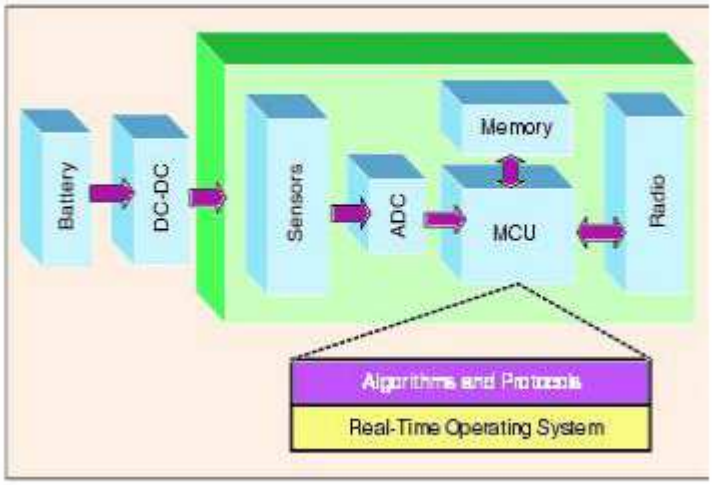

Figure 3. System architecture of a typical wireless sensor node [Bharathidasan 2002]

These constraints concern both the software and the hardware. The software part is handled by the communication protocol stack deployed within the sensor device. It is also constrained by the hardware architecture. In this section, the general hardware architecture of sensor devices is detailed. As it is illustrated in Figure 3, a sensor node contains four basic components listed below.

*2.2.1. **The sensing unit***

The sensing unit typically includes two sub-units, the sensor itself in addition to an analog-to-digital converter (ADC) that converts analog signals produced by the sensors according to the observed phenomenon to digital signals that are transmitted to the processing unit.

2.2.2. ***The processing unit***

The processing unit, usually associated with a small storage unit (memory), carries out the procedures that allow a node to work with the other nodes of the network to give, in the end, the result of the task assigned to the network.

2.2.3. ***The transmission unit***

Connecting the node to the network is managed by the transmission unit. Communications are based on radio frequency-based components that require circuits of modulation, demodulation, filtering, and multiplexing, which increases the complexity of sensor nodes and their production cost. The realization and the use of components of radio transmission in sensor networks low energy consumption is so far a major technical challenge.

2.2.4. ***The power supply unit***

The power supply unit is also one of the most important components in a sensor node. It can be represented by an energy charging system such as solar cells. The sensors are usually battery-powered. Their autonomy is acceptable for applications requiring the transfer of small amounts of data (their original applications). However, when the amount of exchanged data increases, autonomy decreases.

A sensor node may also contain a unit of power management (MM) that controls and adjusts its functions according to the energy budget.

2.3. IEEE 802.15.4 overview

2.3.1. ***IEEE 802.15.4 versions***

Many revisions have been done to the IEEE 802.15.4 standard since its first appearance in 2003. The 2003 version defined two PHYs operating in different frequency bands (one for 868/915 MHz band and one for 2.4 GHz band) with a very simple, but effective, MAC layer protocol. In 2006, a new standard revision [IEEE TG 15.4 2006] added two more PHY options. These optional PHYs proposed a higher rate to the 868/915 MHz frequency bands. It added four modulation schemes that could be used: three for the lower frequency bands and

one for 2.4 GHz frequency band. The MAC was backward-compatible, but it added MAC frames with a variety of enhancements including:

- Support for a shared time base with a data time stamping mechanism
- Support for beacon scheduling
- Synchronization of broadcast messages in beacon-enabled PANs

In 2007, two new PHYs, one for UWB technology and another one used for the Chirp Spread Spectrum (CSS) at 2.4 GHz frequency band, were added as an amendment.

In 2009, two new PHY amendments were approved, one to provide operation in frequency bands specific in China and the other for operation in frequency bands specific to Japan.

The major changes in the current revision (2011) are not technical but editorial. The organization of the standard was changed so that each PHY now has a separate clause. The MAC clause was split into functional description, interface specification, and security specification.

*2.3.2. **IEEE 802.15.4 nodes***

IEEE 802.15.4 defines two types of nodes:

- FFD (Full Function Device): these devices implement the whole protocol stack and can handle packet routing mechanism.
- RFD (Reduced Function Device): RFD node does not have the ability of routing packets. It does not implement the entire protocol stack.

*2.3.3. **IEEE 802.15.4 topology***

2.3.3.1. Star topology

When FFD is activated for the first time, it can establish its own network and become the PAN coordinator. Star networks operate independently from all other star networks. This is possible if a PAN ID that is not used by another network being in the coverage area is chosen.

2.3.3.2. Point-to-point topology

In point to point topology (peer-to-peer), an FFD can communicate directly with other FFD provided they are within radio range of each other. In this topology, there is a single

coordinator as in star topology. Its role is to maintain a list of participants in the network and distribute short addresses.

2.3.3.3. More complex topologies

With the help of a network layer and a data packets routing system, it is possible to develop more complex topologies. ZigBee technology provides a network layer to easily create such topologies with automatic routing algorithms such as cluster tree (tree cells) or mesh networks. The advantage of a cluster tree is the possibility of extending the coverage area of the network, while its disadvantage is the increased latency.

2.3.4. ***Physical layer***

The IEEE 802.15.4 protocol uses the ISM frequency band defined at the following frequencies:

- 2.4 GHz ISM band has 16 channels that are spaced 5 MHz apart with a spectral window of 2 MHz.
- 915 MHz (for USA) has 10 channels that are spaced 2 MHz apart with a spectral window of 0.6 MHz.
- 868 MHz (for Europe) has one channel with a spectral window of 0.3 MHz.

The standard specifies the following four PHY layers:

- An 868/915 MHz direct sequence spread spectrum (DSSS) PHY employing binary phase-shift keying (BPSK) modulation.
- A 2450 MHz DSSS PHY. The modulation format is Offset – Quadrature Phase Shift Keying (O-QPSK) with half-sine chip shaping. This is equivalent to MSK modulation. Each chip is shaped as a half-sine, transmitted alternately in the I and Q channels with one half chip period offset.

In addition to the 868/915 MHz BPSK PHY, which was originally specified in the 2003 edition of this standard, two optional high-data-rate PHYs are specified for the 868/915 MHz bands, offering a tradeoff between complexity and data rate.

- An 868/915 MHz DSSS PHY employing offset quadrature phase-shift keying (O-QPSK) modulation

- An 868/915 MHz parallel sequence spread spectrum (PSSS) PHY employing BPSK and amplitude shift keying (ASK) modulation

The O-QPSK and the ASK PHYs are not mandatory in the 868 MHz or 915 MHz band. If one of them is used by a device in the 868 MHz or 915 MHz band, then the same device shall be capable of transmitting using the BPSK PHY as well.

The data rate of the 2.4 GHz O-QPSK is 250 kb/s. The BPSK PHY is 20 kb/s when operating in the 868/950 MHz band and 40 kb/s when operating in the 915 MHz band.

Table 3 summarizes the main characteristics (frequency, rate, number of channels) of the mandatory IEEE 802.15.4 PHY layers.

Table 3. Frequency band of the IEEE 802.15.4

PHY (MHz)	Frequency Band	Rate (kb/s)	Number of channels	Central frequency (MHz)
868/915	868-868.6	20	1	868.3
	902-928	40	10	906+2(k-1) ; k=1,2,..,10
2450	2400-2483.5	250	16	2405+5(k-11) ; k=11,..,26

We are interested in the 2006 standard version and more specifically the IEEE 802.15.4 2.4 GHz frequency band. We consider that the specification is sufficient enough to study the protocol behavior in WSN.

2.3.4.1. O-QPSK 2.4 GHz PHY

The maximum power emitted by an IEEE 802.15.4 or ZigBee module is not defined by the standard. It depends on the regulatory authority of the area where the transmission is performed, and on the manufacturer according to the application that the node is meant to. However, the typical recommended power is 1 mW or 0 dBm and receiver sensitivity must be better than - 85 dBm at 2.4 GHz (for packet error rate less than 1%).

The IEEE 802.15.4 2.4GHz PHY uses the Direct-Sequence Spread Spectrum (DSSS).

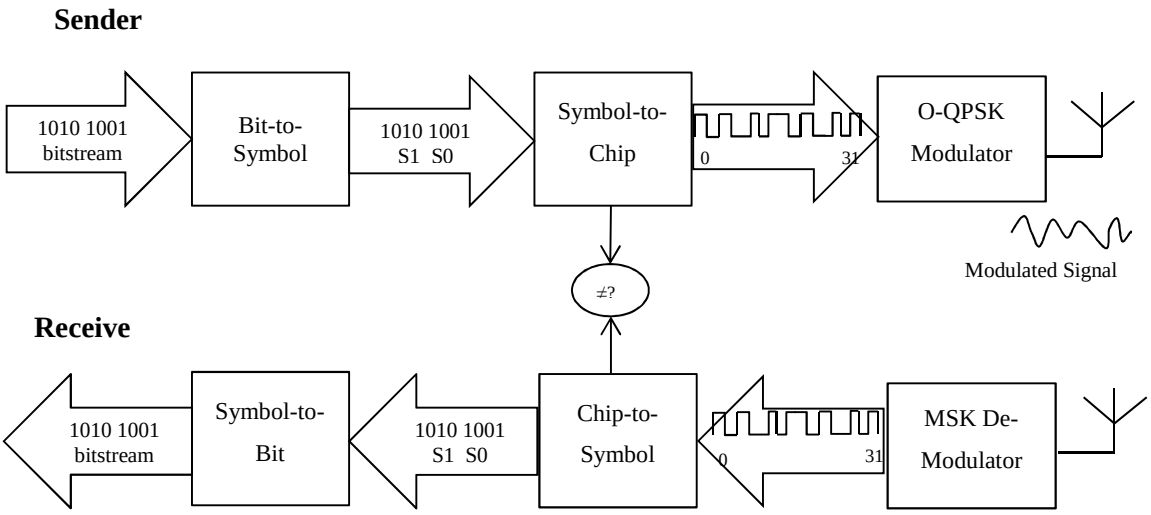

Figure 4. Modulation and spreading functions for the O-QPSK PHYs

DSSS multiplies the data stream with a high-data rate sequence called chip sequence or Pseudo-Noise (PN) sequence. Therefore, the resulting signal determined by the pseudo-random signal can occupy larger bandwidth. Due to its length, the PN sequence seems as a random signal, like noise. However, it is a completely deterministic signal, which enables the reconstruction of the original data stream on the receiver side. The reconstitution is possible even if the signal is distorted during the transfer and the original sequence can still be extracted from the transmission due to its redundancy in the carrying signal. Thus, DSSS istolerant to noise and has the advantage of making the signals of a limited bandwidth like a voice signal more resistant to noise during the transmission. However, spreading the transmit signal power within a larger bandwidth decrease the transmit power.

As it is illustrated in Figure 4, in 2.4 GHz O-QPSK PHY layer, each byte is divided into two symbols, four bits each (S0 and S1). Each symbol is mapped to one out of 16 pseudo-random sequences, 32 chips each. The chip sequences are modulated using O-QPSK. The rate of the 2.4 GHz band is 250 kb/s. The chip sequence is, then, transmitted at 2 MChips/s.

The BER is computed from the SINR and the modulation used. The SINR can be defined as follows:

$$\boldsymbol{SINR} = \boldsymbol{P} * |\boldsymbol{h}|^{\boldsymbol{2}} / \boldsymbol{N_0} + \boldsymbol{I} \quad (1)$$

The numerator is the received power at the base-station due to the user transmission of interest with P denoting the average received power and $|h|^2$ the fading channel gain (with

unit mean). The denominator consists of the background noise N_0 and an extra term due to the interference from the user in the neighboring cell. *I* denotes the interference and is modeled as a random variable with a mean typically smaller than *P* (say equal to *0.2P*).

The bit error probability P_b for QPSK is the same as for BPSK.

$$P_b = \frac{1}{2} * erfc\left(\sqrt{\frac{2E_b}{N_0}}\right) = Q\left(\sqrt{\frac{2\,E_b}{N_0}}\right) \quad (2)$$

$$erfc(x) = \frac{2}{\sqrt{\pi}} \int_x^{+\infty} e^{-t^2}\, dt \quad (3)$$

QPSK modulation consists of BPSK modulation on both the in-phase and quadrature components of the signal. With perfect phase and carrier recovery, the received signal components corresponding to each of these branches are orthogonal. Therefore, the bit error probability on each branch is the same as for BPSK: $P_b = Q(P_b^2)$. The symbol error probability equals the probability of either branch has a bit error:

$$P_s = 1 - (1 - P_b)^2 \quad (4)$$

The *snr* is related to the $\frac{E_b}{N_0}$ in that:

$$\frac{E_b}{N_0} = 2snr \quad (5)$$

During the demodulation stage, the received signal is converted to binary codes. The conversion uses either soft decision decoder (SDD) or hard decision decoder (HDD). If the soft decision decoder is being used, the symbol is decoded and extra information about the most likelihood is determined and gives the probability of the correctness of the decoding.

Let x_k (k = 1 .. N) be the input bits to the encoder of the sender, r the received signal input to the decoder of the receiver. The output of the decoder at the receiver is log likelihood ratio (LLR) for each received bit:

$$LLR(k) = \log\left(\frac{P(x_k=1|r)}{P(x_k=0|r)}\right) \quad (6)$$

The decoded output bit y_k is determined as follows:

$$y_k = \begin{cases} 1 : LLR(k) \geq 1 \\ 0 : LLR(k) < 0 \end{cases} \quad (7)$$

On the other hand, if HDD is being used, each symbol is determined independently of other symbols. HDD uses the Hamming Distance between the received word and the code word (the number of distinct elements between the two words). The SDD is more costly than the

HDD; however, it is more accurate. IEEE 802.15.4 devices usually use a Hard Decision Decoder (HDD) (e.g. the IEEE 802.15.4-compliant ChipCon CC2420).

2.3.4.2. PHY layer services

The PHY layer is responsible for the following tasks:

- the activation and deactivation of the radio transceiver,
- the energy detection (ED) task,
- Link quality indicator (LQI) for received packets,
- Clear channel assessment (CCA),
- Channel frequency selection,
- Data transmission and reception.

i. Energy detection (ED)

The energy detection mechanism allows having an estimation of the received signal power within the bandwidth of the channel with no attempts to identify or decode the signal. The duration of the ED is equal to 8 symbols.

ii. Link quality indicator (LQI) for received packets

When a packet is received by a node, its link quality can then be determined. The IEEE 802.15.4 standard defines the link quality indicator (LQI) as an integer ranging from 0 to 255. However, the calculation of the LQI is not specified in the standard. The LQI measurement is a characterization of the strength and/or quality of a received packet. IEEE 802.15.4 specifies that the measurement may be implemented using receiver energy detection (ED), a signal-to-noise ratio estimation (SNR), or a combination of these methods. The use of the LQI metric by the network or application layers is not specified in the standard as well. Although the calculation of the LQI is not specified in the standard, its definition implies that it depends on the distance between the receiver and the sender.

iii. Clear channel assessment (CCA)

IEEE 802.15.4 nodes use the carrier sense multiple access with collision avoidance (CSMA-CA) mechanism to send packets. The CSMA-CA mechanism is a MAC mechanism (subsection 2.3.5) that consists of listening to the channel before sending packets. A node sends packets if the channel is sensed to be free. In order to do so, the CSMA-CA uses the

CCA PHY mechanism that allows an IEEE 802.15.4 node to listen to the channel during 8 symbols. There are 3 modes of CCA:

- Mode 1: Energy above threshold: the medium is busy if energy above the ED threshold is detected.
- Mode 2: Carrier sense only: the medium is considered busy if the node senses a signal compliant with the standard with the same modulation and spreading characteristics of the PHY that is currently in use by the device. This signal may be above or below the ED threshold.
- Mode 3: Carrier sense with energy above threshold: a combination between the two previous techniques.

iv. Channel frequency selection:

In the initialization of the network, the coordinator has to choose the appropriate frequency in order to avoid collisions between packets that are transmitted in the neighbor networks.

v. Data transmission and reception

The PHY handles the transmission and reception of physical layer protocol data units (PPDUs) across the physical radio channel. PPDU is the information received at the PHY layer and that is composed of control information (a synchronization header (SHR) and a PHY header (PHR) that contains the frame length information) and data (MAC protocol data unit: MPDU).

2.3.5. ***Mac sublayer***

The MAC sublayer is mainly responsible for the synchronization of the network in order to optimize packet transmissions. This is ensured through the beacon management and several other mechanisms (e.g. association, dissociation, channel access, acknowledgment frame delivery, GTS management).

For the sake of simplicity, the MAC personal area network information base (PIB) attributes and MAC constants that are named in this section are given in Some MAC attributes and constants.

2.3.5.1. Beacon management

IEEE 802.15.4 wireless network has a coordinator which always initializes the network defined by an identifier. The coordinator is always an FFD device. There are two types of PANs: non beacon-enabled and beacon-enabled PAN. In beaconless mode, there is no synchronization between nodes. A node wishing to send a message on the channel must first listen on it. If it is free, message can be sent. Otherwise a node has to wait for an interval of time called backoff period and start again. This is handled according to the non-slotted version of the CSMA-CA protocol. The beacon mode is a synchronized mode. Access to the medium is done using the Time Division Multiple Access method (TDMA). The time is divided into superframes. In a non beacon-enabled mode, a node can ask for a beacon by sending a beacon request to the coordinator.

The beacon frame contains essential information about the channel that is used, the PAN identifier (PAN Id), as well as the PAN mode.

2.3.5.2. Superframe format

As shown in Figure 5, each superframe in the beacon-enabled mode consists of an active period in which nodes can receive and transmit and an optional inactive period during which all nodes enter into a low-power mode. The *macBeaconOrder* (BO) is a MAC PIB attribute that defines the beacon interval (BI). BI represents the entire period between two consecutive beacon frames and it is defined as follows:

$$BI = aBaseSuperframeDuration * 2^{BO} \quad (8)$$

where 0 <= BO <= 14 and *aBaseSuperframeDuration* is a MAC constant that represents the minimum duration of a superframe. *aBaseSuperframeDuration* is fixed to 960 symbols.

The *macSuperframeOrder* (SO) is a MAC attribute that defines the duration of the active period called superframe duration (SD). It is defined as follows:

$$SI = aBaseSuperframeDuration * 2^{SO} \quad (9)$$

where 0 <= SO <= BO <= 14 .

The active period is composed of 16 slots (Figure 5). Each beacon interval begins with the synchronization beacon message sent by the coordinator to all nodes of the network. The remaining 15 slots are divided into a contention access period (CAP) and an optional contention free period (CFP). In CAP, the channel is accessed according to the slotted version

of the CSMA / CA protocol. In CFP, the coordinator assigns guaranteed time slots (GTS) that are composed of one or more slots. A node may request GTS assignment from the coordinator during the CAP period.

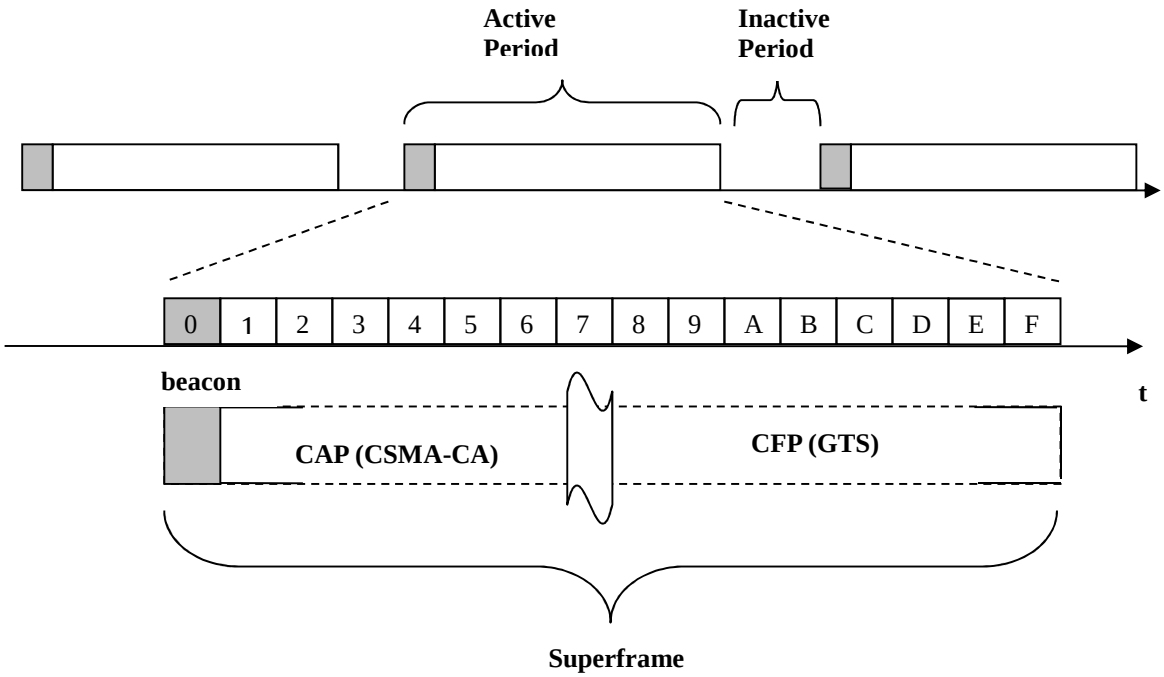

Figure 5. IEEE 802.15.4 Beacon-enabled Superframe

In the beacon-enabled mode, if *macSuperframeOrder* (SO) is set to 15, the superframe does not remain active after the beacon.

In the non beacon-enabled mode, the *macBeaconOrder* (BO) is set to 15 and the *macSuperframeOrder* (SO) value is ignored. In this mode, the coordinator transmits beacon frames only when it is requested to do so, such as on receipt of a beacon request command.

2.3.5.3. Channel access

Depending on the type of the PAN that is defined (beacon-enabled or non beacon-enabled PAN), the channel access is ensured by the CSMA-CA algorithm or by the GTS mode. The standard defines two channel access modes at the media access control sub layer (MAC): the unslotted mode and the slotted mode. If periodic beacons are not being used in the PAN or if a beacon could not be located in a beacon-enabled PAN, the MAC sublayer transmits using the unslotted version of the CSMA-CA algorithm.

i. GTS mode:

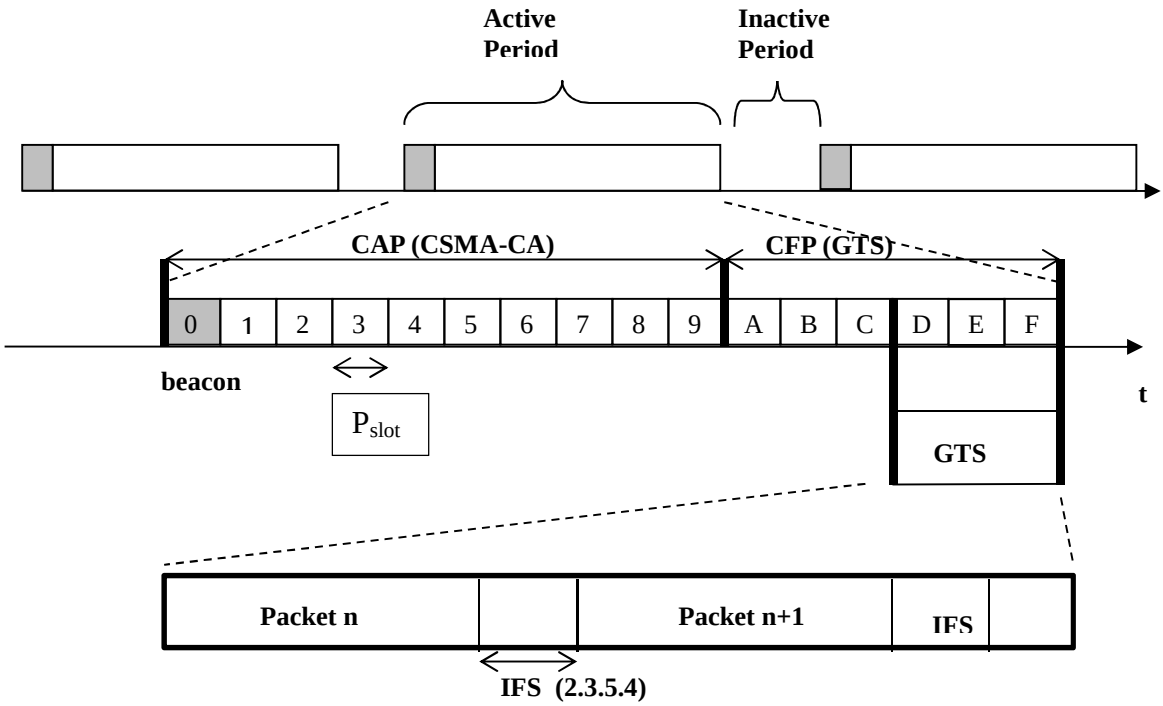

Figure 6. GTS and Backoff slots in IEEE 802.15.4 Beacon-enabled Superframe

A maximum total number of 7 GTSs can be allocated in 1 superframe. A GTS is a portion of the superframe exclusively dedicated to one node so it can transmit or receive packets without collision risks. This can be ensured thanks to the broadcasting of the information about the allocated GTSs and the length of the CAP period in the beacon. The length of an allocated GTS is not limited and the start of the GTS slot has no constraint. However, as it is illustrated in Figure 6, the communication within a GTS must end one interframe-spacing (IFS) (subsection 2.3.5.4) before the actual GTS is ended. A node sends GTS requests to its coordinator in the CAP period using the slotted CSMA-CA mode specifying the number of slots requested and the direction of the transmission (receive or transmit). A data frame transmitted in an allocated GTS uses only short addressing (see 2.4.2). If a device (coordinator or another device) has been allocated a receive GTS, its receiver has to be on during the entire period of the GTS.

On the receipt of a GTS allocation request frame, the PAN coordinator first checks if there is available capacity in the current superframe, based on the remaining length of the CAP and

the desired length of the requested GTS. When the PAN coordinator determines whether capacity is available for the requested GTS, it generates a GTS descriptor with the requested specifications and the 16-bit short address of the requesting device. The GTS descriptor is sent to the requesting node in the beacon frame. GTSs are allocated on a first-come-first-served basis by the PAN coordinator provided there is sufficient bandwidth available. Each GTS descriptor is 24 bits in length and contains the following information:

- The device short address is 16 bits in length of the device for which the GTS descriptor is intended
- The superframe slot (4 bits in length) at which the GTS is to begin.
- The number of contiguous superframe slots over which the GTS is active (4 bits in length).

If a device misses the beacon at the beginning of a superframe, it cannot use its GTSs until it receives a beacon correctly. There is no limit on the GTS use. The GTS is deallocated either on the node request or on PAN coordinator decision (usually because of node's inactivity during a determined number of superframes).

ii. CSMA-CA Algorithm (Annex A)

The CSMA-CA algorithm allows network nodes to share the same channel. It provides a channel access mechanism that avoids collisions between different transmitted signals by listening to the medium before starting to transmit. The transmission is deferred if the channel is found to be busy (used by another transmitting source). This mechanism considerably reduces collision probability. However, collisions still can happen unlike when transmitting during a GTS. Nonetheless, the CSMA-CA mechanism is essential even for the GTS transmission mode since the GTS requests (and all other control frames) have to be sent during the CAP period. Moreover, the GTS mechanism is hard to be achieved in real applications because of the synchronization issue and the risk of clock drift.

CSMA-CA is based on the backoff period unit. The CAP is not considered as a sequence of slots as in the CFP; it is considered as a sequence of backoff slots that have *aUnitBackoffPeriod* period. In slotted CSMA-CA, the start of the first backoff period of each device is aligned with the start of the beacon transmission. In unslotted CSMA-CA, the backoff periods of one device are not related in time to the backoff periods of any other device in the PAN.

Figure 7 describes the CSMA-CA mechanism in the slotted mode. According to the related algorithm, two consecutive CCAs are required before the transmission can start. In Figure 7, the time required for each CCA is denoted T_{CCA}. CCA is performed at the beginning of a backoff period (T_{BP} in Figure 7). The contention window (CW) variable controls the number of CCAs to be performed in each attempt. CW is, therefore, initialized to two and reset each time the channel is assessed to be busy. If the channel is busy, the node has to wait for a computed number of backoff periods. The number of backoff is constrained by a second variable, NB, which is the number of times the CSMA-CA algorithm was required to backoff while attempting the current transmission. This value is initialized to zero before each new packet transmission. Each time a current transmission attempt fails, NB is incremented.

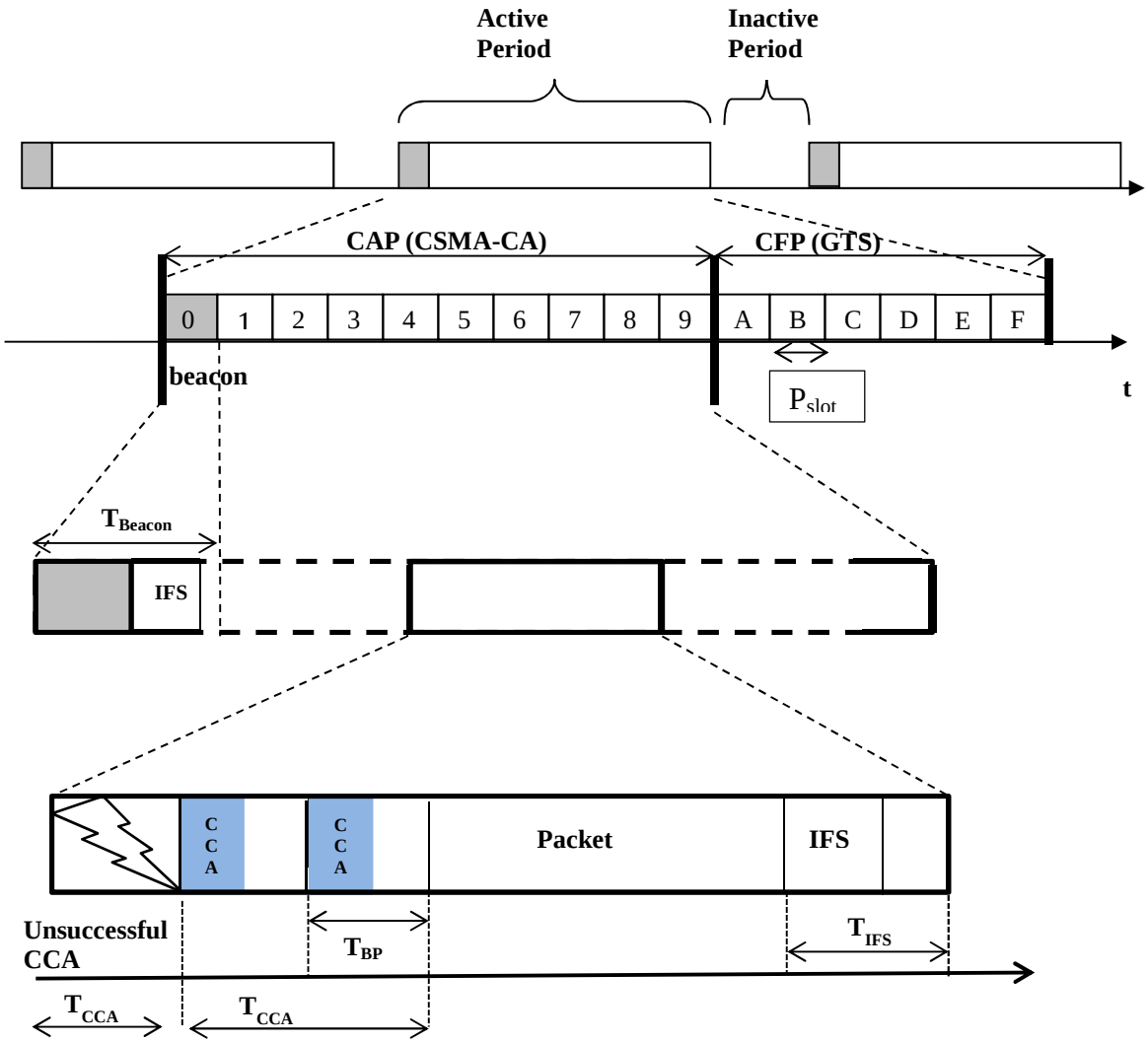

Figure 7. CSMA-CA Algorithm in the slotted mode

If NB reaches a value greater than *macMaxCSMABackoffs*, the current transmission fails. The number of backoff periods a device shall wait before attempting to assess the channel is controlled by a third variable, the backoff exponent (BE). The received beacon contains indication on how to compute BE through the Battery Life Extension (BLE) subfield (1 bit). If BLE subfield is set to zero, BE is initialized to the value of *macMinBE*. If it is set to one, BE is initialized to the lesser of two and the value of *macMinBE*. If the channel is assessed to be busy, the BE is incremented as follows:

$$BE = \min(BE + 1, macMaxBE) \tag{10}$$

The number of backoff periods to wait before attempting the transmission is determined according to the following formula:

$$random(2^{BE} - 1) \tag{11}$$

Thus, if *macMinBE* is set to zero, collision avoidance will be disabled during the first iteration of this algorithm.

As it is shown in Figure 8, in the unslotted systems, only one CCA is required. The unslotted CSMA-CA algorithm uses only the NB and BE variables. NB is initialized to 0 and BE is initialized to the value of *macMinBE*. As in the slotted version, a node has to wait for a random number of backoff periods (BO in Figure 8) then it performs a CCA. If the channel is busy, it increments NB and compute the new value of BE according to the formula given above. The new number of backoff periods before trying to send again the packet is then determined.

In the unslotted CSMA-CA, a transmitting device waits for *turnaround* time (D_{tat} in Figure 8) after a CCA before sending a packet. In Figure 8, Dframe and Dack) are respectively the time required for transmitting a data and an ack frames. Didle_rx is the time taken to switch the radio from idle to receive mode. Before transmitting a packet, a device in a beacon-enabled PAN has to find the beacon first. If the beacon is not being tracked and hence the device does not know where the beacon will appear, it has to enable its receiver and search for at most [*aBaseSuperframeDuration* * (2^n + 1)] symbols, where n is the value of *macBeaconOrder*, in order to find the beacon. If the beacon is not found after this time, the device transmits the frame following the successful application of the unslotted version of the CSMA-CA algorithm. Once the beacon is found, either after a search or due to its being tracked, the frame is transmitted in the appropriate portion of the superframe (either CFP or CAP).

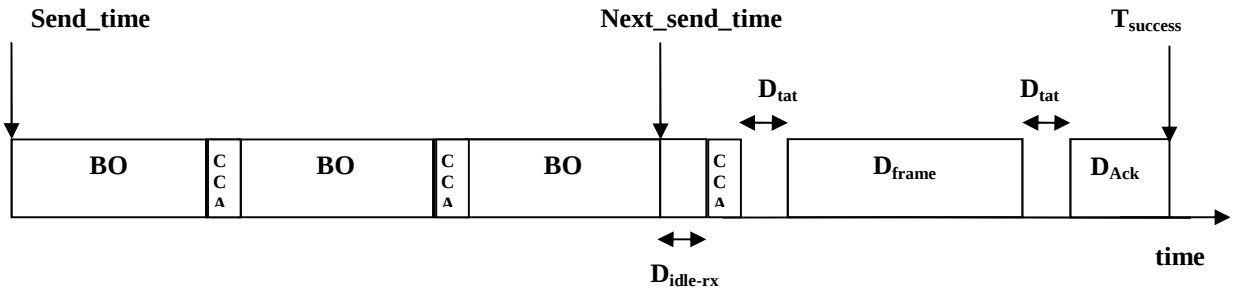

Figure 8. Unslotted IEEE 802.15.4 CSMA-CA

The time spent scanning each channel is [aBaseSuperframeDuration * (2^n + 1)] symbols, where n is the value of the ScanDuration parameter (this parameter is ignored in orphan scan because the node sends a requests then it waits for a macResponseWaitTime for the response).

2.3.5.4. Interframe spacing (IFS)

Two successive frames transmitted from a device have to be separated by at least an IFS period. The IFS period ensures that the MAC sublayer processes the data received by the PHY before switching to another task (e.g. receiving a second packet). If an acknowledgment is required from the first received packet, the separation between the acknowledgment frame and the second transmission has to be at least an IFS period. The length of the IFS period depends on the size of the frame that has just been transmitted.

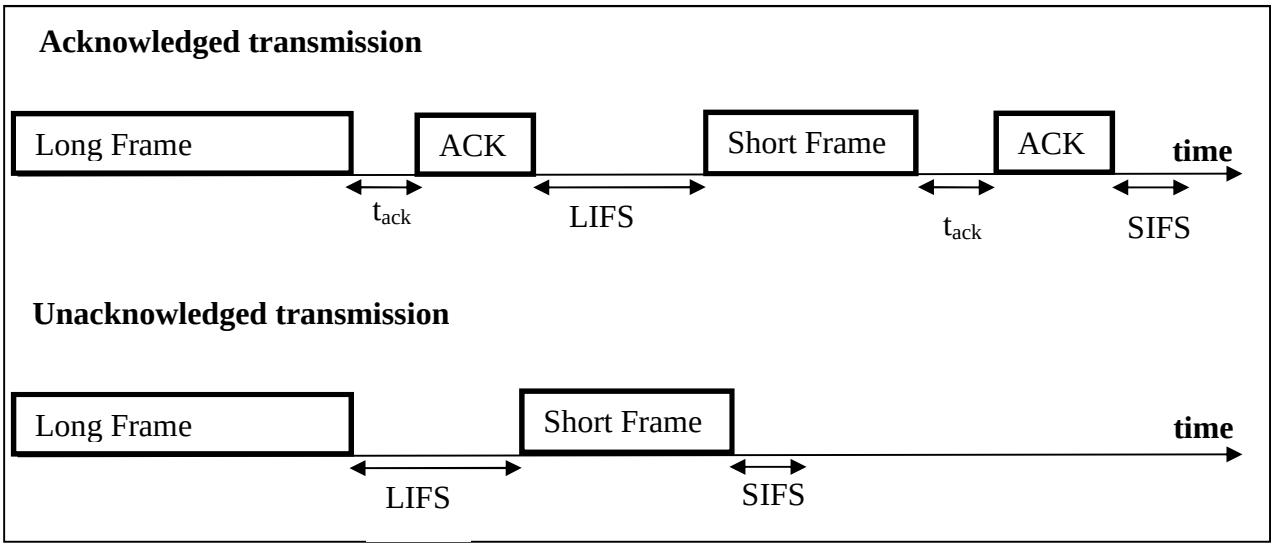

Figure 9. Interframe spacing

If the frame size (i.e., MPDUs) does not exceed *aMaxSIFSFrameSize* bytes, the frame has to be followed by a Short IFS (SIFS) period of at least *macMinSIFSPeriod* symbols duration. If the frame length is greater than *aMaxSIFSFrameSize* bytes, it has to be followed by a LIFS (Long IFS) period of at least *macMinLIFSPeriod* symbols duration. Figure 9 gives the different IFS depending on the frame length and whether or not the acknowledgment is required. If after [aTurnaroundTime + aUnitBackoffPeriod] symbols the acknowledgement is not received, the packet transmission is considered failed. The time to receive an acknowledgement may be deduced according to the following formula:

$$\text{aTurnaroundTime} \leq \text{tack} \leq (\text{aTurnaroundTime} + \text{aUnitBackoffPeriod}) \quad (12)$$

2.3.6. ***Logic Link Control (LLC) sublayer***

In accordance with the family of IEEE 802 standard, 802.15.4 offers a convergence sub-layer type LLC to standardize the interface of layers described by the standard with a top-level layer, typically a Layer 3 compliant LLC. This convergence is ensured by the service specific convergence sublayers (SSCS) described by the standard.

A typical convergence layer must play several roles:

- The verification of the integrity of data received
- Flow control to avoid the saturation of reception buffers and possible loss of data or memory overflows.
- The addressing convergence, that is to say, there is a need to perform the correspondence between addresses Layer 3 (network level addressing is usually globalized throughout the network) and the addresses of Level 2 (link-level, the address is local and sometimes specific to one or wire strand to the area of each radio cell coverage used, etc.)

Under 802.15.4, the sub-layer convergence proposed is very simple for several reasons:

a. Acknowledgment is supported by the management process medium access (MAC) and the standard does not send it up to the SSCS

b. In IEEE 802.15.4, the control flow is implied and realized very simply given the small amount of data exchanged and the small node memory. Data packets are sent according to “send and wait” technique: the upper layer waits for the complete processing of the data packet before sending the next packet (not early).

c. In IEEE 802.15.4, the address management is simplified since there is no conversion to achieve.

2.4. ZigBee protocol [ZigBee]

*2.4.1. **Topology***

ZigBee protocol defines three types of nodes: the coordinators, routers and terminals.

- Coordinator (ZC): FFD type -- It is unique for the entire ZigBee network and is responsible for the creation of the network. It includes the tasks of PAN Coordinator described in IEEE 802.15.4 standard and it acts as a simple router (ZR, see below) once the network is created.
- Router (ZR): FFD -- It must first be associated with the ZC or another ZR. It then accepts other network elements are associated with him, and take on the tasks of 802.15.4 coordinator. The ZR relays messages in a routing protocol that will be presented later. The ZC router is optional in a single network.
- Terminal (ZED): FFD or RFD -- It must first be associated with the ZC or ZR. There is a final element of the network, because it does not accept association, participation in routing messages. The ZigBee end device (ZED) is also optional.
- ZigBee defines three topologies that are represented in Figure 10: star, mesh and cluster tree. In each kind of topology, a unique coordinator must be defined. If many IEEE 802.15.4 PANs are present in the same area, each one has to be defined by a unique identifier called a PAN Id. The beacon mode can only be used in a star or a cluster tree topology. In both topologies, a node wishing to transmit a message to another node has to transmit it first to its coordinator which handles the transmission to the destination node. In a cluster tree topology, each cluster has its own coordinator and its unique PAN Id. All clusters of a same network use the same transmission channel (i.e. the same frequency). A cluster tree network is initialized by a ZigBee PAN coordinator that is considered the root of the tree. A ZigBee coordinator or router can act as a parent device and accept association from other devices in the network. A device connected to a parent device is known as a child device. In this topology, a hierarchical address is assigned to each node of the network, so that hierarchical routing protocol can be used.

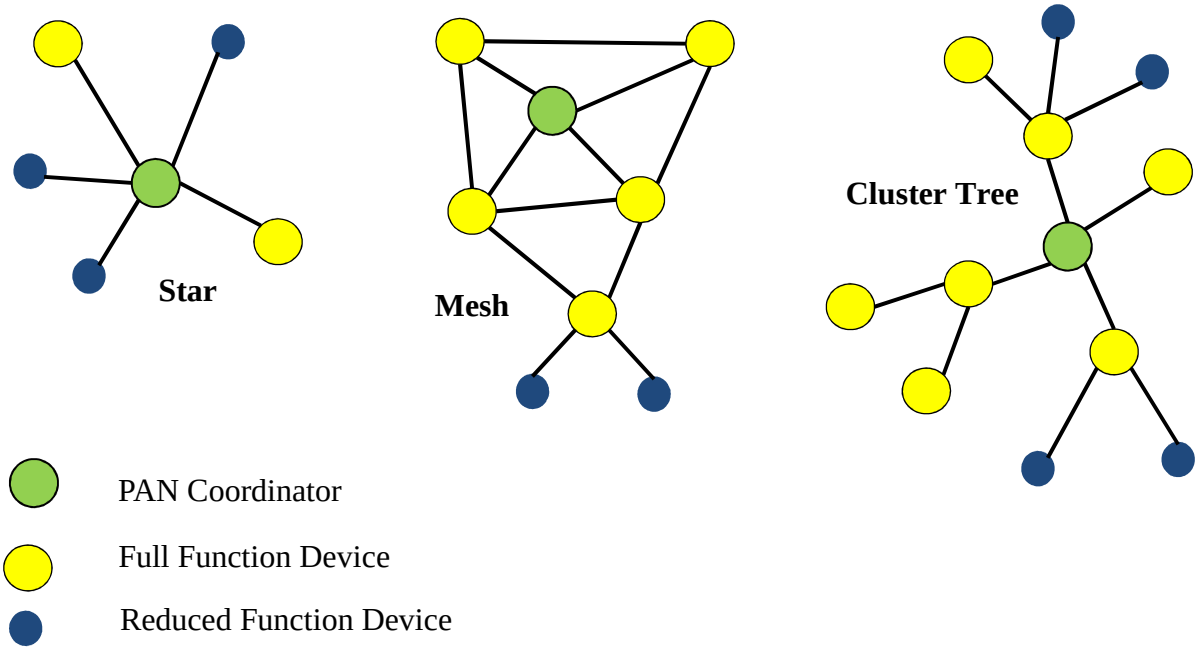

Figure 10. ZigBee topologies

*2.4.2. **Addressing mode***

The network layer defines two types of addresses that can be used whatever the type of the node (coordinator, router or end device):

- The IEEE address (MAC address) that is a unique 64-bit address.
- A short 16-bit address assigned when connecting to a ZigBee network for communication in the network.
- The address distribution algorithm is automatic and decentralized. Layer-3 imposes to layer-2 its address. Layer-3 has a ZigBee configuration mechanism for layer-2 addresses.

The ZigBee specification allows two types of addressing:

- A free address given at the convenience of the top layer (i.e. application framework (Figure 2).
- A hierarchical tree addressing: addresses are distributed according to a hierarchical algorithm used in tree networks.

ZigBee can have wider range than the range of a single node 802.15.4 through the routing process that allows relaying a message by one or more entities to the final destination. This process requires knowledge of the network architecture that is carried out by an automated

discovery algorithm. A ZigBee network can contain up to 65536 nodes (16 bits for each node network address).

2.4.3. ***ZigBee routing protocols***

The general ZigBee packet format is composed of a NWK Header and a NWK Payload. The NWK Header is composed of the frame control field and the routing fields as it is shown in Annex D.

The frame control field includes the frame type and information about the route discovery type. It also specifies if the security in the NWK layer is enabled and if the routing protocol should employ the IEEE Address type for the source or the destination. The route discovery has three options: suppress route discovery, enable route discovery, force route discovery.

Source routing is a technique in which the sender of a packet can specify the route that a packet should take through the network. The source route subframe contains the list of 16-bit short addresses of the nodes that will be used to relay the frame in source routing. The relay count is the number of times the frame is relayed.

The NWK layer can optionally include the 64-bit IEEE address in the NWK layer frames if the IEEE address subfields are set to one. The 16-bit network address of the source and destination are always included in the frame. The value of the sequence number is incremented every time a new frame is transmitted.

2.4.3.1. AODV routing protocol

The on demand routing algorithm proposed by the ZigBee Alliance is close to the Ad hoc On-demand Distance Vector (AODV). AODV routing is a purely "on demand" protocol. In fact, the nodes participating in the routing do not seek to maintain information about the network topology or about the routes.

When a node wants to send a message to another node and it does not have the corresponding entry in its routing table, it starts the path discovery process by broadcasting a *route_request* message. This request is relayed by routers in the neighborhood, and thus, flooding the entire network. When the destination node receives the request, it responds by sending a response message (*route_reply*) but unlike *route_request* who had been broadcasted, the response is only sent to the last router that relayed the broadcast. This process is maintained till reaching the node that originally requested the road. To find the reverse path, each router that

rebroadcasts the *route_request* message has to store the neighbor by which the message was sent in a routing table. The table-driven routing provides optimal routes to the destination.

2.4.3.2. Tree routing

The tree routing is based on the block address allocation mechanism, called C_{skip}. Each device has a set of addresses to distribute to their children. When a device has no capability of routing table and route discovery table, it simply follows the hierarchical tree by comparing the destination address.

This addressing mode can be used in the cluster tree network. The attribution of hierarchical addresses is based on four parameters:

- Maximum number of children per parent (C_m).
- Maximum number of ZigBee routers (R_m) between these children.
- the maximum depth (L_m) of the cluster tree network.
- Depth (d) of a device in a network.
- Network depth defined as the minimum number of hops required for a frame to reach the ZigBee coordinator if only parent/child links are used. The address allocation starts with assigning the zero address to the ZigBee coordinator. To determine the address of the rest of the devices, a function (C_{skip}(d)) is introduced.
- At a given depth d, a function called C_{skip}(d) is used by a node to calculate the addresses A_n of its children. Nodes network addresses are distributed by their parent located at depth d.

$$C_{skip}(d) = \begin{cases} 1 + C_m * (L_m - d - 1) & if\ R_m = 1 \\ \frac{[1 + C_m - R_m - C_m * R_m{}^{Lm-d-1}]}{[1 - R_m]} & otherwise \end{cases} \quad (13)$$

- The address of each end device is assigned using the following equation:

$$A_n = \begin{cases} A_{parent} + C_{skip}(d) * R_m + n & for\ leaf\ nodes \\ A_{parent} + C_{skip}(d) * (n-1) + 1 & for\ other\ routers \end{cases} \quad (14)$$

Figure 11 shows an example of attribution of hierarchical addresses. The ZigBee coordinator's direct children have network depth of 1 because they can send a frame to the ZigBee coordinator directly with a single hop. The ZigBee coordinator itself has a depth of zero. ZigBee standard offers a mechanism to allocate addresses to devices in a tree network.

This is known as the default distributed address allocation. However, application developers are allowed to use their own address allocation method.

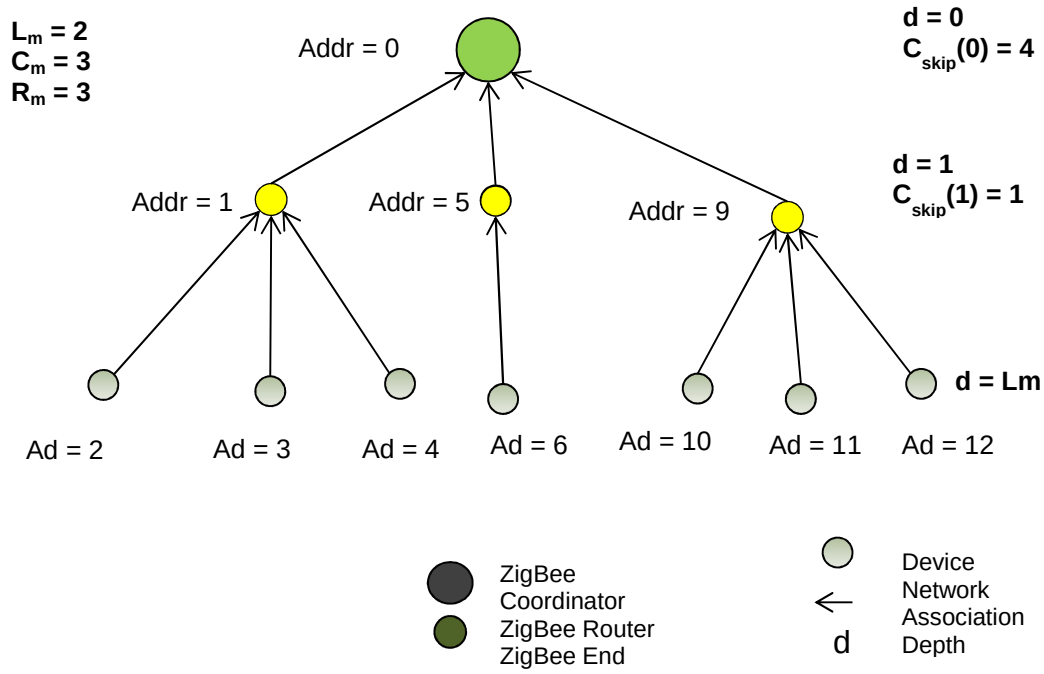

Figure 11. Example of hierarchical addresses attribution

This routing mechanism is based on the short addressing scheme and was initially proposed by MOTOROLA. Each device, upon the reception of a data frame, reads the routing information fields and checks the destination address. If the destination is a child of the device (neighbor table check), the device relays the packet to the appropriate address. If the destination address is not a child, the device must check if the address is a descendent using the condition in (15), where A is the device network address, D the destination address and d the device depth in the network.

$$A < D < A + C_{skip}(d-1) \tag{15}$$

The next hop (N) address when routing down is given by:

$$N = A + 1 + \left\lfloor \frac{D-(A+1)}{C_{skip}(d)} \right\rfloor * C_{skip}(d) \tag{16}$$

If the destination address is not a descendant, the device relays the packet to its parent.

The principle of addressing tree is very interesting because it provides automatic routing based on addresses; therefore, there is no need to additional messages to determine the route

of the packet. The most significant benefit of tree routing is its simplicity and its limited use of resources (e.g. memory used for the routing process). Therefore, any device with low resources can participate in any ZigBee compliant network.

2.5. Energy consumption in IEEE 802.15.4 WSNs

Low energy consumption of sensor networks justifies the growing interest on them. However, low consumption in WSN is generally associated with low data rate and low range. Research in the field of sensor networks try to guarantee a good QoS while, at the same time, use a low energy budget. In order to do so, studies on the limits of the IEEE 802.15.4 protocol and an evaluation of available possibilities have to be carried out. Previous researches agreed that the IEEE 802.15.4 standard as it is defined does not ensure an optimal energy-efficient solution. Tradeoffs as introduced in section 1.2 are required in order to reduce energy consumption which is the first step to guarantee autonomous sensors when they are combined with an energy harvesting system [Sudevalayam 2011].

Energy is consumed in all levels of a sensor node: from the physical layer to the application layer. Optimization of energy consumption can, therefore, be evaluated and optimized in each level. Obviously, for each level, the approaches are different. It is also important to concentrate on the modules (e.g. routing module, network initiation module, mobility module, etc.) that consume the most.

In this subsection, we evaluate the energy efficiency of the IEEE 802.15.4/ZigBee protocol based on the standard protocol and on previous research. An evaluation of the PHY and MAC layers of the IEEE 802.15.4/ZigBee is carried out. For each level, we highlight the most relevant features when studying sensor networks and the main sources of energy consumption.

2.5.1. ***PHY Layer***

Studying the efficiency of the IEEE 802.15.4 PHY layer is important when considering the energy issue in IEEE 802.15.4. In fact, many MAC and routing protocols use the metrics that are obtained at the PHY layer. When the values of the PHY metrics are not accurate, errors at the upper layers will occur, and can have a negative impact on the energy consumption (e.g. retransmission of a packet due to collision). Some inaccuracies cannot be avoided such as the inaccuracies related to the hardware design. In [Zhou 2006] for instance, authors show that

differences may arise from some random factors during the manufacture of sensor devices, which may lead to sensor devices transmitting RF signal at different powers, even though they are the same kind of devices. In addition, after the sensor devices are deployed, the batteries of different sensor devices deplete at different rates, due to different workloads and different environments in which they are deployed. Heterogeneous sending powers combined with environmental factors (e.g. path loss) are the major sources of radio irregularities (variable communication ranges). The effect of these irregularities was observed in their experiments conducted using a CC2420 transceiver. They studied the RSSI and the packet reception ratio (PRR) according to different receiver's directions, but with fixed distance between the transmitter and the receiver. They pointed out that the radio communication range, assessed by the RSSI, exhibits a non-spherical pattern. They also discussed the existence of a non-spherical interference range, located beyond the communication range.

The PHY layer is responsible for the reception of packets and therefore the RSSI and LQI computation that give an estimation of the link quality. However, besides its eventual asymmetric connectivity, the quality of links varies over time [Srinivasan 2010] and space [Zhou 2006] [Zhao 2003] [Reijers 2004]. In [Srinivasan 2006], authors conducted an evaluation of the RSSI and the LQI using experiments with the CC2420 radio for static sensor nodes. Their results showed that RSSI has very small variation over time for a given link. Their results also showed that when the RSSI is above the sensitivity threshold (about -87 dBm), the packet reception rate (PRR) is at least 85%. However, around this sensitivity threshold the PRR is not correlated with the RSSI due to variations in local phenomena such as noise. LQI, on the other hand, varies over a wider range over time for a given link. However, the mean LQI computed over many packets (about 120 packets) has a better correlation with PRR than the RRSI. Therefore, averaged LQI can make more precise estimates, however it decreases reactiveness and increases estimation cost.

During a packet transmission, the signal is sensitive to other signals sharing the same frequency band or to signals that use frequency bands overlapping the original signal frequency band of the IEEE 802.15.4 node. Thus, interferences and disruptions caused by other transmitting sources can occur. As we mentioned earlier, the IEEE 802.11b/g uses the same band as the IEEE 802.15.4 2.4 GHz frequency band. In [Bougard 2005], the coexistence between IEEE 802.11 and IEEE 802.15.4 is evaluated. Results highlighted the negative effect of the presence of IEEE 802.11 transmitting sources on IEEE 802.15.4 networks. In the meantime, it showed that IEEE 802.15.4 signals have no real effect on IEEE 802.11 signals.

According to [Bougard 2005], it should be at least 7 MHz offset between the operational frequencies to avoid IEEE 802.11 signal effect on IEEE 802.15.4 signals.

It is important to notice that IEEE 802.15.4 protocol does not propose an algorithm to adapt transmission power. This may be not the best way to optimize energy consumption even if the signal power is low in comparison to other transceivers [Anastasi 2009] [Francesco 2011]. The influence of the channel on energy consumption was pointed out in [Dessales 2010] using a realistic propagation channel. The BER was used to assess the radio link quality and calculate the energy per successfully transmitted bit. Results showed that gains can be obtained by adjusting the transmission power in function of the link quality.

*2.5.2. **MAC Sublayer***

One of the major characteristics of the IEEE 802.15.4 protocol is the idle and the sleep modes. These status are related to the radio (PHY layer), however, they are handled by the MAC sublayer through the synchronization mechanisms. The synchronization is ensured by sending synchronization beacons in the beacon-enabled mode, while it is defined by the application layer in the non beacon-enabled mode. There is a strong relationship between energy consumption and sleep and idle modes [Xiao 2010] [Kohvakka 2006] [Petrova 2006] [Ramakrishnan 2004] [Österlind 2008] [Dutta 2013]: the lower the duty cycle, the lower the power consumption. In [Jung 2009], a discrete time Markov chain model was used to evaluate performance under low duty cycle in terms of aggregate throughput and average power consumption per packet. It was noticed that low duty cycle saves energy at the cost of packet loss. In fact, in low duty cycles, devices are asleep for a longer period. Therefore, packets generated during this period are sent in burst when the active period resumes and even the energy is wasted because of collisions and retransmissions. A trade-off, then, exists between latency and energy consumption [Ramakrishnan 2004].

The main functionality of the MAC protocol is to provide a channel access mechanism [Lee 2006]. The IEEE 802.15.4 MAC proposes two different ways to do it: the beacon-enabled and the non beacon-enabled modes. Although, the non beacon-enabled mode is simple since there is no superframe structure (no synchronization mechanism), it is more energy consuming since nodes are always active. Thus, the beacon-enabled mode is considered to be more energy-efficient. In the case of non-beacon enabled mode, the energy saving is handled by the higher layers. In [Lu 2004], the performance of the IEEE 802.15.4 standard in terms of

throughput and energy efficiency is assessed based on simulation. Results highlighted some parameters that have an impact on the performance such as the protocol overhead, the number of communicating nodes during the CAP, the payload size, and the number of transmitted beacons. For instance, it was shown that increasing the payload size reduces the per-frame overhead while increasing throughput, and that transmitting more beacons reduces useful throughput (i.e. data payload). However, this work focused on a scenario with few nodes and low channel activity, which significantly diverges from conditions encountered in dense wireless sensor networks. In [Petrova 2006], the properties and performance of IEEE 802.15.4 were analyzed. The RSSI, the PER and the run lengths distribution (sequence of error-free packets) were analyzed through real measurements. The IEEE 802.15.4 MAC protocol was also studied using simulations. It was proved that the simulated throughput is far away from the maximum transmission capacity. Authors figured out that higher throughput can be achieved by relatively small increase in the backoff order (that is defined in subsection 2.3.5). In [Faridi 2010], another analysis of the IEEE 802.15.4 beacon-enabled MAC sublayer was carried out using a Markov chain model. It was noticed that the probability of sensing the channel free (i.e. CCA) is not constant for all the stages of the backoff procedure and varies widely from one backoff stage to another. These differences have a noticeable impact on backoff delay, packet discard probability, and power consumption. They have also shown that the probability of obtaining transmission access to the channel depends on the number of nodes that are simultaneously sensing it.

In [Anastasi 2010], Anastasi and Di Francesco studied the reliability and the energy-efficiency in multi-hop IEEE 802.15.4 wireless sensor networks. They considered several sleep/wakeup strategies and showed that the MAC parameters when their values are the default values do not provide good results in term of delivery ratio and average energy (per node and per message) and thus, the interest of tuning them. In [Zhang 2008], results showed that the CSMA/CA itself has some shortcomings and contributes to the decreased response of the system.

2.6. Summary

This section has first presented an overview of the IEEE 802.15.4/ZigBee protocol. Then, a discussion about its energy efficiency has been conducted. The main characteristic of IEEE 802.15.4 protocol is low energy consumption. Even though IEEE 802.15.4/ZigBee protocol offers mechanisms that reduce the energy consumption such as the use of the idle mode and

the low transmission signal power, the energy efficiency of the protocol has proven not to be optimized. Therefore, a state of the art of previous proposed methods that reduce energy consumption is carried out in the following section. We also present an overview of the major features that we use to conceive a global organization of communicating IEEE 802.15.4 mobile nodes namely the mobility management in wireless networks, the link quality estimation in IEEE 802.15.4 WSN and data rate adaptation in IEEE 802.15.4 WSN.

Chapter 3. **State of the art**

3.1. Introduction

We first present new approaches and algorithms that were proposed to reduce energy consumption. As in the energy efficiency study conducted in subsection 2.5, we sort them out according to the corresponding targeted layers (PHY or MAC layer). Then, we present an overview of the mobility management in IEEE 802.15.4 protocol and in some other wireless networks. We consider that routing and addressing issues (network layer) are strongly related to the topology and thus it is better to include them in the subsection that treats mobility in IEEE 802.15.4 WSN. Next, an overview of link quality estimation in IEEE 802.15.4 WSN is given. Finally, an overview of rate adaptation algorithms in IEEE 802.15.4 WSN is carried out.

3.2. Proposed approaches for reducing energy consumption

3.2.1. ***PHY Layer***

The basic features to look at when attending to propose solutions to reduce the energy consumption at the IEEE 802.15.4 PHY layer are the transmission power level and the appropriate choice of metrics to transmit to the higher layers. At the physical layer, the aim is usually to find a compromise between the strength of the signal sent and the range that can be achieved [Bougard 2005] [Dessales 2010]. Since the different nodes experience different path losses, to achieve maximum energy efficiency, they have to adapt their transmit power. The idea is, therefore, reducing the signal power when transmitting from a very short distance and/or when the channel has a good quality. In some studies, research proposed to adjust the transmission signal power according to the energy budget or the characteristic of links between each couple of sender and receiver. In [Ramakrishnan 2009] for instance, a dynamic power control at the link layer level is proposed so that power transmission is controlled based

on the received RSSI and LQI levels. Another solution based on the kind of link between central node and individual nodes was proposed in [Dessales 2010], the adjustment of the transmission power realized energy gains. In [Castagnetti 2014], authors have proposed a joint duty-cycle and transmission power management approach for energy harvesting WSN. Their global power manager is able to be dynamically adapted to the wireless channel conditions and it controls the transmission power to maintain a good link quality with the base station while minimizing energy consumption. The simulations results have shown that their global power management approach is 15% more energy efficient than a fixed transmission power system.

However, decreasing the transmit power has a cost since it may decrease the throughput [Kouyoumdjieva 2012]. In fact, when the transmission power is low, it is more vulnerable to noise and interferences. Therefore, more transmission failures may occur. In [Bougard 2005], an energy-aware radio activation policy has been proposed. The energy optimal thresholds to switch between transmit power levels was determined according to an analysis conducted based on the CC2420 transceiver parameters. However, the optimization of energy consumption at the PHY layer is proved to be insufficient if it does not come with an optimization at the MAC sublayer (such as strategies of sleep and wakeup, frame length, overhead occurred by the fields of synchronization, error detection of frames). Authors in [Dessales 2010] noticed the importance of a cross-layered approach to optimize effectively the robustness and the lifetime of WSN. However, although the cross layered approach minimizes transfer overhead by having data shared among layers; it removes all the services guarantees offered by each network layer such as security services. To overcome this shortcoming, some works [Papadimitratos 2005] [Mangharam 2007] [Vutukuru 2009] [Francesco 2011] proposed to focus on a set of layers, three layers for instance.

3.2.2. ***MAC sublayer***

The radio energy consumption is of the same order in the reception, transmission, and idle states, while the power consumption drops off at least one order of magnitude in the sleep state [Xing 2009]. Therefore, the radio should be put in sleep mode (or turned off) whenever possible. One of the most obvious solutions is then reducing the duty cycle of sensors so that they enter into sleep mode. This can be achieved thanks to the BO and the SO parameters [Kohvakka 2006] [Petrova 2006] [Neugebauer 2005] [Mirza 2005]. In [Neugebauer 2005], BOAA, a beacon order adaptation algorithm in beacon-enabled mode for star topologies is

proposed. The BO adjustment was done in accordance with the communication frequency required by the sensors based on the maximum frequency at which the most active device had sent messages. However, as it was mentioned earlier, adjusting BO and SO parameters and thus the duty-cycle has an impact on the final throughput and they need to be chosen according to the application requirements (i.e. QoS) and nodes' energy budget.

At the MAC sublayer, reducing the channel access attempts and collisions is the main focus of research. The GTS mechanism is very useful in this case. However, the procedure to assign GTSs is done during the CAP period, which disadvantages communications during this period by increasing collision probability. Besides, the CFP period is very time-sensitive; using it requires a perfect synchronization between the network nodes. However, experiments have shown that because of clock drifts this is not easy to implement [Wang 2009]. In [Mangharam 2007], the solution proposed for this issue was to use a wired external clock that synchronizes all the nodes. Their solution despite its efficiency modifies the IEEE 802.15.4 protocol. Moreover, the deployment of their solution requires an external clock which is not practical.

Synchronization of beacon reception in beacon-enabled mode is another key to decrease collision probability. This issue is even more important when dealing with nodes in a cluster-tree architecture as it will be explained later in subsection 3.3. In fact, the IEEE 802.15.4 MAC sublayer does not offer a robust mechanism to ensure time synchronization between the network nodes. In [Hanzalek 2010], authors tried to overcome this shortcoming by presenting a Time Division Cluster Scheduling (TDCS) technique for a cluster tree WSN that minimizes the energy consumption of the nodes by setting the beacon interval.

Another solution to collision is using multiple channels instead of one [Tang 2011] [Shih 2010] [Österlind 2008] [Ferreira 2007]. A packet forwarding mechanism was proposed in [Österlind 2008]. It was shown that when each transmission is performed on a dedicated radio channel (using multi-channels) the throughput can be increased since collision risk is reduced. In [Tang 2011], another MAC layer is proposed on top of the IEEE 802.15.4 PHY layer, the EM-MAC, a dynamic multichannel MAC protocol for wireless sensor networks. The EM-MAC uses multiple orthogonal radio channels. Each sender is able to accurately and dynamically predict the wake-up channel and wake-up time of receivers. The channels are chosen based on the channel conditions sensed, which enables the node to avoid sending on channels that are currently heavily loaded or that are undesirable such as due to interference or jamming. Moreover, the EM-MAC does not use a control channel, which avoids concentrating control communication on any channel. EM-MAC is therefore high energy-

efficient. However, similarly to [Mangharam 2007], it heavily modifies the IEEE 802.15.4 protocol. In [Shih 2010], an improved mechanism for channel selection was proposed. It uses the sequence of the first three channels of CAP for all communicating nodes with PAN coordinator. Nodes scan the first three channels (SF3C) in order to reduce communicating frequencies among devices and PAN coordinator in star topology. A random double hash function was used to avoid the problem of channel collisions. The channel selection is an important feature in WSN in order to reduce collisions. Results pointed out the effect of communication range on the throughput and the average delay.

Reducing energy consumption can also be achieved by selecting the appropriate values of MAC attributes. In [Kohvakka 2006], authors proposed an adaptive framework for reliable and energy-efficient data collection by collecting information from the MAC and the routing layers. It autonomously tunes the parameters of MAC protocol without requiring modification of the standard. Some of the MAC procedures can be optimized in order to reduce communications over the channel and thus reduce collisions. In [Zhang 2008], a simplification of the association procedure for reducing conflicts and the number of retransmissions was proposed. By changing the association response of the coordinator node from an indirect to a direct mode [IEEE TG 15.4 2006], they succeeded to reduce the risks of collision, the time required for association and the corresponding energy consumption.

3.3. Mobility

In this subsection, we first present the main characteristics of ad hoc and cellular networks. Then, we summarize existing approaches that handle handover in the main cellular network protocols. After that, we describe the mobility management as it is specified in the IEEE 802.15.4 protocol. Finally, we list some of the mobility models that are used in simulation.

3.3.1. ***Ad hoc networks***

The concept of Ad Hoc networks attempts to extend the concept of mobility to all the components of the mobile environment. Here, unlike cell-based communication networks, no central administration is available [Ekici 2006]. These are the mobile hosts themselves, which form an ad hoc way, a network infrastructure. No assumption is made on the size of the ad hoc network; theoretically, the network can contain thousands of mobile units. Ad hoc networks are ideal for applications characterized by the absence of a pre-existing

infrastructure. An ad hoc network is commonly called MANET (Mobile Ad hoc Network). In such environments, the units act as hosts and/or routers.

Ad hoc networks face several challenges that are mainly related to the nature of connections between the nodes. We list below the most relevant ones [Krief 2008]:

- Mobility of nodes: the topology is unstable because nodes are mobile. Therefore it is almost impossible to have a global view of the network topology that reflects the real state of the network.
- The synchronization in ad hoc networks is very difficult given that nodes can appear and disappear independently from each other, it is difficult to coordinate decisions mainly those that concern the allocation of the bandwidth.
- Limited bandwidth: this is explained by the fact that transmission in the same frequency band causes collisions.
- Unstable link capacity: besides collisions, the quality of signals is also affected by other factors such as the distance between communicating nodes and the propagation environment. The link capacity changes then over time.
- Unpredictable transmission delay.
- Variable capacity of link: in dense zones, collisions are important and cause the decrease in the available bandwidth.
- High error probability: retransmissions can even worsen the performance of the network

*3.3.2. **Mobility in cellular networks: different solutions***

Cellular networks are generally composed of two sets of separate entities:

- Fixed sites belonging to a wire-line network called base stations (BS)
- Mobile devices.

Some fixed devices (BS) are equipped with a wireless communication interface for direct communication with the mobile unit (MU) located in a limited geographical area called a cell. Each base station has a cell from which mobile units can send and receive messages via wireless link with limited bandwidth that severely reduces the amount of information exchanged as in ad hoc networks. At a given time, a mobile unit is directly connected to a unique base station. It can communicate with other sites across the base station to which it is

directly attached. All base stations are connected together via a wired communication network, generally reliable and having high throughput. The biggest advantage of cellular networks is the routing of packets between two communicating nodes as long as they do not change the cell. Unlike the ad hoc networks, the topology of cellular networks makes the number of communicating nodes easier to control, which reduces the probability of collisions and guarantee a better capacity of link.

The challenges that are facing today's cellular networks are [Akyildiz 2005]:

- Cellular network management: it is composed of many issues such as the way to set BSs so they cover large area, the way to handle synchronization and association procedures, etc.
- Energy efficiency: similarly to ad hoc networks, mobile devices do not have a high budget of energy; communications have to be optimized in order to reduce energy consumption. Moreover, scan procedure is inevitable in almost all kind of networks; this procedure is energy consuming and has to be avoided whenever possible.
- Mobility management: it is the most important issue in cellular networks. In fact, the goal of using this kind of network is to maintain a good quality of link between communicating nodes. However, when a node goes outside the coverage area of its BS, the communication is interrupted. To overcome this problem, the mobile node has to make a handover to reconnect to a new BS. In infrastructure networks, the first step of a handover is the cell reselection procedure. Many techniques of handover have been proposed for wireless communications. We list some of them below.

3.3.2.1. Mobility management in GSM [Mouly 1992]

The location area (LA) is the basic unit for location tracking. Every LA consists of base transceiver stations (BTS) that communicate with the mobile stations (MSs) over radio links. The GSM defines the mobility management protocol (MM) in order to handle all the aspects of the mobility of a node. The major task of Mobility Management is to update the location of an MS when it moves from one LA to another. The first localization procedure is called attachment to the GSM network and it is achieved when MS is turned on. The node is continuously localized thanks to the mobility management (MM) protocol. Location update procedure is referred to as registration. BTSs periodically broadcasts the corresponding LA addresses to the MSs. The mobile node starts the update of localization when it finds out that it entered a new localization area. This happens when a MS receives a LA address different

from the one stored in its memory. Then, MS has to send a registration message to the network.

Figure 12 describes the procedures of attachment and detachment between the Mobile switching center (MSC) and a mobile station (MS). In the figure, VLR stands for Visitor location register and TMSI stands for Temporary Mobile Subscriber Identity. As it is illustrated in Figure 12, the procedures of attachment/detachment (Attach_request/Attach_accept packets) are initiated by the mobile node. Each mobile node has (thanks to the periodically broadcasted packets) a list of available cells in its localization area.

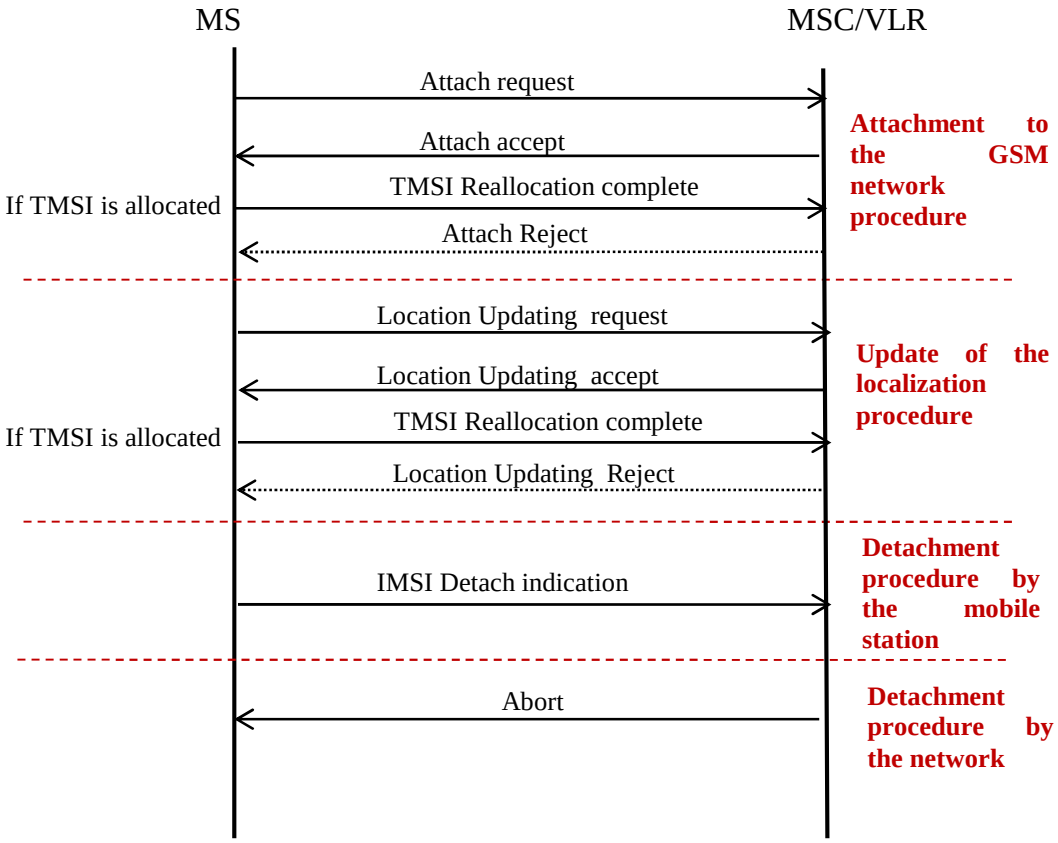

Figure 12. Attachment and detachment procedures in GSM.

3.3.2.2. Mobility management in WiMAX [Wimax]

Mobile WiMAX supports Sleep Mode and Idle Mode to enable power-efficient mobile station (MS) operation. The Sleep Mode provides flexibility for the MS to scan other base stations to collect information in order to assist handoff during the Sleep Mode.

There are three handoff methods supported within the 802.16e standard:

- (HHO)
- Fast Base Station Switching (FBSS)
- Macro Diversity Handover (MDHO).

From these methods, the HHO is mandatory while FBSS and MDHO are two optional modes.

In HHO, the communication is interrupted before beginning HO (break before make). MS stops talking to the serving BS, changes frequency and connect to the new BS. Serving BS can initiate HO procedure (by sending HO request to MS). BSs broadcast messages about neighbor BSs and their channel. BS receives this information from the backbone network. MSs request scanning interval from BS. BS during scanning buffer data incoming to MS. Association is an optional feature and may occur during scanning. The cell reselection is based either on advertisement messages or the scan periods.

When FBSS is supported, the MS and BS maintain a list of BSs that are involved in FBSS with the MS. This set is called an Active Set. In FBSS, the MS continuously monitors the base stations in the Active Set. Among the BSs in the Active Set, an Anchor BS is defined. When operating in FBSS, the MS only communicates with the Anchor BS for uplink and downlink messages. Transition from one Anchor BS to another (i.e. BS switching) is performed without invocation of explicit HO signaling messages. A FBSS handover begins with a decision by an MS to receive or transmit data from the Anchor BS that may change within the active set. The MS scans the neighbor BSs and selects those that are suitable to be included in the active set. The MS reports the selected BSs and the active set update procedure is performed by the BS and MS. The MS continuously monitors the Anchor BS based on the signal strength. An important requirement of FBSS is that the data is simultaneously transmitted to all members of an active set of BSs that are able to serve the MS.

3.3.2.3. IEEE 802.11.f (IAPP standard) [IEEE 802.11f 2003]

The principle of IEEE 802.11.f is identical to the principle of handover of the GSM and UMTS networks. The connection to an access point AP is realized in two steps:

- Authentication (pass word, WPA/WEP key, etc.)
- Association

The handover procedure is handled by the layer-2 (MAC). If a mobile node M wants to re-associate to a new access point nAP, it sends a re-association frame to nAP. The access points

watch continuously the access to the distribution system DS (a system enabling the interconnection of access points in an IEEE 802.11 network) and have to stop all activities if they lose the connection to the DS. Each new association, the AP communicates in multicasts that the other APs update their tables of correspondence: AP/mobile station.

When a node sends a re-association request to the nAP, the nAP sends to the old AP (i.e. oAP) a request to inform it. This technique presents many shortcomings, and was definitively aborted in 2006 also because manufacturers did not have the will to propose an interoperable solution that may affect their profits.

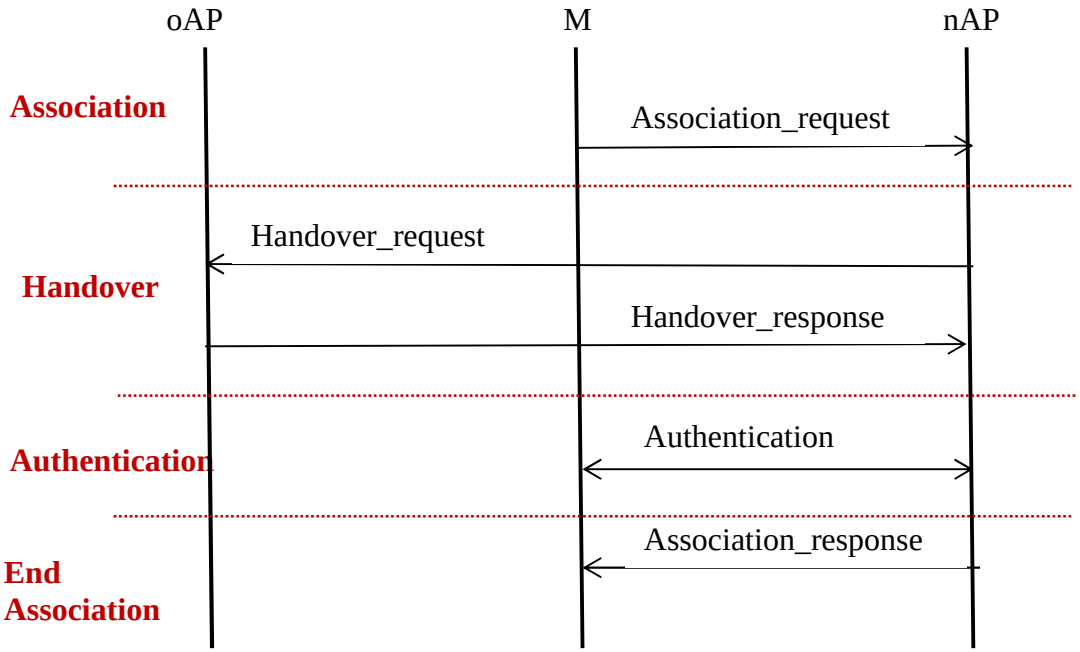

Figure 13. Handover in IEEE 802.11f

*3.3.3. **Mobility in IEEE 802.15.4***

In many wireless networks such as GSM, IEEE 802.11 and WiMAX, the procedure of reselecting cell is a layer-2 procedure (mainly the MAC sublayer) and is based on scanning periods. This supposes that a mobile node has to listen to neighbor attachment points periodically so that it updates its neighbor list. Challenges are not the same when using IEEE 802.15.4 WPAN protocol [IEEE TG 15.4 2006]. In fact, the received signal strength range is much lower, which imposes that delay of cell change must be very short. Moreover, IEEE 802.15.4/ZigBee nodes usually have less energy capacity, thus mobility management approach has to ensure low energy consumption during reselecting cell procedure.

During movement, a node can leave the coverage area of its PAN and enter a coverage area of another one. Mobility in IEEE 802.15.4 is handled in a very basic way. A loss of a coordinator of association requires an orphan scan operation during which the node looks for its current coordinator of association. This procedure is triggered if the node fails to listen to four consecutive beacons of its current coordinator. If this step fails, the node, then, begins a new association procedure by making an active or a passive scan. For each scanned channel, if a coordinator is discovered, the mobile node saves its corresponding parameters into a PAN descriptor structure. This structure contains some parameters of the beacon frame such as the PAN Id, the logical channel, the coordinator address and the link quality indicator (LQI) value of the received beacon.

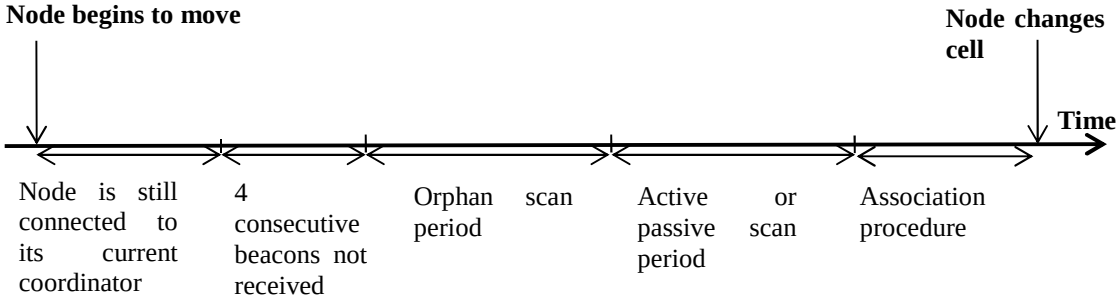

Figure 14. Mobility management in 802.15.4 standard

At the end of this scan, the node chooses a coordinator from a list of discovered coordinators for association and sends an association request (assocRqt) using the CSMA/CA protocol. As it can be seen in Figure 15, when the node receives an association request acknowledgment (Ack) from the coordinator, a macResponseWaitTime timer is set to wait for the processing of the association request. The macResponseWaitTime is a MAC attribute defined in the IEEE 802.15.4 specification as “the maximum time, in multiples of *aBaseSuperframeDuration*, a device shall wait for a response command frame to be available following a request command frame”. When this period expires, the node sends a data request command to the coordinator. Then, the coordinator sends an association response (AssocRsp). The node is considered to be associated to the PAN when an association response (AssocRsp) that contains a new network address and a status indicating a successful association is received.

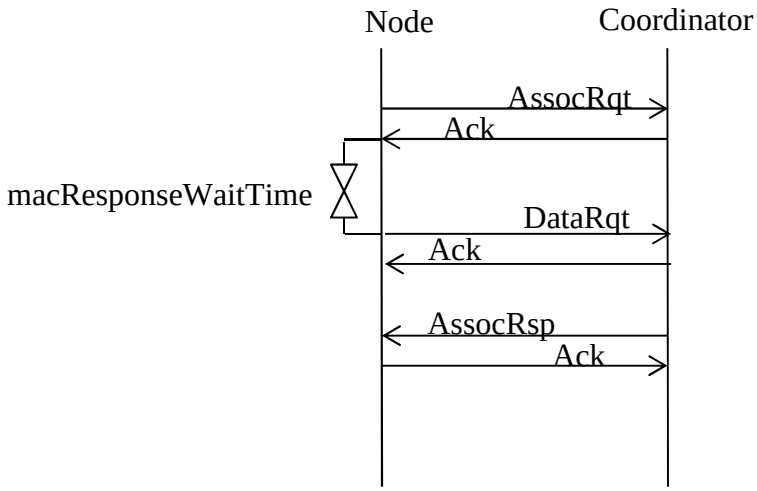

Figure 15. Association procedure in IEEE 802.15.4 standard protocol

A communication between different PANs coordinators is not possible unless they belong to the same cluster tree or if they define a common transmission channel. In both cases, the performance of the network is not optimized.

Several studies have investigated the mobility management for IEEE 802.15.4. In [Sun 2007], a comparison of the mobility was made in many kinds of IEEE 802.15.4 networks by varying some parameters, such as the type of communicating nodes, their number and their speed. This study shows that mobility is highly dependent on network topology. Moreover, network performance decreases when the number of mobile nodes is increased or when the node is moving fast. These studies do not cover the case where many coordinators are present in the same area and when each one is transmitting on a different channel. The most important aspect of the mobility management is the association procedure which is costly in terms of time and energy due to the scan phase and the mechanism of CSMA/CA [Anastasi 2011]. Authors in [Zhang 2008] show that the CSMA/CA itself has some shortcomings and contributes to the decreased response of the system. Therefore, they propose a simplification of the association procedure for reducing conflicts and the number of retransmissions. This involves changing the association response of the coordinator node from an indirect to a direct mode. The proposed method thus reduces the risks of collision, the time required for association and the corresponding energy consumption. In conclusion, the more the number of channel access is reduced, the better the mobility is managed. Extending the range of a network usually consists in using many nodes and letting them communicate via multi hop. Reducing energy consumption in the

network layer amounts to saying that routing protocol does not need to send too many control messages in order to find the appropriate route between two communicating nodes if a route breaks down (e.g. in case of mobility or if the energy budget is over). In fact, nodes energy consumption is different depending on the amount of data transmission and processing. Therefore, nodes that drain their battery first may cause a loss of connectivity in the network. In [Taha 2013], authors proposed an energy-based scheduling schema that they integrated with AODV protocol and they showed that their scheme extended the WSN lifetime. The schema achieved better packet delivery ratio. On the other hand, the fairness in network resources share was affected slightly. They proposed to integrate energy based scheduling to other routing protocols.

In [Singh 1998], authors presented a case for using new power-aware metrics that are based on battery power consumption for determining routes in wireless ad hoc networks. They evaluated the proposed shortest-cost routing algorithm and showed that it reduced the cost per packet of routing packets by 5-30% over shortest-hop routing. They pointed out that using power aware metrics in routing protocols is very beneficial because the difference in battery consumption between various nodes is reduced, which increases the network life time. They showed that larger networks have higher cost savings and that the cost savings are best at moderate network loads and negligible at very low or at very high loads. Dense networks exhibited more cost savings in general.

It is worth noticing that many studies focused on routing in ad hoc networks and proposed many routing protocols. However, the design of routing protocols for wireless mesh networks is still an active research area [Akyildiz 2005]. Designing routing protocol for mobile nodes in WSN is more complex and involves other considerations such as network architecture design and providing a mechanism for locating mobile nodes giving that the exact location of nodes is not always available to other nodes or to a base station. For instance, one has to ensure the maintaining of the connectivity so that each node remains within the range of at least some other nodes [Cassandras 2005].

Previous studies have shown that using multi hop increases the probability of losing synchronization frame between the different nodes [Koubaa 2008]. In [Ferreira 2007], authors investigated the possibility of extending the network and reducing channel access conflict by using multi frequencies in the same network. However, the mobility case was not considered.

Mobility is not handled efficiently in the IEEE 802.15.4/ZigBee protocol. In [Anastasi 2011], an evaluation of mobility for the IEEE 802.15.4/ZigBee protocol was carried out. A

comparison between the mesh and the cluster-tree networks was done. Results showed that the performance of the network significantly decrease when the number of mobile nodes increases or when their speed increases (speed between 1 m/s and 5 m/s). Results also highlighted that the mesh topology is more efficient than the cluster tree topology in mobility use cases.

Performance also changes according to the topology. Table 4 summarizes the main characteristics of the topologies proposed by the standard.

Table 4 Topologies characteristics

Topology	Characteristics
Star	The network is more energy-efficient The extension of the network is limited
Mesh	Mobility has more important impact on RFD Routers are robust (no explicit need to change address). Routers do not send periodically beacons. Network extension is possible
Tree	Use of hierarchical addressing The mobility of a router causes an address changing of all the nodes that are associated to the router Routers can use beacons Network extension is possible

Many research studied mobility in IEEE 802.15.4 sensor networks and different mobility use cases were evaluated. Evaluations concerned mainly the movement of nodes [Abbagnale 2009] [Vlajic 2011] [Koubaa 2008], nature of mobile nodes (whether they are routers or end devices) [Braem 2010] [Nia-Chiang 2006] or network architecture [Braem 2010]. For instance, in [Nia-Chiang 2006], authors are interested in ZigBee mesh network and precisely in the impact of the nature of mobile nodes (routers or end devices). They indicate that the ZigBee mesh routing algorithm exhibits significant performance difference when the number of reduced functional devices (RFD) is highly different from the number of full functional devices (FFD) in the network. Routing performance in ZigBee network does degrade when the network includes an increasing number of ZigBee end devices. In [Vlajic 2011], the purpose of the study is the evaluation of deployment of path-constrained mobility of sinks.

*3.3.4. **Mobility models***

Using mobility models to define mobility scenarios of nodes is necessary to handle the complexity of setting movements of multiple nodes in simulation scenarios. In addition to that, it allows having scenarios that approaches real cases. Thus, the chosen mobility model has to fit the targeted application.

3.3.4.1. Random waypoint model (RWP)

It is the most simplistic and common mobility model. Destination positions are determined randomly and selected speed is uniformly distributed between a minimum and a maximum value. The minimum speed, the maximum speed and the maximum pause time periods are the parameters that can be tuned.

3.3.4.2. Gauss-Markov mobility model (GM) [Camp 2002]

In this mobility model, two parameters are updated in each period to determine the next destination position. These parameters are the speed and the movement direction. They are chosen from a normal distribution of previous values.

3.3.4.3. Manhattan Mobility Model (MHT) [ETSI 1998]

The Manhattan mobility model is proposed to model movement in an urban area. In the Manhattan model, a mobile node is allowed to move along the horizontal or vertical streets of an urban map. At an intersection, the mobile node can turn left, right or go straight. Figure 16 shows node movements according to this model. TurnProb is the probability that a node changes its current street. The velocity of a mobile node at a time slot is dependent on its velocity at the previous time slot. Also, a node velocity is limited by the velocity of the node preceding it on the same lane of the street.

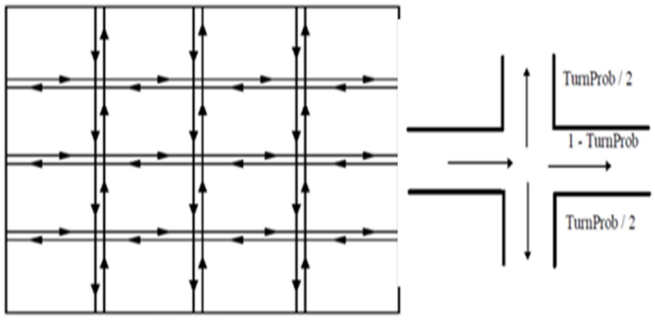

Figure 16. Manhattan mobility model

3.4. Link Quality Estimation

The link quality estimation is an important feature that is useful in many protocol decisions (e.g. handover, rate selection, transmitted power strength, routing, packet retransmission technique [Jamieson 2007] [Srinivasan 2008], packet recovery [Jamieson 2007], etc.). The accuracy of estimating the status of the transmitting channel at a given time is related to the parameters to consider. However, high accuracy is not easy to guarantee since there are many parameters that characterize the channel and that are difficult to assess.

We highlight below the most relevant parameters that impact the rate adaptation algorithm. Then, we present the most relevant link quality estimators.

3.4.1. ***Considered parameters***

3.4.1.1. Sensor-related constraints

Sensors are small devices that are basically designed to be autonomous and usually working on battery. Thus, the main issue when designing sensor network applications is the energy consumption. Application designers have also to consider hardware limitations (e.g. memory, computing limitations).

Therefore, our solution should limit computation requirements and has to consider the energy budget of mobile nodes.

3.4.1.2. Signal power vs. bit rate

If the SNR exceeds a defined threshold the transmit power could be decreased to reduce energy consumption instead of increasing the bit rate. On the other hand, if the transmit power is low; a rate adaptation algorithm may decrease the network performance or may even be not feasible. In IEEE 802.15.4, the maximum transmit power does not usually exceed 0 dBm. In [Lanzisera 2009a], authors used a power amplifier to transmit at 5 dBm. They showed that according to their experiments varying the data rate leads to greater energy savings.

A tradeoff between the transmit power and the bit rate has to be done in order to optimize the energy consumption.

3.4.1.3. Coherence time

The main issue that impacts the quality of link estimation is the coherence time which is approximately the duration over which fading effects remain the same. Thus, during the

coherence time, the channel disruptions effects are assessed static. In mobile networks, the coherence time is strongly related to the communicating nodes' mobility. In fact, if the Doppler spread in frequency due to mobility is equal to f, then the coherence time of the channel is roughly equal to 0.4/f [Tse 2005]. However, it is not easy to estimate since channel model cannot be known accurately.

In mobility scenarios, coherence time is too short. Our rate adaptation algorithm should be therefore very responsive.

3.4.1.4. Packet interval vs. bit rate

The IEEE 802.15.4 slotted CSMA-CA protocol requires that the sender makes two Clear Channel Assessments (CCAs) before transmitting a packet. If a packet transmission fails, the sender has to wait for a random backoff period before resuming the packet transmission. CSMA-CA mechanism does not take into consideration coherence time, if the channel conditions during retries are still the same or worse, successive failures occur and latency is increased. Network performance would improve if the packet interval depends on the time coherence of the channel. If the interval is too small compared to the coherence time, packet error rate will be high and vice-versa. The packet interval management may also involve the application layer. However, since backoff parameter is a MAC-layer parameter, designing a PHY-aware MAC layer would give extra information to handle packet interval more efficiently. Srinivasan et al. [Srinivasan 2008] proposed a new metric: the β-factor to adjust backoff periods according to channel conditions. In order to increase the reception ratio, they used an opportune transmission approach. The node transmits one packet each defined time interval. However, if the link is bursty, the node transmits packets until one packet failure occurs. In this case, the node stops the transmission. Then, it resumes it at the start of the next interval.

3.4.1.5. Packet size vs. link quality estimation

The IEEE 802.11b standard uses the DSSS spreading technique. Studying the rate adaptation algorithms used for IEEE 802.11b networks may help us to figure out how we can adapt rate in an IEEE 802.15.4 network.

In IEEE 802.11b standard, the size of the frame was proven to be enough to give good link quality estimation. However, the maximum packet size in IEEE 802.15.4 protocol is 133 Bytes (266 PN-Codes). Even if the rate in IEEE 802.15.4 is much lower than the 802.11b bit

rates (1, 2, 5.5 and 11 Mbits/s), we have to check if the packet size is large enough to get accurate information about the channel. Besides, in SoftPHY hint [Vutukuru 2009] for instance, a collision detection mechanism was proposed. Only the packet portions without errors caused by interferences were considered in the computation of the estimated BER. We should investigate whether it is possible to eliminate errors caused by interferences in IEEE 802.15.4 packets when estimating the link quality. At this phase of the study packet size seems not too important since what matters is the time required to transmit a packet. Some previous works consolidate this assumption. In [Heinzer 2012], a correlation between the chip error rate and the packet reception ratio was demonstrated. In [Wu 2010b], Wu et al. analyzed the chip error patterns of IEEE 802.15.4 packets in two different scenarios: attenuation and mobility. Based on their study, we can verify that chip error patterns depend on the cause of occurred errors within the received data stream. However, in [Wu 2010b], the combined effect of mobility and attenuation was not studied and the synchronization phase analysis was ignored.

3.4.2. ***Overview of link quality estimators***

In this subsection, we present the most relevant link quality estimators that were proposed to estimate the quality of IEEE 802.15.4 links.

3.4.2.1. Link estimation in the CC2420 RF transceiver

The CC2420 is a 2.4 GHz IEEE 802.15.4 compliant RF transceiver designed for low-power and low-voltage wireless applications. It is widely utilized in sensor networks. It uses the Chip Correlation Indicator (CCI) also referred to as Link Quality Indicator (LQI) to give an estimation of the link quality during the packet transmission time. Its datasheet specifies that soft decisions are used in the correlator, and that the average correlator output for 8 symbols from the preamble are averaged to calculate LQI.

3.4.2.2. β factor [Srinivasan 2008]

This factor is used as a metric to measure the link burstiness (i.e. links stable in the short term). The β factor assesses if losses happen in burst or almost equally distributed based on conditional probability delivery functions (CPDFs). CPDFs are derived from packet delivery traces of received and non-received packets. Here are some notations used to define the β factor:

- The conditional packet delivery function C(n) is the probability that a packet will be received after n successive successful transmissions if n > 0 or after n successive failures if n < 0.
- Independent losses: the probability of reception is independent of any history.
- Ideal bursty link: the link is ideal if {C(n>0) = 1 and C(n<0) = 0}
- Kantorovich-Wasserstein (KW) distance: the average of the absolute differences of a link from an ideal bursty link.

In order to introduce the β factor formula, let us consider Figure 17 as an example. The distances e_1 – e_6 are the distances between the CPDF elements of the example link and the CPDF elements of the ideal bursty link. The distances i_1 – i_6 are the distances between the CPDF elements of the corresponding independent link and the CPDF elements of the ideal bursty link.

In this example β formula is as follows:

$$\beta = \text{mean}\,(i_1,..,i_6) - \text{mean}\,(e_1,..,e_6) \,/ \text{mean}\,(i_1,..,i_6) \tag{17}$$

In general,

$$\beta = (KW(I) - KW(E)) \,/\, KW(I) \tag{18}$$

Where KW() is the distance from the ideal bursty link, E is the CPDF of the empirical link, and I is the CPDF of an independent link with the same PRR.

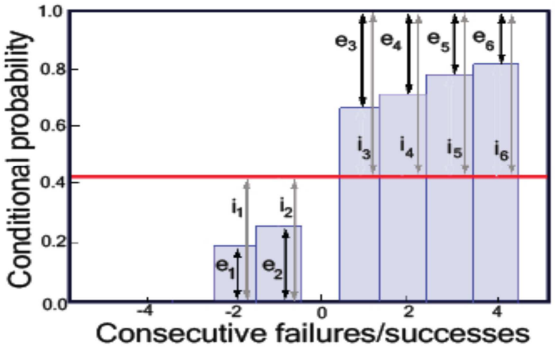

Figure 17. Conditional probability [Srinivasan 2008]

A perfectly bursty link has a β =1, while a link with independent deliveries has a β =0. Negative β values are permitted. This happens when there is a negative correlation in packet

reception: as more packets are received the next packet is more likely to fail and as more packets are lost the next packet is more likely to be received.

The study in [Srinivasan 2008] showed the effects of time (the interval between packets affects the reception ratio distribution) and frequency (channel selection). Over shorter periods, links have a higher chance of being perfect or non-existent. Over longer periods, the chance of being intermediate increases. Authors demonstrated that their method improved PRR, the end-to-end path routes and minimize the route cost.

3.4.2.3. SoftPHY interface [Vutukuru 2009]

SoftPHY is an expanded physical layer interface that provides PHY-independent hints to higher layers about the PHY's confidence in each bit it decodes. BER is computed using per-bit confidences referred to as SoftPHY hints [Jamieson 2007]. The estimated BER is interference-free. The method allows the receiver to estimate the BER even using a frame that was received with no errors. For each packet transmission, the average BER is calculated based on the average bit error probability over all packet bits. The bit error probability p_k is calculated based on:

- x_k (k = 1 .. N): the input bits to the encoder of the sender.
- r: the received signal input to the decoder of the receiver.
- The output of the decoder at the receiver is log likelihood ratio (LLR) for each received bit (i.e. formula given in (6)).
- The decoded output bit yk (formula given in (7))
- s_k: the softPHY hint of the bit k.

$$sk = |\mathrm{LLR}(k)| \tag{19}$$

The probability p_k of error of a bit k is determined as follows

$$pk = \frac{1}{1+ e^{sk}} \tag{20}$$

The average BER of the channel during the packet transmission is the average p_k over all bits of the frame.

Interferences are detected as sudden jumps in BER. The collision detection algorithm is calculated as follows:

Let S be the number of symbols per frame. Each symbol contains N_{bps} bits, for a total of N = N_{bps} x S bits per packet. p_k is computed for each bit k = 1 … N. p_k is averaged N_{bps} at a time for each symbol j to obtain p_j.

$$Avg(pj) = \frac{1}{Nbps} \sum_{i=1}^{Nbps} pi + (j - 1).Nbps \quad (21)$$

The collision detection algorithm is a simple threshold on the difference d_j defined as:

$$d_j = |avg(p_j) - avg(p_{j-1})| \quad (22)$$

The algorithm detects interferences that start after the receiver has synchronized.

Note that, in addition to BER estimation, SoftPhy proposes a postamble scheme [Jamieson 2007] to recover data even when the packet preamble is corrupted and not decodable at the receiver. In order to recover symbol losses, Jamieson et al. defined a threshold η that allows the identification of the packet portions to be retransmitted. In fact, if the hamming distance of a symbol is above the η threshold, misclassification of correct and incorrect symbols is high. In experiments, hard decision decoder (HDD) was used. Results showed that when the preamble is received correctly, the threshold η is under 2.

3.4.2.4. Chip error based link quality estimator [Heinzer 2012]

In [Heinzer 2012], the correlation between chip errors and PRR was investigated. Only the symbols received after the synchronization were considered. It was demonstrated that for many environments, there is a clear correlation between the chip error rate per symbols (CEPS) and the PRR for the whole range of PRR values between 0 and 1 in all scenarios: the higher the PRR, the lower the chip errors per symbols. Even links with a PRR lower than 10% do not exhibits more than 2 CEPSs. This is because when too many chip errors occur in the preamble or the start of frame delimiter, the receiver does not succeed to synchronize and the packet is simply ignored.

Heinzer et al. tried to determine if the burstiness of chip errors is a useful indicator for the PRR. The β factor [Srinivasan 2008] was applied to chips instead of packet losses. No way was found to correlate the chip β-factor to the PRR in an accurate form. Even the combination of the chip β-factor and the chip errors per symbols in each packet did not exhibit an improvement compared to the case where only the chip errors per symbol is used as a link quality indicator.

The model proposed is a Geometric Linear Model defined as follows:

$$PRR_{\text{CEPS}} = \begin{cases} 0 & if\ Avg(CEPS) > Chiplimit \\ 1 - \frac{Avg(CEPS)}{Chiplimit} & if\ 0 \leq Avg(CEPS) \leq\ Chiplimit \end{cases} \quad (23)$$

In order to compute the Avg(CEPS), only symbols that have the most chip errors were considered (e.g. 10%). Authors showed that already four symbols provide an estimate close to the estimation obtained by considering the whole payload. This study proved to be more accurate than SRN-based estimators especially in mobile scenarios.

Before choosing the rate selection algorithm it is important to have an accurate estimation of the link quality. Table 5 gives an overview of link estimators used in the literature. Each one relies on a specific metric(s) (the input of the link estimators) and requires different number of received packets. Link quality estimation efficiency strongly depends on whether nodes are mobile or not. This fact will be detailed in the next sections. Thus, the table also specifies whether the mobility is considered. Moreover, there is a major constraint when investigating link quality estimator techniques. The best way to do it would be through experiments. However, for large scale networks this may not be possible to realize. This is the reason why simulations are widely used instead.

Good link quality estimation requires an accurate and responsive method. In [Srinivasan 2008], Srinivasan et al. demonstrated that the conditional probability of packets is an accurate estimation. However, their method requires the analysis of many packets. Moreover, this method may not be suitable in case of mobility since the coherence time when nodes are mobile is short. In [Heinzer 2012], authors tried to find a correlation between the packet reception ratio (PRR) and the chip errors per symbols (CEPS). They proposed a geometric linear model to estimates the PRR given the chip error rate per symbol. However, they only considered the correctly received packets.

Using the RSSI or the LQI to characterize the channel is proved to be sufficient in some previous rate adaptation techniques [Lanzisera 2009a]. LQI and RSSI are calculated based on the 8 first symbols following the start of frame delimiter (SFD). However, the coherence time of the channel in some strong noisy environment is too short, thus RSSI and LQI values could not give all the information about the channel changes during the whole packet transmission period.

Table 5. Overview of link quality estimators

Method	Input parameter(s)	Method	Required number of packets	Protocol	Mobile scenario	Evaluation tool
DRACER [Lanzisera 2009a]	Signal strength or Chip Correlation	Thresholded LQI or SNR	1 packet (133B, 15 min interval)	IEEE 802.15.4 3 rates are added	No	Simulation (not specified)
LA in Body Network [Martelli 2011]	Signal strength	Estimation of the SNR and the (probabilistic) SIR.	1 packet (beacon) (transmit power 0 dBm)	IEEE 802.15.4 3 rates are added	Small move-ment of the body	Simulator written in C
β-factor [Srinivasan 2008]	Packet statistics	conditional probability delivery functions (CPDFs)	More than 1 packet	IEEE 802.15.4 IEEE 802.11b [802.11]	No	CC2420 [CC2420] + TinyOS [TinyOS]
SoftPHY [Vutukuru 2009]	BER free-interference	log likelihood ratio (LLR) for each received bit	1 packet Calibration of the thresholds	IEEE 802.11 ACK frame modified	Yes	NS-3 [NS-3] PHY layer replaced by traces collected from software radio experiments
CEPS [Heinzer 2012]	Chip errors	Geometric Linear Model	1 Packet	IEEE 802.15.4	Yes	USRP2 [USRP] + RFX2400 daughterboard [RFX]

3.5. Rate adaptation in IEEE 802.15.4

Optimizing the throughput through adjusting the transmission bit rate of mobile sensor nodes according to the channel conditions can considerably increase the network QoS since it optimizes the use of the superframe. Rate adaptation is composed of two major stages that are the link quality estimation and the selection of the bit rate. There are many parameters that can characterize the quality of link; most of them are determined by the physical layer. Based on the physical layer link estimation, the MAC layer has to determine the most suitable physical layer bit rate for the outgoing frames. In WLAN networks (e.g. IEEE 802.11), several rate adaptation methods were proposed [Biaz 2008]. Some of WPAN sensor protocols

offered multiple rates such as the cc2500 transceiver protocol [CC2500]. However, they did not propose a mechanism for rate adaptation. Moreover, these protocols are proprietary.

In this subsection, we list the available rates in IEEE 802.15.4 2.4 GHz frequency band and the most relevant rate adaptation algorithms for IEEE 802.15.4.

3.5.1. ***Available rates in IEEE 802.15.4***

So far, rate adaptation has not been thoroughly investigated in IEEE 802.15.4/ZigBee sensor networks mainly because sensor protocols do not offer multiple rates. In IEEE 802.15.4 2.4 GHz frequency band, the bit rate is 250 Kbps. However, previous studies [Mehta 2012] [Lanzisera 2009a] [Martelli 2011] demonstrated the feasibility of having three additional rates for IEEE 802.15.4: 500 kbps, 1 Mbps and 2 Mbps. These rates are obtained by modifying the chip mapping of symbols in the DSSS modulation. Thus, if the channel conditions are good, using fewer chips per symbol may increase the rate without decreasing the signal quality and without changing much of the hardware design. The proposal suggested that the number of chips per symbol should be variable (16, 8 or 4 chips per symbols). Therefore, for each rate, a chip mapping is defined. Table 6 gives the different numbers of chips per symbols, their corresponding bit rate, and the corresponding symbol period.

Table 6 Available rates

Rate	Chips per symbol	Bit rate	Symbol Period
1	32	250 Kb/s	16 µs
2	16	500 Kb/s	8 µs
4	8	1 Mb/s	4 µs
8	4	2 Mb/s	2 µs

As it can be seen in Annex D, the IEEE 802.15.4 standard specifies a synchronization header in the PPDU frame consisting of a preamble followed by a two-symbol start of frame delimiter (SFD). Three SFDs are added to denote the three additional data rates. The SFDs specify the rate at which the PHY payload is sent [Lanzisera 2009a] [Mehta 2012]. In fact, the defined protocol standard preamble is not changed and it always corresponds to the protocol standard data rate. The preamble and the start of frame delimiter (SFD) are always sent at the standard rate (250 Kbps) whatever the data rate used. When a packet is being received, the physical layer recognizes the current data rate of the incoming packet by checking the value

of its SFD. Based on this value, the appropriate detection scheme is used to decode to PHY payload. The speed of electronics is higher than the transmission data rate; therefore, changing the code set between symbols is not a concern.

3.5.2. ***Overview of proposed rate adaptation algorithms for IEEE 802.15.4***

Rate adaptation techniques are either a function of packet delivery ratio (PDR) [Lacage 2004] or a function of signal strength [Holland 2001] or a combination of both of them (hybrid algorithms) [Lanzisera 2009a] [Martelli 2011]. Both methods in [Vutukuru 2009] and [Srinivasan 2008] try to estimate the link quality by removing interferences that distort the estimation. The proposed SoftRate algorithm in [Vutukuru 2009] was based on the estimation of interference-free BER. The method proposed in [Srinivasan 2008] was based on the estimation of SNR and signal-to-interference ratio (SIR).

3.5.2.1. The SoftRate Algorithm [Vutukuru 2009]

The SoftRate receiver uses SoftPHY hints that were introduced in subsection 3.4.2 to compute the average BER for each received frame, employing a heuristic to detect and excise portions of the frame subject to strong interference. The SoftRate receiver then sends the interference-free BER estimate to the sender in a link-layer feedback frame. At the sender's link layer, the SoftRate algorithm uses the per-frame BER feedback to pick the best transmit bit rate for the next frame. To ensure reliable delivery of feedback, SoftRate always sends its link-layer feedback frame at the lowest available bit rate in a "reserved" time slot, much like 802.11 link-layer ACKs. Feedback is sent whether or not the frame was in error, as long as the frame's preamble and header are decoded correctly. To correctly determine the identities of the sender and receiver even when the frame has an error, link-layer headers are protected with a separate CRC. If the frame has no errors, then the BER feedback is one component of the link-layer ACK. SoftRate protocol incurs a little extra overhead compared to existing protocols: a CRC in the link-layer Header and a BER measurement in the link-layer ACK.

The SoftRate algorithm uses a heuristic to predict channel BER at a few other bit rates using the BER estimate at one bit rate. The algorithm is divided into three phases. In the first phase, it uses a heuristic to predict channel BER at a few other bit rates using the BER estimate at one bit rate. In the second phase, the algorithm computes optimal thresholds α_i and β_i for each rate R_i such that, when the BER at rate R_i is in the range (α_i , β_i), then R_i is the optimal transmit bit rate. The computation of optimal thresholds is based on the observation that BER

at a given SNR is at least a factor of 10 higher than BER of the next-lower bit rate. The computation of these thresholds depends on the link layer's error recovery mechanism. It is a configurable parameter depending on experiments. In the third phase, given interference-free BER estimate from the receiver and optimal thresholds at each bit rate, the SoftRate sender adjusts its bit rate.

The sender increases the rate if the most recent estimate free-interference BER b_i of the current rate R_i is such that $b_i < \alpha_i$. And it lower the rate if $b_i > \beta_i$.

3.5.2.2. IEEE 802.15.4 DRACER [Lanzisera 2009a]

The DRACER rate adaption algorithm is based either on the LQI or the SNR predefined thresholds. In case of packet transmission failure (no ACK), four different backoff schemes were evaluated:

- Backoff scheme A: The transmitter continues to send at a higher data rate until it is successful, with no reduction in rate.
- Backoff scheme B: Upon a packet failure, the transmitter drops down one data rate and transmits at that rate until receiving an ACK.
- Backoff scheme C: The transmitter drops to the standard IEEE 802.15.4 data rate (i.e. 250 kbps) upon a single packet failure.
- Backoff scheme D: The transmitter reduces the transmit rate one step for each packet failure until it hits the legacy 802.15.4 rate.

Results showed that the DRACER rate adaptation algorithm reduces average network energy consumption. Moreover, results are better when the LQI metric is used to define thresholds. The energy saving was up to 41% when the LQI thresholding and the backoff scheme D were used.

3.5.2.3. Link adaptation in body area networks [Martelli 2011]

The proposed rate selection algorithm is based on SNR and signal-to-interference ratio (SIR). From the measure of the received beacon power, each node estimates the SNR: if the estimated SNR is below a threshold Th_{SNR}, the node decrements its bit rate. Otherwise it estimates the SIR through the evaluation of a failure probability, denoted as P_F which is the probability that a packet is not received by the coordinator. This probability is given by the ratio between the number of unacknowledged packets (i.e., packets for which the ACK is not received) and the number of packets sent on the channel (including retransmissions):

$$P_F = \frac{Not\ received\ ACK}{sent\ packets} \quad (24)$$

P_F is evaluated over a window of 20 superframes. If P_F is above a defined threshold Th_{PF}, the node is in a situation where many of its packets are lost and, since the channel quality is good (high SNR), these losses are due to interference. Thus, in this case the bit rate is incremented, in order to reduce the packet transmission time and the probability of collision. If $P_F < Th_{PF}$ the node does not change the current bit rate.

3.6. Summary

In this section, we have presented an overview of the main issues that have been addressed during this thesis. First, we have summarized the approaches proposed to reduce energy at the PHY and MAC layers. We have been interested in the properties that are related to the protocol specification (e.g. signal strength, node active periods, CSMA-CA protocol). Then, we have pointed out that unlike some other wireless protocols (GSM, WiMAX, IEEE 802.11f), the IEEE 802.15.4 does not include an efficient mobility management policy. Moreover, mobility impact in IEEE 802.15.4 varies depending on the network architecture and the mobility characteristics of IEEE 802.15.4/ZigBee nodes. After that, we have noted that the link quality estimation depends on many parameters that are not only related to the hardware design and the channel characteristics (e.g. noise, interferences) but also to the application characteristics (e.g. packet interval, mobility). Therefore, link quality estimators are various. Table 5 summarizes some of the most relevant link quality estimators that were proposed for IEEE 802.15.4 links. It gives the parameters that each estimator takes into account, the required packet number for the estimation, the used evaluation tool and it indicates whether or not the node mobility has been considered in the evaluation. Finally, we introduced the rate adaptation feature in IEEE 802.15.4 protocol. It is a fairly new feature that offers many new possibilities to enhance network performance and reduce the energy consumption. However, it also raises new issues such as the accurate link quality estimation and the selection of the appropriate bit rate.

The state of the art conducted during this chapter has contributed in the work presented in [Courtay 2010].

In the next section, we start by proposing a global network architecture then an enhanced mobility management approach in order to reduce the energy consumption and the delay related to the mobility of IEEE 802.15.4/ZigBee sensor node.

Chapter 4. An Enhanced Mobility Management Approach for IEEE 802.15.4 protocol

4.1. Introduction

The first purpose of our study is to propose a solution that reduces the cost of IEEE802.15.4/ZigBee sensor nodes' mobility and that maintains communication between mobile devices. The proposed mobility management strategy has to take into account the small energy budget of sensor nodes. Our study examines both the energy of the communicating device itself and the monitoring of all network devices in an optimized network topology. The mobility cost in terms of energy and delay is related to the network topology. An efficient mobility management approach has to be aware of the network topology or at least of some of its characteristics (e.g. anchor nodes, end devices or coordinators, etc.). Our study is in the scope of the 2.4 GHz PHY layer since it uses the unlicensed ISM frequency band and offers 16 channels. In order to optimize the performance of our proposed approach, we first propose a global network architecture that makes use of the beacon-enabled mode. Then, we propose and evaluate a new approach that anticipates the link disruption between a mobile node and its coordinator based on the LQI. After validating the efficiency of using LQI metric in our approach, we introduce and evaluate a new formula for the LQI threshold. The new mobility management approach uses a speculative algorithm that predicts the new coordinator of association. We conduct several simulations in order to evaluate our approach for different mobility models. We also verify the efficiency of our approach in a noisy environment. Afterwards, we study the impact of modifying the speculative algorithm on the global performance of the network.

4.2. Proposed network architecture

The proposed architecture should be in compliance with the following pre-established requirements:

- End devices can be mobile inside the network coverage area.
- Our approach has to reduce as much as possible the non-disruption of a communication when changing coordinator.
- The protocol should offer a routing protocol and an addressing mode that take account of the changings in the network (mainly caused by the mobility of nodes).
- The protocol has to be adapted according to the mobility cases in order to handle the association and the dissassociation of end devices to and from the base stations.

4.2.1. ***Network topology***

Sensor nodes use the idle mode in order to reduce the energy consumption. The most optimized configuration is when nodes only wake up (i.e. turn the RF transceiver on) when they have to send or to receive packets. This implies that nodes have to be synchronized. The IEEE 802.15.4 beacon enabled mode is, thus, used for communication between end devices and the corresponding coordinators. The use of the beacon enabled mode requires the use of a star or a cluster tree topology. In both topologies, a node wishing to transmit a message to another node has to first transmit to its coordinator which handles the transmission to the destination node. In a cluster tree topology, each cluster has its own coordinator and its unique PAN ID. All clusters of a same network use the same transmission channel. Given that the cluster tree topology guarantees the possibility to enlarge the network coverage area, it is retained in our approach.

Our study mainly focuses on end devices that use IEEE 802.15.4 protocol given its energy consumption characteristics. However, the communication between other eventual types of nodes may use another protocol. In order to reduce interferences and optimize the use of the superframe, we choose to connect the coordinators via a wired protocol.

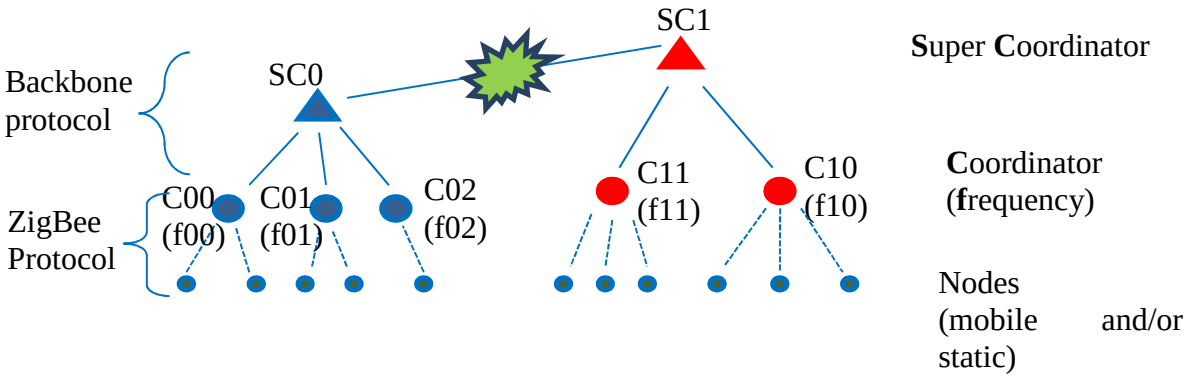

Figure 18. Network Organization

Figure 18 shows the topology of the proposed network. We define three types of nodes:

- Mobile end devices: the objective is to reduce the energy consumption of these devices as we assume they are power supplied by an energy harvesting system. They are RFD nodes.
- Static coordinator: they are on power supply and their energy consumption is not a constraint. They are FFD nodes.
- SuperCoordinator: this special coordinator is added in order to wire connect all coordinators. It is an FFD node responsible for the initiation of the network and of the address attribution. This is important since our approach is required to be centralized and since mobile nodes do not have to make energy consuming decisions.

We assume SuperCoordinators are connected using a backbone network (e.g. internet).

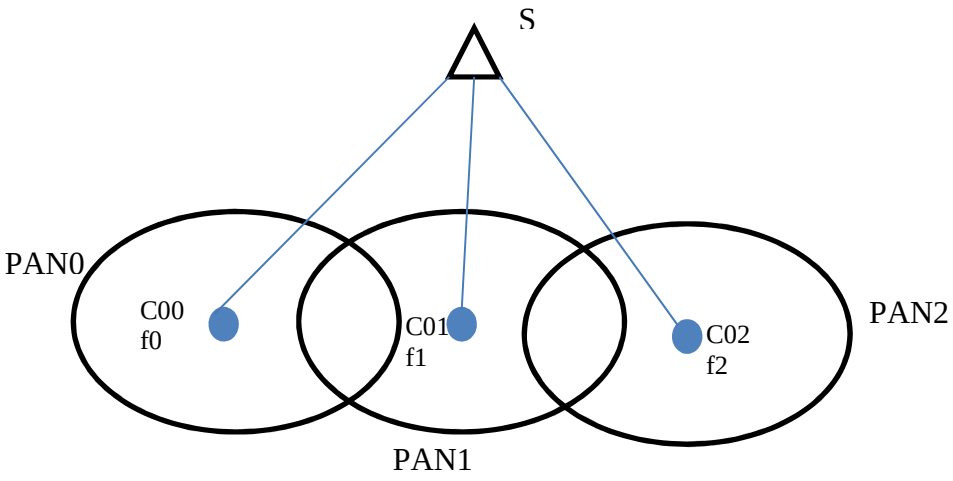

Figure 19. Proposed network topology

A coordinator is initialized when the SuperCoordinator attributes to it an address and a channel on which it has to communicate. Each coordinator is responsible for initiating and maintaining a PAN independently defined by a unique PAN identifier (PAN id) and an operating frequency fi, as it is illustrated in Figure 19. The adjacent cells have to ensure that they have different operating channel frequencies. The SuperCoordinator may have an IEEE 802.15.4 interface and be a coordinator. In this case, it may permit association for end devices. The communication between SuperCoordinators is out of the scope of this study. We name road a set of geographically aligned coordinators.

*4.2.2. **Addressing and routing***

The used addressing mode is the hierarchical addressing in order to optimize the routing procedure. So far, it has been noticed that the hierarchical addressing mode is not suitable when nodes are moving. One of the benefits of using a SuperCoordinator is to overcome this issue.

4.3. Simulation tools and general simulation setup

The choice of the appropriate network simulator is crucial. In fact, there are many available simulators. However, the modeling of the protocol layers and the available modules vary from one simulator to another. The choice of the simulator has to consider the following requirements:

- Open source: so we can implement new algorithms.
- IEEE 802.15.4 beacon-enabled mode: Synchronization is required in our study and packets have to be send according to the slotted CSMA-CA algorithm.
- IEEE 802.15.4 Association procedure: This requirement is crucial since we need to assess the cost of cell change (i.e. loss or end of synchronization with a coordinator and re-association with a new one) in order to determine the efficiency of our approach.
- Mobility support: It is obvious that the node location at a given time has an impact on the quality of link (e.g. attenuation due to path loss). Besides, node's coordinator of association is chosen based on parameters that are strongly dependent on the node location at a given time.
- Hierarchical addressing and routing: Our global network architecture is a cluster tree network that uses the hierarchical addressing and routing methods.

- LQI computation: Although the standard does not present a formula for computing LQI, it gives some instructions to interpret the definition so one proposes a formula compliant with the specification (e.g. LQI is computed based on the RSSI or SNR or both of them). As it is detailed in the following parts of this section, LQI estimation is required in our work.
- Channel modeling: In order to obtain accurate link estimation and thus accurate evaluation results, the channel modeling has to include propagation models. It also has to consider interferences and errors induced by noise. The granularity of processed information impacts the accuracy of the channel transmission. The biggest granularity is the whole packet whereas the finest granularity is the bit. However, the finest the granularity, the longest the simulation run time is.

Table 7 shows whether these requirements are available in three free network simulators: NS-2 [NS-2], OMNET++ [OMNET] and WSNet [WSNet]. In addition to that, it gives enlightenment on some characteristics of each simulator.

Table 7. Network simulators

	NS-2	OMNET++	WSNet
Open source	**Yes**	**Yes**	**Yes**
IEEE 802.15.4 beacon-enabled mode	**Yes**	**Yes**	No: A very important work is required in order to implement this procedure.
Association procedure	**Yes**: The implementation is accurate and compliant with the standard.	No: A very important work is required in order to implement this procedure.	No: A very important work is required in order to implement this procedure.
Mobility support	**Yes**	**Yes**	**Yes**
Hierarchical addressing and routing	**Yes**: An extension is available [Zbr Routing].	No: A considerable implementation effort has to be made in order to implement these algorithms.	No: A very important work is required in order to implement these algorithms.
LQI computation	**Yes** Formula based on the SNR and the RSSI	No It is possible to implement the formula	No It is possible to implement the formula

Channel modelling	Acceptable: Based on the analysis of the whole packet. Interferences are considered. Propagation models are available. Possibility of injecting errors within the packet.	Acceptable: Based the analysis of the whole packet. Interferences are considered. Propagation models are available. Possibility of injecting errors within the packet.	**Accurate**: Possible BER for each byte in a packet. Interferences are considered. Propagation models are available. Possibility of injecting errors within the packet.

The lack of an accurate network simulator modeling is the first challenge that confronts us. A tradeoff has to be made depending on the modules availability and modification cost of the source code. It is also important to notice that accurate modeling implies an increase of simulation run time.

Based on Table 7 we choose the NS-2 simulator. The LQI is computed in NS-2 using the SNR and the signal strength power. It is an integer that varies from 128 to 255. Of course, we have had to modify the IEEE 802.15.4 implementation. The main changes than have been made to it are:

- Adding the hierarchical addressing and routing [Zbr Routing]
- A mechanism of assigning addresses and frequencies in accordance to the network architecture
- A heterogeneous routing mechanism that handles IEEE 802.15.4 and Ethernet protocols.
- Modifying the implementation of the CSMA-CA protocol so it can handle some additional cases that are related to the change of cell procedures.
- Implementing our proposed mobility management approach
- Implementing an additive white Gaussian noise generator into the NS-2 simulator.
- The main difficulty in modeling an accurate AWGN is the faithful representation of the normal distribution $N(0,\sigma)$ that has zero mean and a standard deviation σ. We use the Box-Muller transform [Box 1958] which is an efficient method for generating normally distributed random numbers. Since most pseudorandom number generators output uniformly or nearly-uniformly distributed values, it is commonly used in combination with the pseudorandom number generators to create normally distributed values, which are useful in simulation data sets with known mean (average) and variance.

- In order to generate mobility scenarios, we use the BonnMotion tool [Aschenbruck 2010].

We base our energy consumption evaluation on the CC2420 RF transceiver specification [CC2420].

Table 8 gives the power consumption values of the CC2420 transceiver and Table 9 provides the common simulation setup of the current section (i.e. Chapter 4).

Table 8 CC2420 energy consumption values [CC2420]

RF transceiver	CC2420
Transmission power	0 dBm
Supply Voltage (V)	1.8
Consumption during the transmission (W)	0.03132
Consumption during the reception (W)	0.03384
Idle (W)	0.0007668

Table 9 Common simulation setup for the mobility management approach

BI (no inactive period)	245.76 ms
Distance between two consecutive coordinators	25 m
Routing protocol	ZigBee Routing (zbr) [Zbr Routing]
RF transceiver	CC2420
Transmission power	0 dBm
Propagation model	Two-ray-ground [Fonseca 1996]

4.4. Energy consumption in the standard procedure

Table 10 gives the energy consumption for a mobile node moving on a straight line from a coordinator C1 to coordinator C2 spaced of 25 meters. It can be seen that the energy consumption related to the scan periods are very important in comparison with the association procedure itself. It can be deduced that if we reduce the energy consumption during the first two stages of the change of cell, the energy consumed would significantly drop.

Table 10 Energy consumption Evaluation of the standard procedure

	Orphan Scan	Active Scan	Association Procedure

Energy consumption (10^{-3} J)	7,534	3,995	0,774

Sensor devices may contain, depending on their application field a localization system. It is often assumed that a GPS tracking system within a sensor node has an accuracy of at least 5 meters [Guglielmo 2012]. However, this assumption is not reliable for wireless sensor networks because of the short range of sensor nodes. Another approach proposed in [Polastre 2004] consisted in providing a limited number of nodes with GPS (anchor nodes) and helping other nodes to find their position using anchor nodes. In [Lee 2010], authors presented an IP mobility performance enhancement using an appropriate IEEE 802.16 L2 trigger based on an ARIMA prediction model. Signal strength is predicted either through scanning of neighbor base stations (BS) or from periodic serving BS measurement. However, signal strength prediction is achieved without any assumption on the statistical properties of the nodes' movement. Their method aims at reducing handover latency and packet drops. Although obtained results have demonstrated their efficiency, their method still requires that mobile nodes listen to neighbor attachment points. Our purpose is to avoid scan periods during cell change procedures in order to reduce both energy consumption and latency.

If a mobile node knows the geographical distribution of coordinators it would start directly the association procedure just after locating the superframe boundaries without making expensive scan procedures. However, mobile devices in our global organization should not take decisions in order to save energy. Therefore, it is the role of coordinators and the SuperCoordinator to handle their association to the network. Moreover, coordinators are related to each other via the SuperCoordinator that has a full knowledge of the coordinator locations. Therefore, the Supercoordinator can choose the most appropriate next coordinator in the case of each mobile end device. In our approach, the Supercoordinator determines the next coordinator identifier, its address and its related frequency channel.

In the remainder of this section, we detail our mobility management approach starting by the handover procedure in subsection 4.5. We then show in subsection 4.6 that anticipating the link disruption and selecting the appropriate coordinator reduces energy as well as packet delivery latency. Afterwards, we propose two mechanisms: the first one handles the link quality estimation and is detailed in subsection 4.7; the second one is a speculative algorithm that predicts the next coordinator of association (subsections 4.6.2, 4.8 and 4.9).

4.5. Handover procedure

The Figure 20 illustrates how messages are exchanged between a mobile node and coordinators during an enhanced change of cell. When a mobile node M receives a beacon frame or a data packet with an LQI lower than a threshold denoted $LQI_{threshold}$, it informs its coordinator C1 by sending to it an LQI notification (lqiNot) message. This frame contains the LQI value of the last received beacon. If the lqiNot is successfully received by C1, it has first to acknowledge the request of the mobile node. If the maximum number of lqiNot frame sending attempts is reached (fixed to four attempts in our case) without receiving the acknowledgment frame (Ack), it is considered that the mobile node has left the coverage area of its current coordinator. Then the node has to begin an active scan. If the acknowledgment is received, the mobile node M sets a *macResponseWaitTime* timer to wait for the response from its coordinator C1. After sending the acknowledgment, C1 sends a handover request (HRqt) to the SuperCoordinator SC which chooses the new PAN of association.

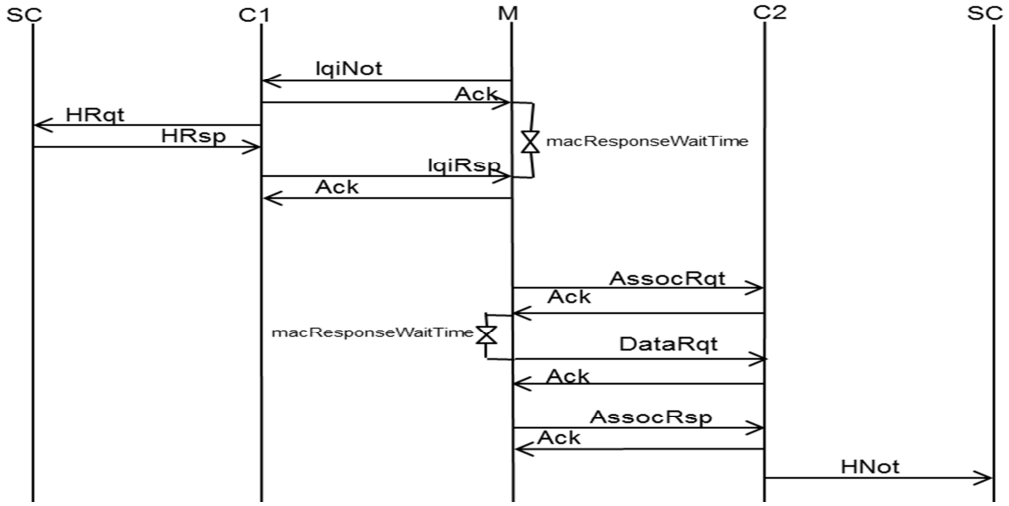

Figure 20. Changing cell procedure

The choice of the next coordinator is based on a speculative algorithm performed by the SC. SC answers C1 with a handOver frame (HRsp) containing the new association PAN Id, the address of the next coordinator (C2), as well as the next logic channel identifier. Then, the coordinator C1 sends to the mobile node M an LQI response (lqiRsp) frame which contains the information sent by SC. The mobile node M starts, after locating the C2 superframe boundaries, an association procedure to synchronize with C2. The association procedure is not modified compared to the standard IEEE 802.15.4 protocol. If the association procedure ends successfully, C2 sends a handover notification (HNot) to SC that contains the new address of

the corresponding mobile node. However, if the procedure fails at any of these steps, the IEEE 802.15.4 standard procedure will be performed starting with an active scan. Note that the orphan scan is no longer performed.

4.6. Efficiency of using LQI in mobility management

In this subsection, we first evaluate the use of an $LQI_{threshold}$ by varying its value. The evaluation has been conducted in terms of the cell change procedure success rate, the energy consumption and the latency for mobile end devices. The procedure of changing cell is considered to be successful if all nodes do not perform a scan during changing cell procedure.

4.6.1. ***Network architecture and initialization***

The algorithm of selection of a new coordinator is based on the knowledge of the geographical distribution of coordinators. In Figure 21 for instance, there are four sets of geographically aligned coordinator, thus four roads. The initialization of coordinators is organized according to their geographical location so that coordinators belonging to the same road (e.g. r1 in Figure 21) have successive addresses. To avoid the case where the SuperCoordinator attributes to an end device an address that is between two-coordinator addresses, coordinators addresses are attributed decreasingly starting from the highest hierarchical address attributed to the first initialized coordinator, to the lowest address attributed to the last initialized coordinator in the network coordinators.

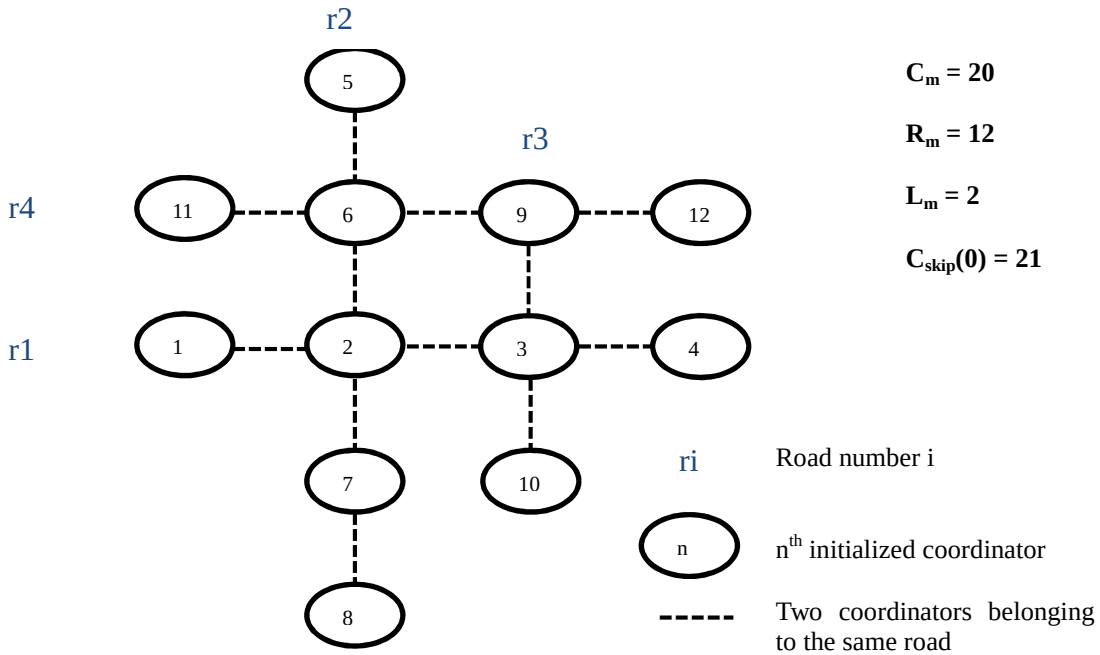

Figure 21. A multi-road network

The address attribution method implies that the last coordinator of a road I must be initialized before the first coordinator of the road I+1. In the example illustrated on Figure 21, the address of the node 5 of r2 has a lower address than its predecessor node 4 of r1. If a coordinator from a road I+1 has already an address because it belongs to another road (e.g node 2 in Figure 21), the first address is preserved. Let A_0 be the address of the SuperCoordinator and A_n be the n^{th} initialized coordinator. Addresses are given according to (26) by n'of (25). (26) is obtained by replacing n in (16) of subsection 2.4.3.2.

$$n' = R_m - n \tag{25}$$

$$A_n = A_0 + C_{skip}(0) * (n' - 1) + 1 \tag{26}$$

n' corresponds then to the n^{th} initialized coordinator

Let Rt_m be the maximum number of roads in the network. An R_m-by-Rt_m *Nt* matrix is used by the SuperCoordinator to describe the network in order to choose the new coordinator of association. Columns of the *Nt* matrix are roads that form the network.

$$Nt[i,j] = \begin{cases} n & if\ the\ n^{th}\ coordinator\ exists \\ 0 & otherwise \end{cases} \tag{27}$$

*4.6.2. **Selection of the new coordinator***

Our speculative algorithm favors the movement of nodes on the same road. By default, it is supposed that nodes move from the coordinator having the highest hierarchical address to the coordinator having the lowest hierarchical address. The choice of the coordinator is based on the previous coordinator of association and on the current road of a mobile node. If the address of the previous coordinator is higher than the address of the current coordinator, the direction of movement is supposed to be changed. Let *hist* be a vector containing the *n* value of the previous coordinator of association of each mobile node M. Let *rd* be a vector that corresponds to the current road of a mobile M. The *hist* and *rd* vectors are updated at the end of each new successful association (HNot frame in Figure 20). The choice of the next coordinator of association is done according to the *Nt* matrix. *Nt[i,j]* corresponds to the entry of the *Nt* matrix that refers to position *i* of the current coordinator of M in the current road *j*. The corresponding pseudo code for this algorithm can be described as follows:

```
j = rd[M]
If (hist[M] == Nt[i+1,j] and hist[M] != 0 and i >=1)
        Then   return Nt[i-1,j]
Else if Nt[i+1,j]!= 0
        Then   return Nt[i+1,j]                    // e.g at the first cell changing
Else
        return Nt[i-1,j]                           // e.g the last coordinator of a road
End If
```

*4.6.3. **Simulation use cases***

The $LQI_{threshold}$ and mobile nodes speed have been varied in two different use cases. In the studied networks, the SuperCoordinator does neither send beacon frames nor permit mobile nodes association. The mobile node speed varies from 1 to 7 m/s. Nodes are considered to be in an ideal environment, without noise and where the signal is only affected by the distance and interferences caused by transmitting nodes that are present in the network. We start our

evaluation with a single-road use case (Figure 22) where mobile nodes are configured to correctly choose association coordinators. Then, we evaluate a multi-road use case (Figure 21). We examine the cell change success rate procedure in both use cases. Afterwards, we evaluate the efficiency of our approach in terms of energy and delay.

4.6.3.1. Single-road use case

As illustrated in the Figure 22, in this use case the network is composed of one SuperCoordinator (node 0), three aligned coordinators (nodes 2, 3 and 13 in red), and 12 mobile end devices (in green color). The corresponding *Nt* matrix for this single road use case is the following:

$$Nt^{-1} = (1\ \ 2\ \ 3\ \ 0\ \ \ldots\ 0)$$

Mobile nodes move in the coverage area of the three coordinators following a straight trajectory. Before nodes start to move, all of them are associated and LQI value of each received packet is the highest value (255). In this study, the simulation duration has been fixed to 300 seconds. $LQI_{threshold}$ is varied from 127 to 250. All nodes move only once. Nodes initially associated to C13 moves to the C3 coverage area. Nodes initially associated to C3 moves to the C13 area. Nodes initially associated to C2 moves to the area of C3. The next coordinator of association is, then, properly chosen. As a consequence, the failure of the procedure is only due to packet loss. The Figure 23 presents results of the successful rate of changing cell procedure depending on $LQI_{threshold}$ and on the speed value *Vi* which is equal to *i* m/s. Based on these results, we consider that the $LQI_{threshold}$ values can be classified into three zones whatever the speed of the node.

- *Zone 1*: The mobile node is close to the next coordinator. Therefore, synchronization with its current coordinator may be lost before the $LQI_{threshold}$ is reached. Moreover, in this case, if the $LQI_{threshold}$ is reached, the lqiNot and the lqiRsp frames may not be successfully received. The success rate decreases when the speed increases.

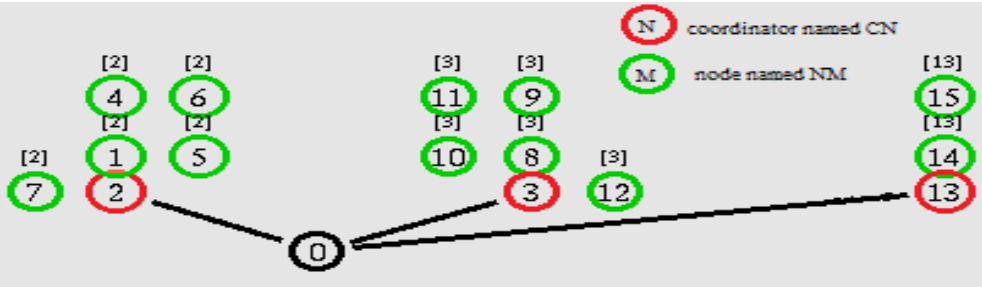

Figure 22. Single road use case for different $LQI_{threshold}$

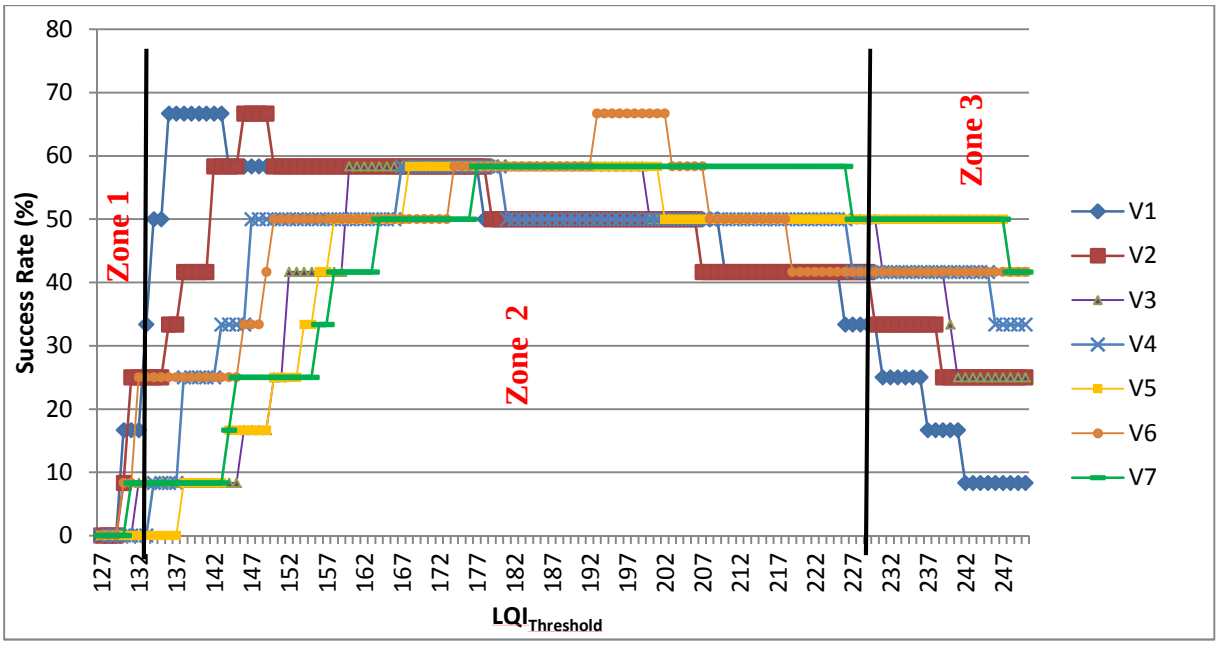

Figure 23. Success rate vs. $LQI_{threshold}$ and speed

- *Zone 2*: A mobile node is close enough to its current coordinator when it communicates with it. The probability that lqiNot and lqiRsp frames are successfully received is better than in the zone 1. At the receipt of lqiRsp, a node may be enough close to the next coordinator to communicate with it. When $LQI_{threshold}$ is between 164 and 206, the success rate is greater to 50% whatever the speed.
- *Zone 3*: The node is close to its current coordinator. The probability that lqiNot and the lqiRsp frames are successfully received is higher than in the first zone. However, since the node is close to its current coordinator, messages related to the association procedure (with the new coordinator) may not be successfully received. In this zone, the success rate increases when the node speed decreases.

4.6.3.2. Multi-road use case:

The geographical organization of the multi-road use case is described on the Figure 21. The network is composed of one SuperCoordinator (node 0), 12 coordinators and 7 mobile nodes (nodes 13, 14, 15, 16, 18 and 19). The SuperCoordinator and the mobiles nodes are not shown on the Figure 21. The Coordinators are grouped into 4 roads (r1, r2, r3 and r4). The

corresponding *Nt* matrix for this multi roads use case is the following (only the first 5 representative lines of the matrix are presented):

$$Nt = \begin{pmatrix} 1 & 5 & 9 & 11 \\ 2 & 6 & 3 & 6 \\ 3 & 2 & 10 & 9 \\ 4 & 7 & 0 & 12 \\ 0 & 8 & 0 & 0 \end{pmatrix}$$

All mobiles nodes are associated before they start to move. The simulation lasts 400 seconds. Mobile nodes randomly start moving 70 seconds after the beginning of the simulation. As in the single road use case, we have performed simulations in order to determine the successful rate of changing cell for mobile nodes having different speeds. The $LQI_{threshold}$ is set to values going from 165 to 195. This corresponds to the zone 2 previously mentioned.

As shown in Figure 24, the successful rate of changing cell procedures is lower than in the first case. However, this result was expected because nodes move randomly and the geographical organization of the network is more complex. Nevertheless, it can be observed that even in this complex use case, the successful rate may be up to 40% for a speed of 5m/s.

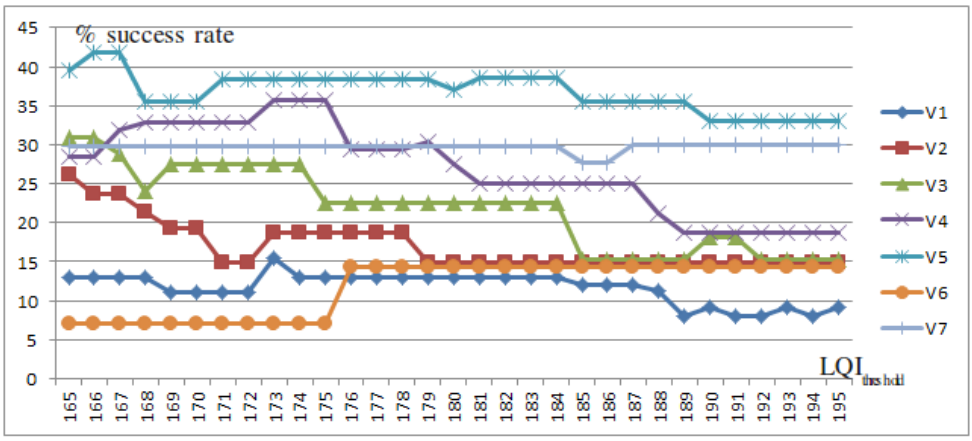

Figure 24. Success rate vs. $LQI_{threshold}$ and speed

4.6.4. Gain in energy and delay for both scenarios

In our enhanced changing cell approach, the optimization of energy consumption of mobile nodes is based on the LQI metric. The objective of the approach is to reduce the energy consumption and changing cell delay in comparison with the original IEEE 802.15.4 protocol. The delay of a changing cell procedure is calculated from the time a node receives the last beacon to the time that it is successfully associated to a new coordinator. Let the initial node

energy be the energy when a node sends an lqiNot or when it begins to make a scan just after a beacon receipt. The energy consumption of a node is the difference between the initial energy and the final energy corresponding to the energy at the end of the procedure. Figure 25 and Figure 26 respectively show the gains in energy and delay obtained using our approach. SI corresponds to the mobile nodes speed value I m/s. For each speed and all $LQI_{threshold}$ values, both the average energy consumption and the average delay for all changing cell procedures are computed. In the Single-road scenario $LQI_{threshold}$ varies from 127 to 250 and in the Multi-road scenario $LQI_{threshold}$ varies from 165 to 195.

As it can be observed, in the single-road use case, our new approach reduces up to 70.42% the average energy consumption of mobile nodes while the average delay can be decreased up to 73.9%.

In the multi-road use case, results show that we can reduce the average energy consumption of mobile nodes up to 58.17% as well as the average delay up to 49.75%. Of course, in a multi-road configuration, the probability of success for changing cell is lower than in the single road use case. In fact, although the number of mobile nodes is reduced (6 instead 12), nodes are moving randomly over a longer duration. As a consequence, the probability that they access the medium simultaneously is greater, thus increasing the number of collisions and backoff periods. Moreover, the probability to get a wrong next coordinator of association (i.e. wrong next coordinator in the lqiRsp frame) is increased.

When a node only moves from a coordinator zone to a neighbor coordinator one, the changing cell procedure will certainly successfully end by the association of the mobile node to the coordinator. In this case, if the mobile node’s speed is high, it will be faster within the new coordinator area. Thus, changing cell procedure delay and consumption average energy will be lower. As a consequence, the gain in energy and delay is higher when the speed is higher. However, when it enters within a coverage area of many coordinators while moving at a high speed, the node may begin a changing cell procedure with a coordinator and then leave its coverage area before the end of the procedure. In this case, the gain in energy and delay is higher when the speed is lower as obtained in the second use case.

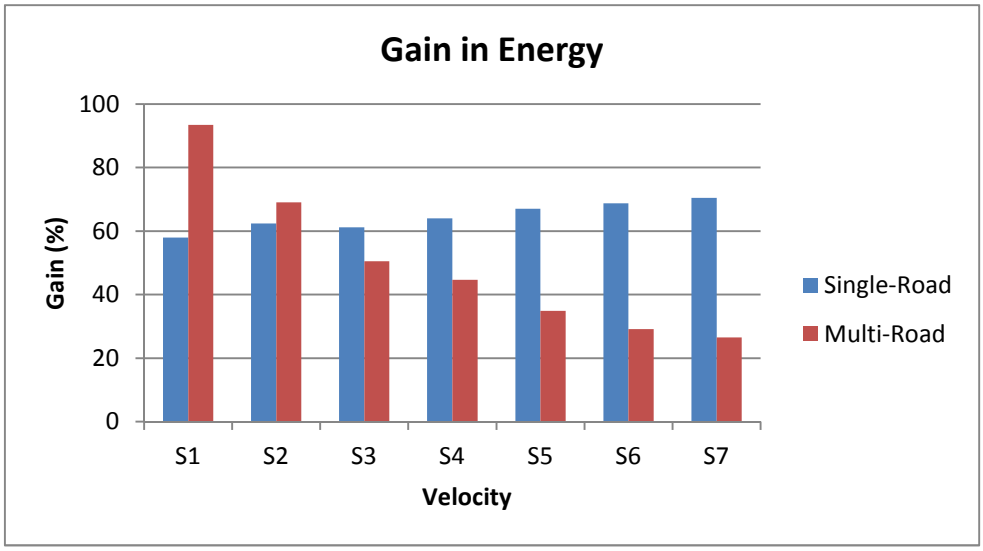

Figure 25. Energy gain for the Single-road and the Multi-road use cases in comparison to the standard

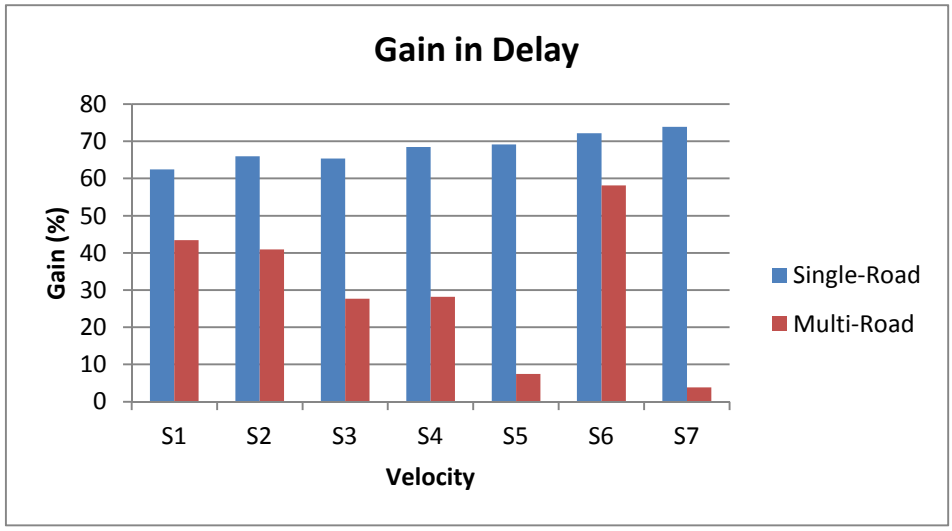

Figure 26. Energy gain for the Single-road and the Multi-road use cases in comparison to the standard

4.7. An $LQI_{threshold}$ formula for mobility management

In the subsection 4.5, we have presented a new approach for mobility management for IEEE 802.15.4/ZigBee mobile nodes in a cluster tree topology. Simulations in subsection 4.6 have demonstrated that anticipating the cell change before the loss of connection coupled with the right selection of the next coordinator reduces the energy consumption average of mobile nodes. It has also been boosted that the link quality has an important impact on the

performance of our approach. In consequence, $LQI_{threshold}$ has to be adjusted according to the channel conditions. A connection between the mobility behavior of nodes and our mobility management approach efficiency has been figured out by varying speed of nodes and simulation use cases. Therefore, we examine our approach efficiency for the Manhattan and the random waypoint mobility models.

In the previous evaluation, the $LQI_{threshold}$ was a constant value identical for all nodes. In this subsection, we propose a formula to compute $LQI_{threshold}$.

4.7.1. $LQI_{threshold}$ *formula*

In IEEE 802.15.4 beacon-enabled mode, end devices are periodically receiving beacon messages. Cases where LQI decreases due to interferences during the beacon time slot are ignored since all associated nodes are not allowed to transmit. Thus, for a defined level of noise, the LQI of a beacon packet depends only on the distance between the sender and the receiver. However, during the contention access period (CAP) the LQI may depend on interferences caused by communicating nodes.

As it can be observed in Figure 27, when a node is moving through a coordinator (C) coverage area, it can be associated to C after a scan period and/or an association procedure. As soon as M receives an association response from C, an LQI_{init} based on the first received beacon frame is stored. A handover procedure is started as soon as the LQI of a received packet is less than an $LQI_{threshold}$. The time when the handover procedure must be started, i.e. the $LQI_{threshold}$ choice, has to be determined carefully, neither too early nor too late.

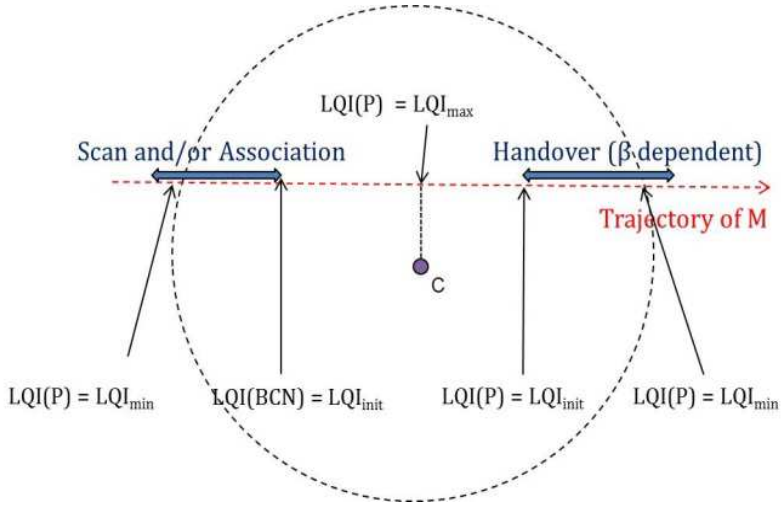

Figure 27. LQI value during node movement through a cell

As illustrated in Figure 27, during the association procedure, packets can be exchanged between a mobile node and its coordinator. During this interval, these packets have an LQI lower than LQI_{init} and higher than LQI_{min} in all cases. It can be concluded that the $LQI_{threshold}$ has to be within this interval and it must also take into consideration some network parameters that can have an impact on LQI. Parameters that can be also included to determine $LQI_{threshold}$ value are the number of end devices in the cluster, the number of transmitting nodes, the distance from the coordinator, the node velocity, etc.

So far, only the distance and the velocity of mobile nodes have been taken into account. The proposed formula to compute the $LQI_{threshold}$ is as follows:

$$LQI_{threshold} = LQI_{init} - (LQI_{init} - LQI_{min}) / \beta \quad (28)$$

Where LQI_{min} is a constant and $\beta \geq 1$.

Note that LQI_{min} is RF transceiver dependent. It can be noticed from (4.7-1) that the higher β is, the earlier the handover procedure is started (and vice-versa). In Figure 27 only a straight trajectory is represented for M. In fact, a mobile node may have any other trajectory.

4.7.2. ***Impact of β parameter***

We conduct some experiments in order to evaluate the impact of β in the $LQI_{Threshold}$ computation. In this use case, coordinators form a grid as shown in Figure 28. The mobile end devices' number and the β parameter value have been varied and the average total energy that is consumed during cell reselection procedures has been computed. Results are given in Figure 29. So far, this average energy has only corresponded to the power required by the RF transceiver.

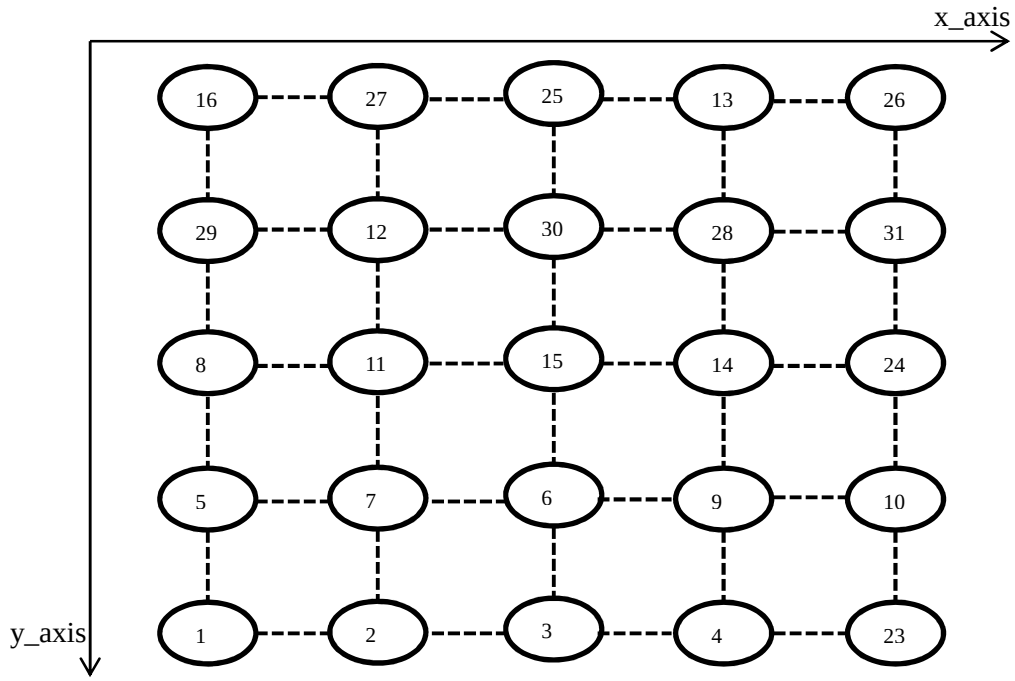

Figure 28. Coordinators in the grid architecture

Figure 29(a) presents results for the random waypoint mobility model, while Figure 29(b) provides results obtained using the Manhattan model. As simulations have been done with NS-2 simulator, LQI_{min} is equal to 128 and LQI_{max} is equal to 255. The communication channel is considered to be without noise and interferers. Simulation duration is 2400 seconds and other setup parameters are specified in Table 11. Manhattan *TurnProb* parameter is set to 0.2, meaning that a node has a 0.2 probability to change its current road (i.e. to turn left or right). It is important to note that in this case, energy consumption in cell reselection procedures may also be due to errors of the speculative algorithm. To eliminate the influence of this kind of errors, we have varied the velocity of a mobile node M that goes back and forth between the two extremities of a grid road. The next coordinator of association of M should then be correctly chosen each time. There are 24 other mobile nodes (plus node M) that move randomly during the simulation period. The success rate is computed for each velocity value given a β value. Figure 30 presents the percentage of handover success rate according to different node velocity values as well as different choices of β value. The results highlight that the success rate decreases when the velocity increases. Combining the average energy (Figure 29) and the success rate metrics (Figure 30), a β value of 2 represents a good tradeoff.

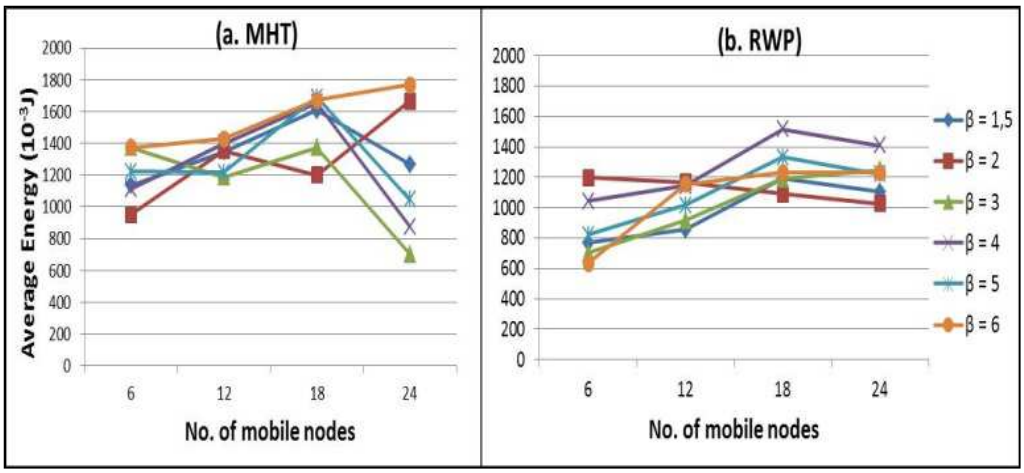

Figure 29. Energy spent in cell reselection procedures for different β values

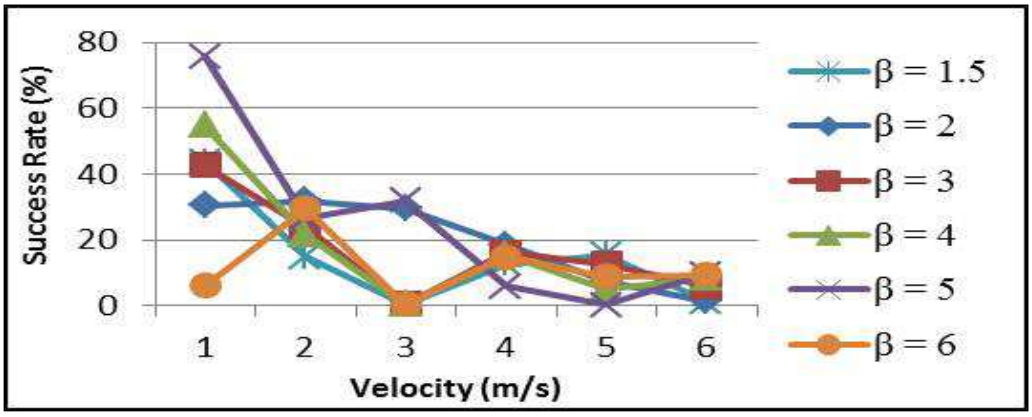

Figure 30. Success rate Vs. Velocity of node for different β values

4.8. Same-road speculative algorithm

The first speculative algorithm that has been introduced in subsection 4.6.2 favors the movement of nodes on the same road. In 4.6.2, the initialization of coordinators was organized in relation to their geographical positions and coordinators belonging to the same road had to be sequentially initialized so that they have successive addresses. Each road in the previous proposed speculative algorithm was therefore represented by a column in the *Nt* matrix. A shortcoming of this organization is that some roads may not be explicitly represented. This is for instance the case when all coordinators of a road are already initialized in previous defined roads. As a consequence, in this case, some handover procedures will fail. In this subsection, we propose a new matrix structure without constraints on the initialization time of coordinators. Columns of the new matrix describe vertical roads and its rows describe

horizontal roads of the grid. The matrix is then a purely spatial representation of the network topology. This organization of the matrix allows an easier and more efficient management of mobility.

The choice of the next coordinator of association for a mobile node is based on the previous coordinator of association and on its current road. A default road corresponds to the horizontal road containing the coordinator of association. A default direction is also defined and corresponds to the x_axis (Figure 28) vector for nodes moving on horizontal roads, and to the y_axis vector for those moving on vertical roads. If the previous coordinator is situated on the left of the current coordinator, then the next coordinator will be the coordinator which is on the right of the current one (and vice-versa). Of course, in mobility scenarios, nodes can turn left or right; which leads to some wrong selections of the next coordinator. A network matrix (*Nt* Matrix) in the SuperCoordinator is used to describe the geographical distribution of coordinators.

Let *rd* be a vector of size N that corresponds to the current road of a mobile M. We use the vector *hist* of size N that contains the value of the previous coordinator of association for each mobile node M. The *hist* and *rd* vectors are located in the SuperCoordinator which updates them at the end of each new successful association. The position of the current coordinator in the matrix is determined based on two attributes which are the current road of the mobile and the position of the coordinator in the matrix (*pos*). The enhanced algorithm of selecting the new coordinator is defined as follows:

```
road = rd[M]

If (road isVertical)
        If (hist[M] == Nt[pos+1,road] and hist[M] != 0 and pos ≥ 1)
                Then  return Nt[pos-1,road]
        Else If (Nt[pos+1,road] != 0)
                Then   return Nt[pos+1,road]                  // e.g. at the first cell changing
        Else
                return Nt[pos-1,road]                         //e.g. the last coordinator of a road
```

```
        End If
Else //horizontal movement
        If (hist[M] == Nt[road,pos+1] and hist[M] != 0 and pos ≥ 1 and Nt[road,pos+1] != 0)
                Then   return Nt[road,pos-1]
        Else If (pos ≥ 1 and Nt[road,pos-1] != 0)
                Then return Nt[road,pos+1]                    // e.g. at the first cell changing
        Else
                return Nt[road,pos-1]                         //e.g. the last coordinator of a road
        End If
End If
```

*4.8.1. **Simulation setup***

Coordinators are organized according to the grid architecture shown in Figure 40. In simulation scenarios, all nodes are already associated before they begin to move. For each mobility model scenario, all end devices are mobile and their number is varied. We use the simulation setup given in Table 9. Table 11 gives the remainder setup parameters for all mobility scenarios evaluated in this subsection.

Table 11 Simulation setup

Parameter	Definition	Value
Xdim (m)	Size of the grid on x-axis	100
Ydim (m)	Size of the grid on y-axis	100
N	Number of coordinators per road	5
Duration (s)	Duration of the mobility scenario	300
speedChangeProb	Probability for the mobile to change its speed	0.2
minSpeed (m/s)	Mobile's minimum speed	0.5
meanSpeed (m/s)	Mobile's mean speed	3.0
pauseProb	Probability for the mobile to pause	0

4.8.2. ***Evaluation of the proposed approach***

In this subsection, some parameters of mobility models are varied in order to study their impact on the node energy consumption and the cell reselection delay.

4.8.2.1. Impact of mobility model on network performance

Different simulations have been performed in order to figure out the performance of the network in term of energy and cell change delay when nodes are moving according to one of the three different mobility models: the random waypoint (RWP), the gauss-markov (GM) and the Manhattan (MHT). In these simulations, nodes do not have pause periods. The turn probability (*TurnProb*) in Manhattan mobility model scenarios is set to 0.2. The number of moving nodes has been varied from 6 to 30 with a step of 6. Figure 31 shows the average energy (Figure 31 (a)) and the average delay (Figure 31 (b)) for the three different mobility models when using the standard mobility management procedure as defined in IEEE 802.15.4 protocol. Average gain in energy and delay when using our approach are shown in Figure 32 (respectively in (a) and (b)). As it can be observed in Figure 31, the average energy and delay consumed during procedures of change of cells in Manhattan is higher than the other two models. In fact, in Manhattan model, nodes are moving along roads. Thus, even though their trajectories may be slightly deviated, they still have more or less straight trajectories to reach a cluster coverage area during change of cell procedure.

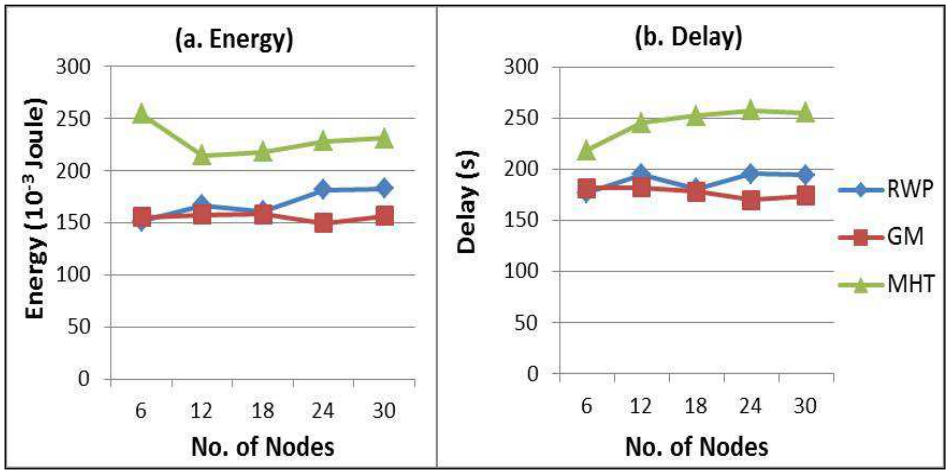

Figure 31. Average energy and average dalay during cell reselection procedures

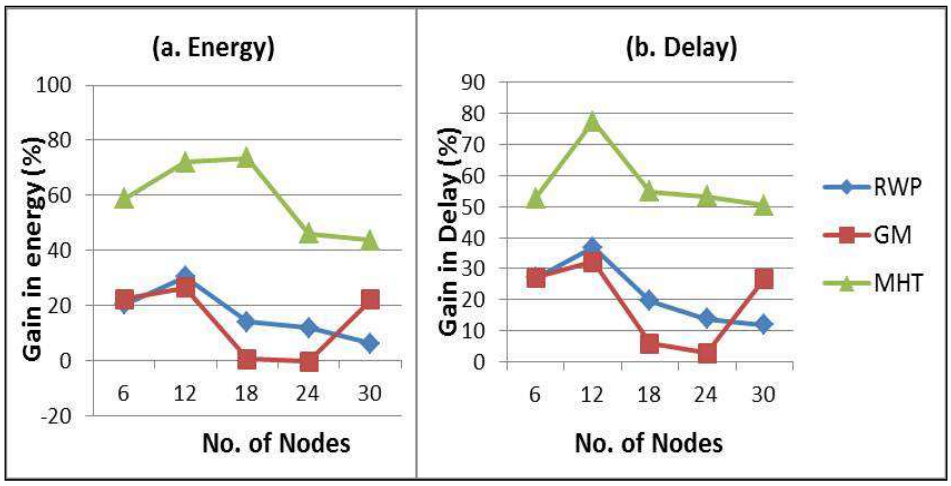

Figure 32. Gain in average energy and average delay using 3 different mobility models

However, the standard procedure requires that nodes enter in a scan period before beginning the association procedure. As a consequence, nodes may leave the coordinator coverage area before they finish the association procedure. In Figure 32, it can be seen that the average gain in delay and energy is higher when the Manhattan model is used. In fact, since coordinators cover all the grid area, when using Manhattan; nodes enter more rapidly the next coordinator coverage area. Using our scan-free approach, packets sent during association procedures are then more likely to be successfully received; thus decreasing the amount of control packets as well as the delay of the procedure. In our case, this improvement is also due to our speculative algorithm since, in Manhattan, nodes are more likely to stay on the same road (*TurnProb* 0.2).

4.8.2.2. Evaluation of the approach with Manhattan mobility model

In the previous paragraph, the turn probability was set to 0.2. Thus, the probability that nodes stay on the same road is very high (0.8). This represents almost the best case as our speculative algorithm favors movement of nodes on the same road. In this subsection, we present simulation results when *TurnProb* changes (0.2, 0.5 and 0.8) and when the number of mobile nodes varies from 6 to 24 with a step of 6. Two cases have also been considered: with pause (WP) and without pause (WOP) of mobile nodes. In the first set of simulations (WP) pause probability is equal to 0.1.

Figure 33 shows the average energy spent in change of cell procedures when our approach is used. WP 0.2 means that *TurnProb* is equal to 0.2 and nodes are having pause periods. It can be seen that the enhanced procedure is more efficient when pause periods are allowed. In fact, since the grid area is covered by coordinators, when a mobile node stops moving for a period

of time, it is more likely that it successfully finishes a handover procedure in a short period of time. However, if it is moving for a longer period, it may not have enough time to finish a handover procedure and leaves the average area of the new association coordinator before the end of the procedure. In this case, the number of transmitted control packets (association request/response, handover request/response, data request, beacon request) increases. So does the energy. Figure 34 and Figure 35 respectively represent the corresponding gains in energy and delay compared to the standard procedure. It can be noticed that they are both important when *TurnProb* parameter is low (0.2). That is expected due to our speculative algorithm. However, even if *TurnProb* parameter is higher (0.8), the gain is still around 20% for 24 mobile nodes.

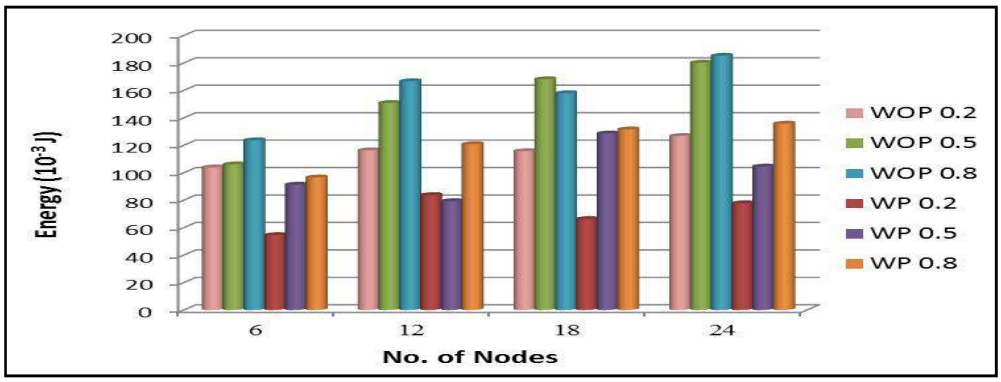

Figure 33. Average energy spent in cell reselection procedures (MHT model)

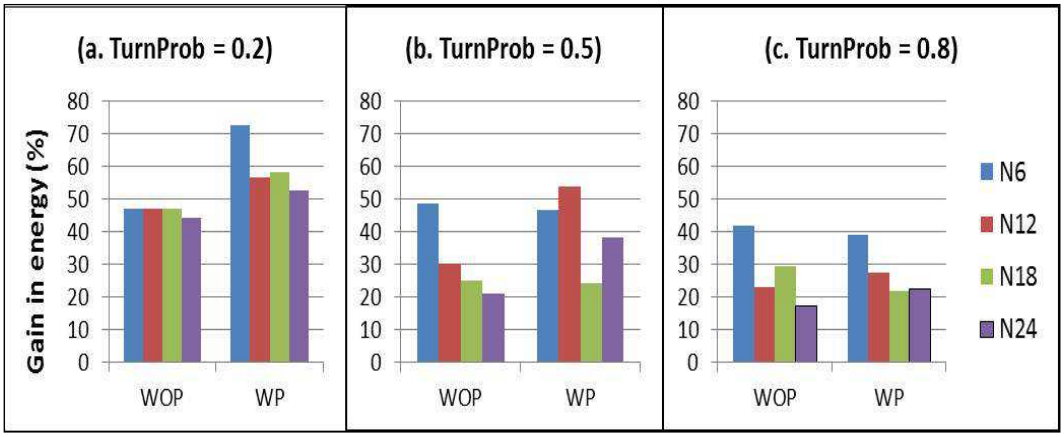

Figure 34. Gain in energy (MHT model)

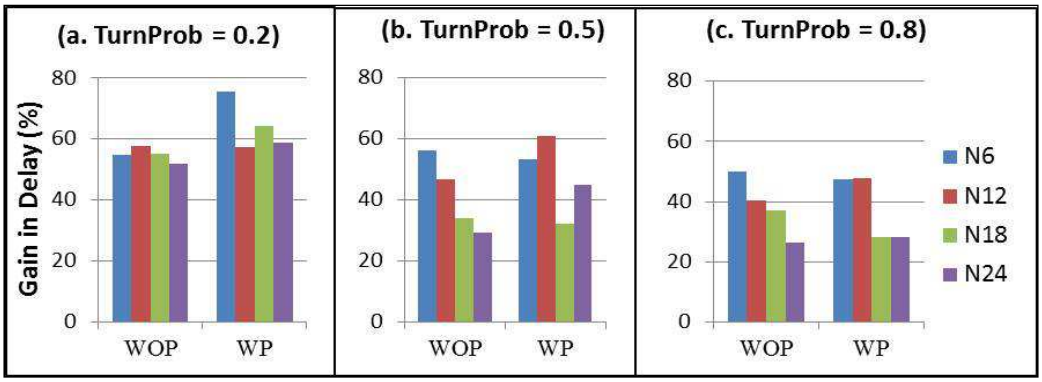

Figure 35. Gain in delay (MHT model)

4.8.2.3. Analysis of the energy consumption of a mobile node

So far, evaluation has dealt with the average energy and delay of all the mobile nodes for different mobility models, with or without pause, and different number of mobile nodes. In this subsection, the objective is to study the behavior in terms of energy consumption of a specific mobile node called M (instead of all the nodes) for different network conditions. For instance, M keeps the same trajectory while the number of mobiles varies. Pause probability value is the same for all mobile nodes in each scenario. Common simulation parameters are set as in Table 9 and Table 11.

Given the pause probability, two sets of simulations are defined. In the first set of simulations, we do not define pause periods. In the second set, pause probability is equal to 0.1. Turn probability is set to 0.2 in all simulations. Trajectories of other end devices are different in each simulation. Figure 36 shows the remaining energy in M at the end of the simulation when the total number of mobile end devices varies for both scenarios (WP and WOP) using our approach (ENH) and the standard (STD). Globally, the remaining energy decreases when the total number of mobile nodes increases. This is expectable since increasing the number of communicating nodes increases collisions and thus retransmissions of packets. Network conditions (here the number of mobile nodes and trajectories) have then an important impact on the energy consumption of a mobile node M having the same trajectory. We can also observe that the remaining energy is in some cases higher using the standard protocol than using our approach. The reason is that the mobile node M is synchronized for a longer period of time to network coordinators. This is observed on Figure 37. This figure illustrates the number of received beacons by the mobile node M for the same scenarios that correspond to Figure 36. As it can be seen, the number of received beacons is higher using our enhanced

handover procedure than when using the standard. This is verified for any value of the pause probability. So, having a mobile node synchronized for a longer period is energy consuming but the energy is spent for good reasons, mainly for maintaining a good link and reducing the latency.

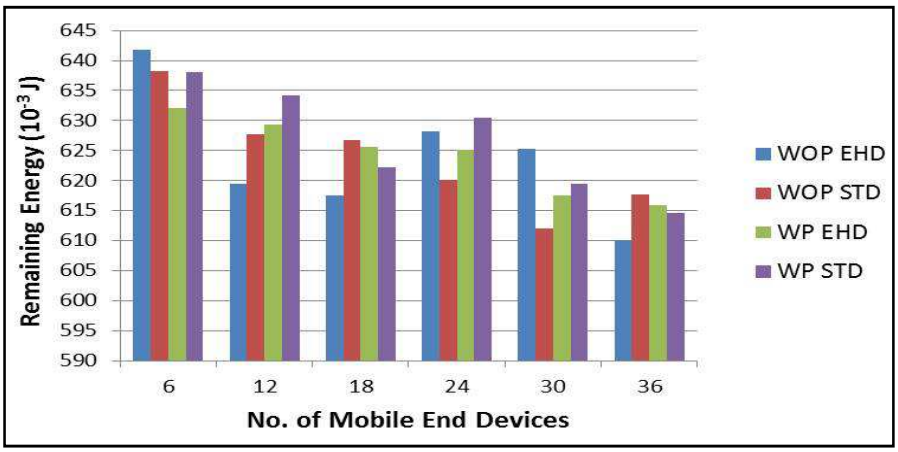

Figure 36. Remaining energy of node M vs. number of end devices

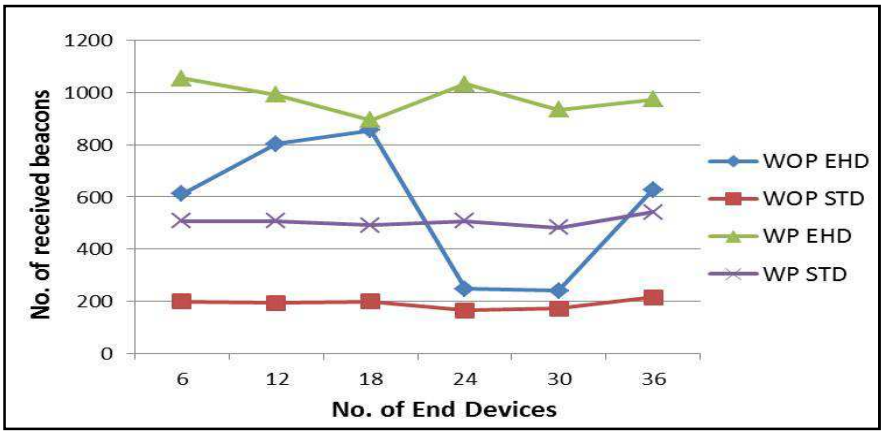

Figure 37. Number of received beacons by node M vs. Number of end devices

4.8.2.4. Impact of noise on the new mobility approach

So far, our approach has been evaluated without considering noise that is very common in realistic use cases. Moreover, we have based our $LQI_{threshold}$ formula on making the

assumption that the same level of noise is assessed during the movement of an end device within a coordinator coverage area. In this subsection, we evaluate the efficiency of our approach including the $LQI_{threshold}$ formula using an additive white Gaussian noise (AWNG).

Table 12. Simulation setup for noisy environment

Duration (s)	Duration of the mobility scenario	300
Variance	The variance of the AWGN model	0.3

We used the same network architecture described in subsection 4.8.1 and summarized in

Table 9, Table 11 and Table 12. For each mobility model scenario, all end devices are mobile and their number is varied. End devices are periodically receiving beacon messages. Nodes do not send data. In our simulation scenarios, due to noise effect, some nodes may not be associated before they begin to move.

Each mobility model scenario has been simulated first without considering the noise, and then with an AWGN model. MHT_N, RWP_N and GM_N correspond to the simulation scenarios when the noise is considered. The results of the scenarios without considering noise (MHT, GM and RWP) correspond to the results shown in Figure 31 and in Figure 32. The speculative algorithm that favors node movements on the same road is used. The Figure 38 shows simulation results that correspond to the average energy (Figure 38.a) and the average delay (Figure 38.b) during cell reselection procedures. The Figure 39 shows simulation results that correspond to the gain in energy (Figure 39.a) and in delay (Figure 39.b) during cell reselection procedures in comparison with the standard IEEE 802.15.4 procedure.

Due to the random behaviour of the noise combined with the pseudo-randomness of packet transmissions (MAC backoff period), simulation results with a noise model are not always worse than those that did not. Moreover, the results demonstrated that even when the noise is considered, the energy consumption and the delay can be reduced up to 42% and 58% respectively. Thus, we verify that the proposed $LQI_{threshold}$ formula is efficient even in a noisy environment.

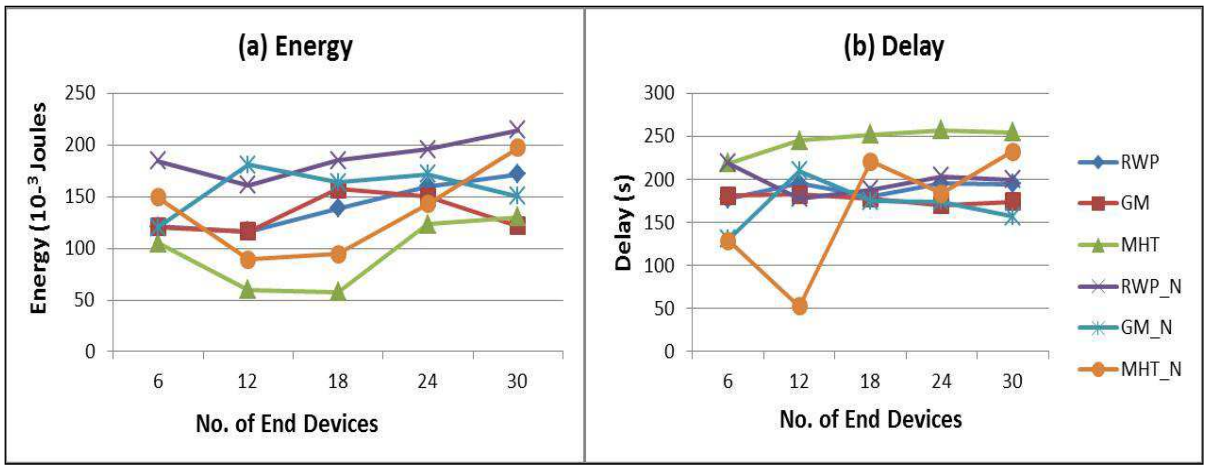

Figure 38. Average energy and average delay during cell reselection procedures

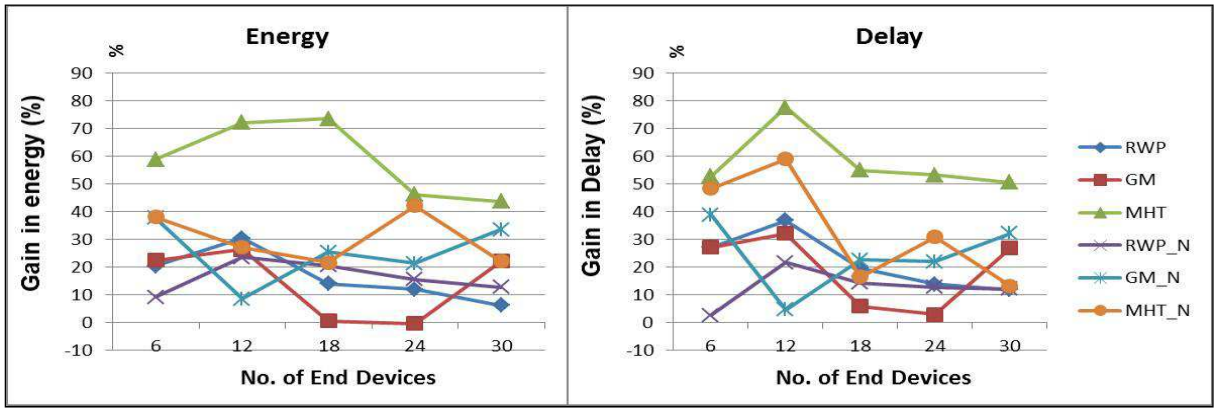

Figure 39. Gain in average energy and average delay using 3 different mobility models

4.9. Probabilistic speculative algorithm

So far, the speculative algorithm (subsection 4.8) that has been evaluated has only favored the movement of a node on the same road. A default road has been defined which corresponds to the horizontal road containing the coordinator of association and a default x_axis vector direction (Figure 40). According to this algorithm, if the previous coordinator is situated on the left of the current coordinator, then the next coordinator is the coordinator which is on the right of the current one (and vice-versa). The method did not take into consideration the fact that nodes are able to turn left or right. Moreover, a node may leave the coordinator coverage area before it finishes the association procedure, which may be due to its speed, to the delay of the reselection cell procedure or to the noise. In this case, even if the previous coordinator

of the mobile node and its current coordinator belong to the same vertical road, the default horizontal direction will be used.

In this subsection, we propose a new speculative algorithm that takes into consideration the cases where nodes change roads (turn left or right) and the cases where the previous coordinator and the current coordinator of a mobile node are not two successive coordinators of the same road.

Both speculative algorithms are compared. The first algorithm that was proposed in 4.8 supposes that nodes stay on the same road. We name it the same-road algorithm. The second algorithm is a probabilistic speculative algorithm that randomly selects the direction of a mobile node. The probabilistic speculative algorithm is detailed in subsection 4.9.1 and a comparison of both algorithms is conducted in 4.9.2.

4.9.1. ***Description of the Probabilistic Algorithm***

Let (i,j) be the coordinates of the current coordinator of association in the *Nt* matrix and let (i',j') be the coordinates of the previous coordinator of association in the *Nt* matrix. As shown in Figure 40, around the current coordinator (i.e. the red circle in Figure 40), the grid can be divided into four zones (A, B, C, D). The previous coordinator of association is located in one of these zones (denoted previous zone). The previous zone is determined by comparing the coordinates (i',j') of the previous coordinator in the *Nt* matrix and the coordinates (i,j). The results of the comparison are given in Table 13**.** The previous zone is randomly chosen if the previous coordinator and the current coordinator are the same or if it is the first cell reselection of the mobile node.

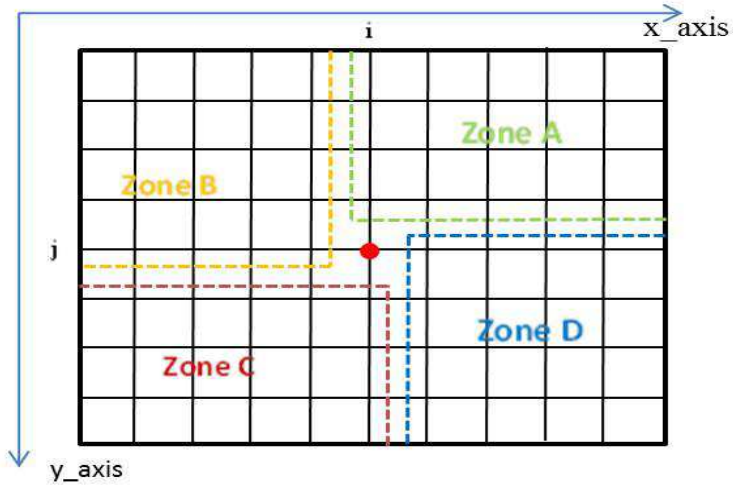

Figure 40. Grid architecture

Table 13. Zones of a coordinator

Previous Coordinator X-coordinate	Previous Coordinator Y-coordinate	Previous Zone
i' ≥ i	j' < j	A
i' < i	j' ≤ j	B
i' ≤ i	j' > j	C
i' > i	j' ≥ j	D
i' = i or i' undefined	j' = j or j' undefined	Random

The new speculative algorithm uses the previous zone and a random direction determined using a normal distribution of a set of 3 possible directions:

- Straight (S): the probability of S is 0.5
- Right (R): the probability of R is 0.25
- Left (L): the probability of L is 0.25

The algorithm first predicts the next zone to which the mobile node is moving using the rotation table given in Table 14. Then, it determines the coordinated of the next coordinator of association based on Table 15.

Table 14. Rotation Table to determine the next zone

		Predicted Direction		
		S	L	R
Previous Zone	A	C	D	B
	B	D	A	C
	C	A	B	D
	D	B	C	A

Table 15. Coordinates of the next coordinator

Next Zone	X-Coordinate	Y-Coordinate
A	i	j – 1
B	i – 1	j
C	I	j + 1
D	i + 1	J

If the current coordinator is in the extremity of the grid, then some zones are not available. The algorithm has to choose a direction corresponding to one of the available zones. For instance, if $i = 0$ and $0 < j < N - 1$, where N is the maximum number of coordinators per road, zone B is eliminated from the direction prediction algorithm.

4.9.2. ***Gains in energy and delay of the probabilistic algorithm***

The Figure 41 shows simulation results that correspond to the gain in energy when the probabilistic speculative algorithm is used in comparison with the same-road algorithm. The Figure 42 shows simulation results that correspond to the gain in delay when the probabilistic speculative algorithm is used in comparison with the same-road algorithm.

As it can be seen in Figure 41 and Figure 42, for the random waypoint scenario, the probabilistic algorithm is better than the same-road algorithm. When the Manhattan model is used, the same-road algorithm gives better results. This can be explained by the fact that the *turnProb* parameter (the probability that the node turns left or right) is relatively low (0.2). The gain in energy and delay is almost equal to zero for the Gauss-Markov mobility model.

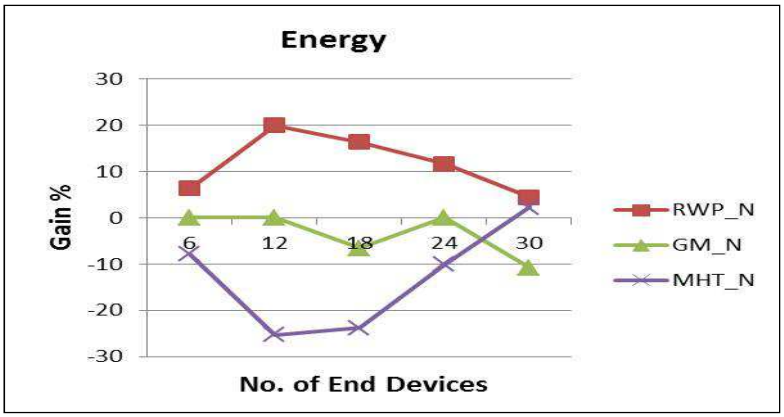

Figure 41. Gain in energy of the probabilistic speculative algorithm in comparison with same-road algorithm

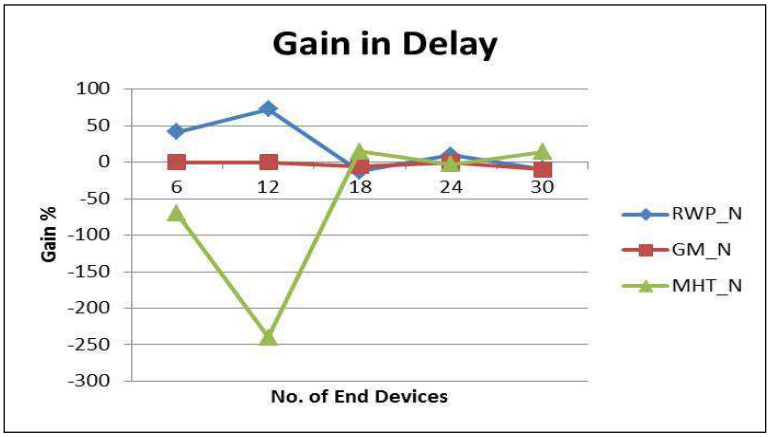

Figure 42. Gain in delay of the probabilistic speculative algorithm in comparison with same-road algorithm

4.10. Summary

In this section, a global network architecture that efficiently handles mobile IEEE 802.15.4/ZigBee end devices has been proposed. A new mobility management approach has been presented and evaluated using simulations. The proposed mobility management approach anticipates the link disruption by controlling the LQI value of each received packet and uses a speculative algorithm. An $LQI_{threshold}$ formula and two speculative algorithms (respectively denoted same-road and probabilistic) have been proposed and evaluated in a grid network. Results obtained in simulation with different parameters related to mobility (mobility models, speed, number of nodes, etc.) lead to the following conclusions:

- The gains in energy and delay of our mobility approach in comparison to the standard protocol procedure are important. Moreover, the mobility management approach has proven its efficiency even in a noisy environment
- The mobility behavior of end devices has a great impact on performance. It includes the speed of nodes, the mobility model, and some parameters such as the probability of pause and the Manhattan Model *turnProb* parameter. Nevertheless, simulation results demonstrate that our approach always improves performance (in energy and delay) when compared to the standard procedure

The work that has been conducted in this chapter has been presented in several papers. The approach for mobility management has been first proposed in [Chaabane 2011]. In [Chaabane 2012a], the efficiency of $LQI_{threshold}$ has been proven. In [Chaabane 2012b], the $LQI_{threshold}$ formula and the node mobility behavior have been investigated. Finally, we have presented the probabilistic speculative algorithm and the impact of noise in [Chaabane 2013].

In addition to the mobility management, other features can be explored in order to even more reduce energy consumption while maintaining a good link quality. In the next section, we propose to investigate the rate adaptation capability in IEEE 802.15.4 networks to improve the power consumption of mobile nodes.

Chapter 5. **Rate adaptation algorithm**

5.1. Introduction

As mentioned above, the problem of rate adaptation in sensor networks has almost not been investigated. In section 3.5.2, we have presented the most relevant studies that focused on rate adaptation in IEEE 802.15.4 WSN. However, in these studies, nodes' mobility cost and impact on the link estimation and rate selection was not a major concern. In mobile networks, wireless channel conditions are constantly changing. Thus, assessing the channel conditions using the channel history (i.e. statistics of packets delivery ratio (PDR)) may lead to irrelevant estimations. Thus, more accurate parameters than PRR have to be used in the design of a PHY-aware MAC protocol. In this section we propose two rate adaptation algorithms and we adjust the data rate according to information from the last received packet. As it has already been done in [Lanzisera 2009a], we add three start frame delimiters (SFDs) corresponding to the three additional data rates.

We have presented in the previous section a new mobility management approach and we have proved its efficiency in terms of energy and delay. It is interesting to evaluate this approach when combined with a rate adaptation algorithm. Therefore, we present in subsection 5.2 a mobility-aware rate adaptation algorithm based on the LQI parameter and using the $LQI_{threshold}$. We evaluate our approach using the NS-2 simulator.

Then, in subsection 5.3, we propose a second rate adaptation algorithm that uses a more accurate link quality estimation based on the chip error rate of received packets. Given the limitations of the NS-2 simulator channel modeling, we use another simulator, WSNet, to evaluate this second approach using an ad hoc IEEE 802.15.4 network with a non beacon-enabled mode.

5.2. A Mobility-aware Rate Adaptation Algorithm

In order to reduce the energy consumption of IEEE 802.15.4 mobile end devices, we propose a hybrid approach that combines mobility management and rate adaptation. We evaluate the efficiency of this approach in an IEEE 802.15.4 cluster tree network connected to a backbone network.

5.2.1. ***Rate selection algorithm***

We estimate the link quality using the LQI of the last received packet. The appropriate rate to be used is then determined according to the LQI value. Regardless of the current data rate, the next packet data rate is selected based on the most recent LQI at that frequency.

Our method defines LQI thresholds to be used by the rate adaptation algorithm. The range of possible LQI values is determined based on the maximum and the minimum LQI value of a packet. Given that our rate adaptation algorithm is used with our mobility management approach, the $LQI_{threshold}$ is the minimum value that can be taken into account. Therefore, for each new successful handover the LQI range is computed again and thus the rate adaptation LQI thresholds. Obviously, if a node is static, the minimum possible LQI value is LQI_{min}. Then, after determining the available range corresponding to the link between the mobile node and its new coordinator, four intervals are determined based on the rate adaptation LQI thresholds _ each one is assigned to a rate.

Let LQI_{MAX} be the maximum value of LQI, *ppduLQI* the LQI of the last received packet and *setRat*e() the function used to update the rate of a given link. Our proposed algorithm is as follows:

LQI_{RA} = ceiling((LQI_{MAX}- $LQI_{threshold}$)/4)

If (ppduLQI ≥ LQI_{MAX} – LQI_{RA})

    Then setRate(8);

Else If (ppduLQI ≥ LQI_{MAX} – LQI_{RA} * 2)

    Then setRate(4);

Else If (ppduLQI ≥ LQI_{MAX} – LQI_{RA} * 3)

    Then setRate(2);

Else

```
        setRate(1);
End If
```

Based on the $LQI_{threshold}$ formula given in (28), it can be noticed that LQI_{RA} is a function of LQI_{init}, LQI_{min} and LQI_{MAX}. When LQI_{init} is high, LQI_{RA} is low. In this case, the LQI values' range for each rate is small. Therefore, rate selection algorithm is more sensitive to the channel condition changes: when the quality of channel worsens (i.e. LQI of the received packet decreases), it is more likely that the data rate drops. Actually, if a node is entering a new coordinator coverage area then the longer the handover procedure, the more likely the LQI_{init} is to be higher. In this case, the channel conditions have not been good enough to establish a new association for lower LQI values. However, when the channel conditions are good, the association is quickly successfully established and thus the corresponding LQI_{init} is low. The rate adaptation algorithm uses this information in order to dynamically adjust its rate adaptation LQI thresholds computation regarding the handover procedure conduct.

In our approach, the acknowledgments (ACKs) have to be enabled so that both sender and receiver are able to estimate the link quality of each packet sent. Acknowledgments are sent according to the last computed rate. The beacon frame is always broadcasted using the legacy rate in order to ensure its reception probability. The beacon request frames are also sent using the legacy rate given that nodes that are requesting beacons have not been associated yet and do not have a full knowledge of the channel conditions.

5.2.2. ***Evaluation of the Approach***

Simulations are performed in order to evaluate the performance of the network in terms of energy and synchronization time when nodes are moving. As mentioned earlier, when a node does not receive a beacon, it does not send data packet and has to enable its receiver in order to find the beacon. Therefore, the higher the number of received beacon, the longer communications can be assured. Thus, the synchronization time is estimated by the number of received beacons.

First, we compare the network performance when using the mobility-aware rate adaptation algorithm (RA+MM approach) to the mobility management approach (MM) and to the standard protocol procedure (STD). We vary the number of mobile nodes from 6 to 30 by a step of 6. This first set of simulation scenarios are intended to evaluate the efficiency of the

RA+MM for the whole network. Then, we focus on its efficiency for a given communicating node that can be a sender or a receiver. The rate adaptation algorithm is strongly dependent on the channel conditions that vary over time. Therefore, the performance of our algorithm is evaluated when the packet interval changes.

5.2.2.1. Simulation Setup

The noise model is an additive Gaussian white noise (AGWN) generated using the Box-Muller method [Box 1958] and the variance is set to 0.3. Simulations are carried out using the NS-2 simulator [NS-2]. . A two-ray ground propagation model is used. We use the Manhattan mobility model without pause periods and with a turn probability (TurnProb) set to 0.2.

Table 9 and Table 16 summarize setup parameters for all mobility scenarios.

Table 16. Simulation setup in mobility-aware rate adaptation algorithm evaluation

Variance	The variance of the AWGN model	0.3
Duration (s)	Duration of the mobility scenario	1800

5.2.2.2. Network Performance of the Mobility-aware Rate Adaptation Algorithm

The average number of received beacon by end devices as well as the average remaining energy are determined for each scenario and given in Figure 43 and in Figure 44. As it can be seen, the average number of received beacon and the remaining energy are more important for both RA+MM and MM approaches compared to the standard IEEE 802.15.4 protocol. Despite the difference between the average number of received beacons when using either the RA+MM or MM approach is not very important, the remaining energy when using the RA+MM approach is more important. As a consequence, one can verify the energy efficiency of the RA+MM approach.

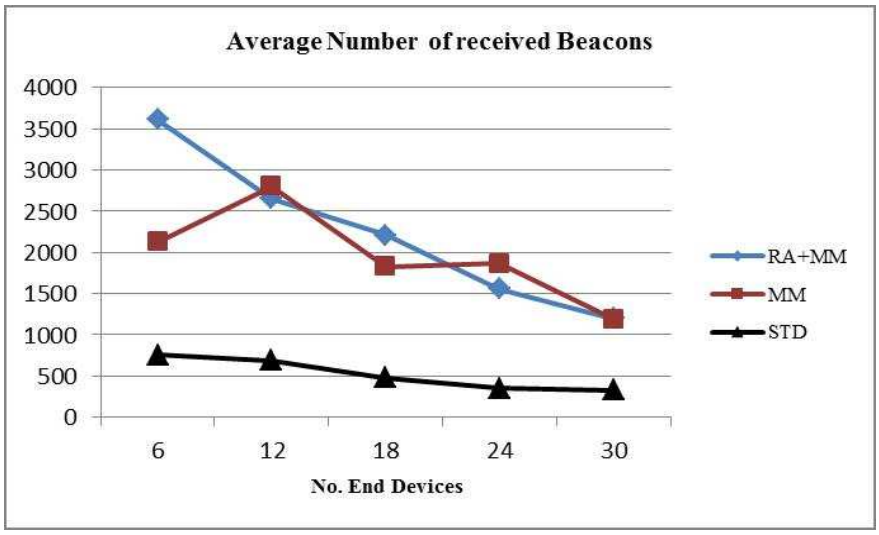

Figure 43. Average number of received beacons

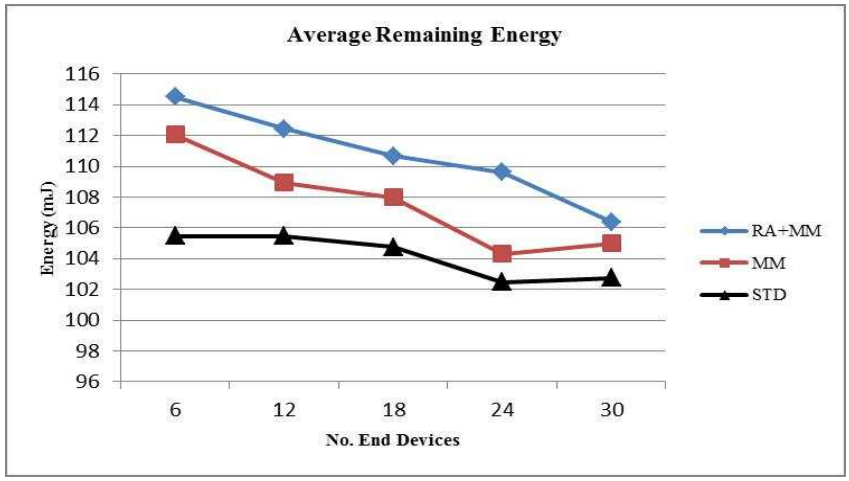

Figure 44. Average remaining energy

5.2.2.3. Performance Analysis of a Communicating End Device

So far, we have not considered the case where end devices are communicating. In this subsection, we conduct simulations where two nodes are communicating. In the beacon-enabled mode, packets sent from a source (Src) to a destination (Rcv) are routed by the corresponding coordinators of Src and Rcv even if they share the same PAN (same coordinator for both the sender and the receiver). In our approach, if the Src and Rcv are not in the same PAN, packets are routed from the coordinator of Src to the coordinator of Rcv through the SuperCoordinator. This hybrid routing mechanism is implemented and added to NS-2 simulator. When an end device receives a packet with an LQI lower than the $LQI_{thresholds}$, it has to trigger the change of cell procedure by sending an LQINot message to its coordinator.

When it receives the LQIRsp, it has to begin the association procedure with the new coordinator. At this stage, the node cancels the packet transmission and resumes it at the end of the association procedure. If nodes are receiving data packets, the probability that they trigger this procedure more often is higher. Moreover, when end devices are sending or receiving data packets, the amount of exchanged packets with their corresponding coordinators is more important. In consequence, end devices are able to update the data rate more quickly.

iii. Energy, synchronization and PDR evaluation

Simulations are conducted using both RA+MM and MM approaches as well as the IEEE 802.15.4 standard protocol (STD). We study the impact of communication on the remaining energy and the synchronization time of both sender and receiver. In our simulations, packets' length is 113 bytes (physical layer) and they are sent using a constant bit rate transmission every 10 seconds. The packet delivery ratio is determined in each simulation.

It can be seen in Figure 45 that the number of received beacons for both the sender and the receiver is consistent with the general network evaluation results shown in Figure 43. It can also be seen that the received beacons' number of both sender and receiver is higher than the average beacon number from Figure 43. Moreover, as it is illustrated in Figure 46, the remaining energy in the RA+MM approach is higher than in the MM approach. However, unlike the results obtained in the previous simulations (Figure 44), the remaining energy when using the standard protocol is the highest among the three approaches. Actually, when using the standard protocol, the time during which nodes are not synchronized is the longest. Therefore, the number of sent and received data packets is the lowest. As a result, the energy spent in data communication is lower than in the RA+MM and MM approaches. We can also deduce from Figure 44 and Figure 46 that data transmission has a stronger impact on the remaining energy than the cell change procedures which is mainly due to the length of data packets. Figure 47 gives the packet delivery ratio (PDR) for the different approaches. It can be seen that there is a slight variation between the RA+MM and the MM approaches. However, PDR is always better than in the STD case.

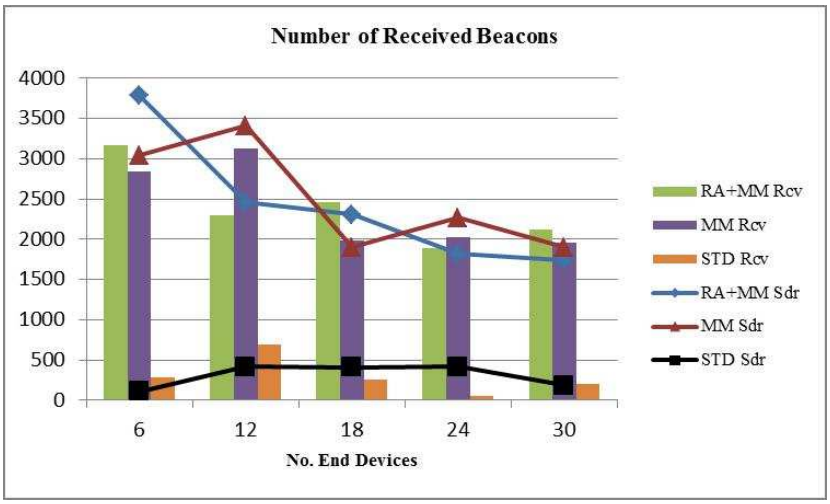

Figure 45. Number of received beacons for communicating nodes

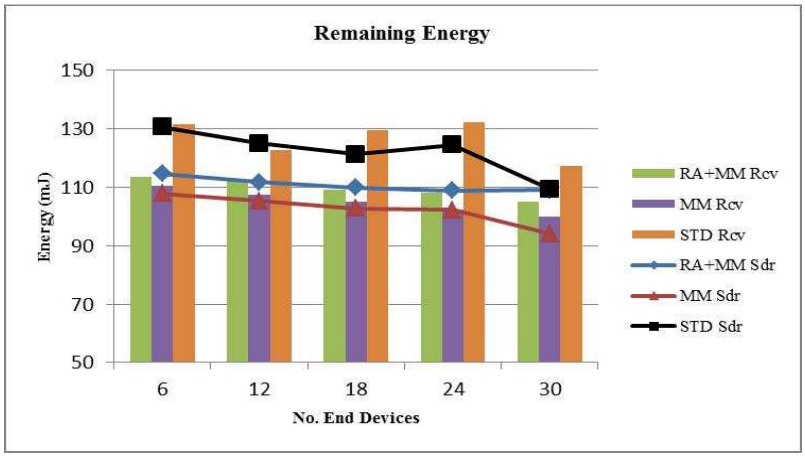

Figure 46. Remaining energy of communicating nodes

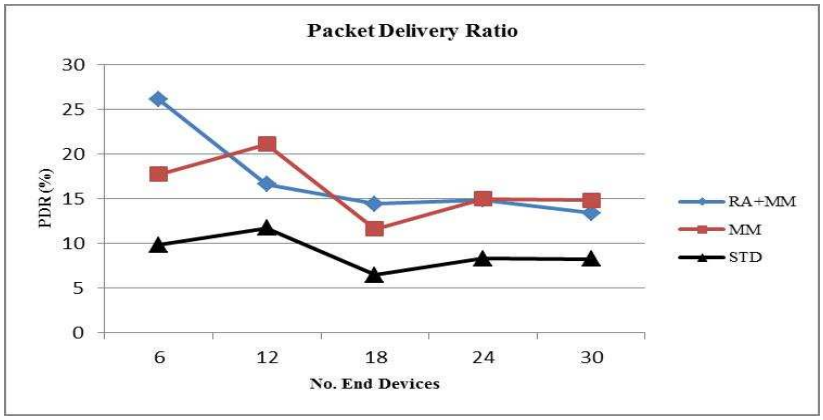

Figure 47. Packet delivery ratio

iv. Impact of packet interval

As it has been evoked in subsection 3.4.1, the IEEE 802.15.4 slotted CSMA/CA protocol uses backoff periods to overcome packet transmission failures. In fact, if a packet transmission fails, the sender has to wait for a random backoff period before resuming the packet transmission. However, this period is computed independently from the channel coherence time.

In this section we highlight the impact of modifying the packet interval using simulations. For that, we vary the packet transmission interval (1, 5, 10, 20 and 60 seconds) of the CBR (Constant Bit Rate) application. The number of mobile nodes in the scenarios is set to six including a sender and a receiver. As it can be seen in Figure 48 and in Figure 49, the remaining energy in RA+MM approach is always higher with a slight difference in the number of received beacon. In Figure 50, one can see the impact of changing packet transmission interval on the packet delivery ratio.

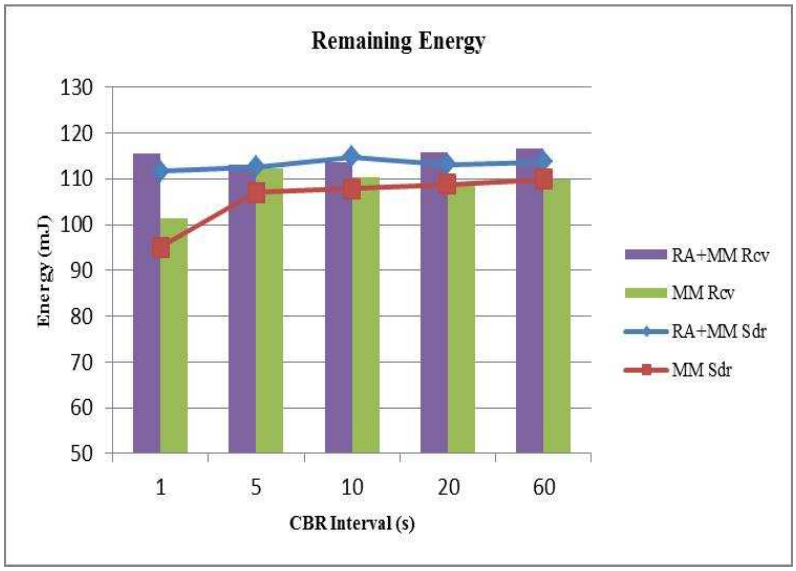

Figure 48. Remaining energy of communicating nodes Vs. CBR interval

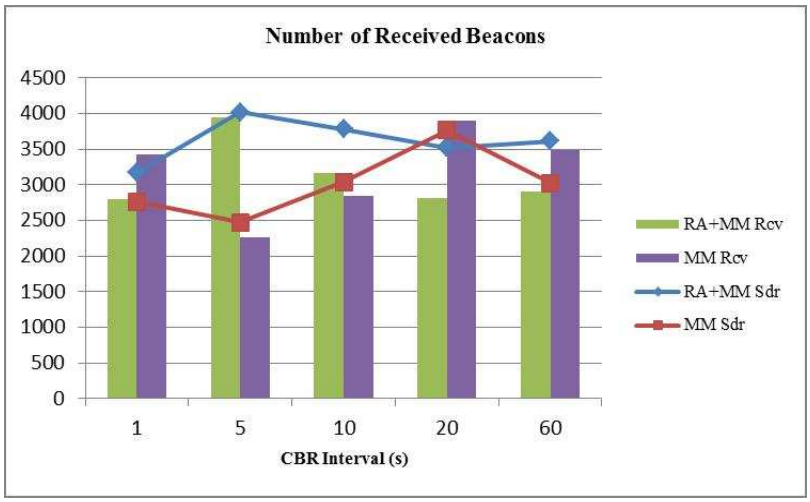

Figure 49. Number of received beacon of communicating nodes Vs. CBR interval

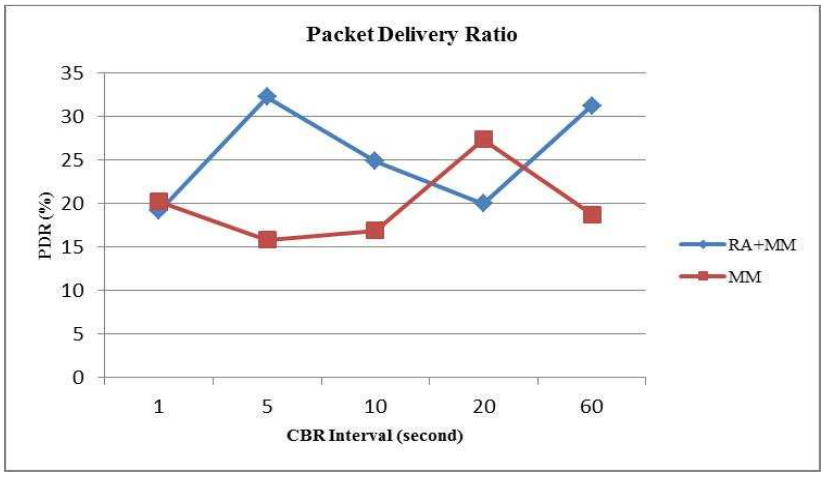

Figure 50. Packet delivery ratio of communicating nodes Vs. CBR interval

5.3. An adaptive rate adaptation algorithm

The basic approaches of link estimation use either the signal strength (SNR) or the packet statistics. In SNR-based techniques, the BER at a giving SNR might vary by many orders of magnitude between environments. SNR measurements also require hardware specific calibration [Zhang 2008]. Besides, SNR measured in the beginning of the reception of a frame does not capture the variation that might occur during the transmission of the packet due to fading. On the other hand, Frame-level schemes are not responsive to channel variations that occur on short timescales. Some hybrid solutions that combine metrics based on both signal strength and packet statics have been proposed [Fonseca 1996]. Packet errors may also occur

due to interferences that are not a channel characteristic. Accuracy of estimators depends on the elimination of the interference effects.

In IEEE 802.15.4, chips are the smallest information entity transmitted over the channel and are therefore more responsive to channel conditions. The most suitable way to adapt the bit rate in an IEEE 802.15.4 network with mobile nodes should therefore be based on chip error rate.

In this subsection, we propose a hybrid method for rate adaptation based on the chip error rate to evaluate the efficiency of the current data rate and the packet delivery ratio (PDR) of the current transmission data rate to adjust our metrics' thresholds. We first present a new method to estimate the link quality in subsection 5.3.1. Then, we present our proposed rate adaptation algorithm in subsection 5.3.2. In subsection 5.3.3, the simulation setup is described. The experimental results of our approach are given in subsections 5.3.4 and in 5.3.5.

5.3.1. ***Link Quality Estimation Metrics based on chip error rate***

In DSSS and in spread-spectrum systems in general, the receiver correlates a locally generated signal (i.e. the predefined code words in DSSS) with the received signal (pseudo random noise code, i.e. PN-Code). In fact, during the decoding phase, packets are sampled symbol per symbol. In the IEEE 802.15.4 PHY, if the chip error per PN-Code (CEPP) is lower than the correlator error threshold, the symbol will be correctly received. For each symbol, if the HDD is used, the Hamming distance (HD) is determined. In our study, we use the Hamming distance to determine the chip error per pseudo random noise code (CEPP). In [Wu 2010b] for example, the HD was used and the HD threshold (i.e. correlator error threshold) was set to 11. Thus, up to 10 chips out of a total of 32 in a PN-Code could be corrupted without negating the receiver's ability to recover from the original data. In contrast, if any one of the CEPPs in a frame reaches the CEPP correlator error threshold, this frame is dropped. In our study, we set the correlator error threshold (i.e. HD threshold) to 10 (i.e. up to 9 chip error per symbol are accepted). This value is close to the value used in [Wu 2010a] (i.e. threshold set to 11). However, we choose to decrease it in comparison to [Wu 2010a] in order to reduce the probability of packet misclassification (when one or more PN-Codes are wrongly decoded). In fact, our channel is noisy and that our network can support a large number of communicating nodes (in our modeled transmission environment, errors may occur frequently). This value is high in comparison with the values determined in [Srinivasan 2008]

and in [Heinzer 2012] given that in network simulators the synchronization process (reception of the preamble and the SFD) is the same as decoding any other symbol. In our approach, even if the receiver encounters a PN-Codes HD higher than the HD thresholds, it continues the decoding process until the end of the frame even though it is obviously corrupted. Continuing to decode corrupted packets was used in [Wu 2010a] and in [Wu 2010b] in order to determine and distinguish chip error patterns related to mobility from those that are related to noise. However, authors did not propose any metric that can be exploited.

Our link quality estimation method uses the CEPP to define new metrics that are used by the proposed data rate adaptation algorithm. We determine CEPP of both the correctly received and the corrupted PN_Codes. We introduce two new metrics in order to examine the chip error distribution:

- Percentage of the total chip error in the packet denoted *Pctg(CEPP$_{kt}$)* which is an integer corresponding to the total number of chip error in the packet divided by the total number of chips in the packet.

$$Pctg(CEPP_{kt}) = (integer)\ \frac{\text{total number of chip error per packet}}{\text{total number of chips per packet}} * 100 \qquad (29)$$

- Percentage of the total number of corrupted PN-Codes in the packet (if they exist) denoted *Pctg(NCP)* which is an integer corresponding to the total number of corrupted PN-Codes in the packet divided by the total number of PN-Codes in the packet.

$$Pctg(NCP) = (integer)\ \frac{\text{total number of corrupted PN\_Codes per packet}}{\text{total number of PN\_Codes per packet}} * 100 \qquad (30)$$

Pctg(CEPP$_{kt}$) and *Pctg(NCP)* are calculated based on the total length of the received packet since packet size is variable. Therefore, this method is independent of the packet size. The chip error per symbol is a known value at the physical layer. Using only two integers (instead of using all the information that can be retrieved from the physical layer) has the advantage of reducing the computation cost, and thus the processing time and energy cost.

5.3.2. ***Rate Selection Algorithm***

Estimating the link quality is crucial to propose an efficient rate selection algorithm. Several rate selection algorithms were designed for IEEE 802.11 networks. However, given the physical layer differences between IEEE 802.11 and IEEE 802.15.4 many techniques are not applicable in IEEE 802.15.4. We have listed in subsection 3.5.2 the most relevant rate selection algorithms that are proposed for IEEE 802.15.4 networks. In [Lanzisera 2009a] and [Martelli 2011], the proposed algorithms were based on SNR or LQI and it has been shown that these metrics are not accurate in mobility use cases. In [Vutukuru 2009], SoftPHY rate algorithm used BER thresholds defined for each rate in order to select the next data rate. However, this algorithm was only evaluated using IEEE 802.11 nodes.

Our approach requires acknowledgment frames in order to quickly update the rate used between the receiver and the sender. In fact, enabling acknowledgments (ACKs) allows both radios to measure channel conditions for each packet sent since the acknowledgement is also sent using the most recent selected data rate.

Our approach is evaluated using an Ad hoc IEEE 802.15.4 network. All nodes use the same channel frequency and the unslotted CSMA-CA algorithm. Nevertheless, the approach can be extended to a star or a cluster tree network. In this latter case, rate adaptation algorithm is performed for communications between nodes and their coordinators since the beacon-enabled mode and the slotted CSMA-CA algorithm are used. Only the handling of the transmission of the beacon and the beacon request frames has to be added in order to ensure sending these frames using the standard data rate as explained in subsection 5.2.1.

Hereafter, we consider two nodes that are communicating as described in Figure 51. If a node (node N_j in Figure 51) wishes to transmit a packet to node N_i, it must first use the 250 kbps standard bit rate. The node N_i then calculates the $Pctg(CEPP_{kt})$ and the $Pctg(NCP)$ of the received data packet, and determines the appropriate bit rate to be used by the sender. Each node keeps a log of the nodes that is communicating with, the corresponding rate at which packets have to be sent and the packet reception ratio (PRR) corresponding to the current rate. Upon the reception of a data packet from N_j, N_i sends the ACK frame (Annex D) to N_j using the computed rate. If the ACK is successfully received, the sender N_j updates the transmission rate and the number of successful transmissions that are both relative to its communication with N_i. If an ACK is not received by N_j, the next packet from N_j to N_i is sent at the rate recorded by N_j corresponding to the last successfully received packet.

Each link between two communicating nodes is, then, evaluated independently from other links. However, if a node wishes to broadcast a message, it has to use the lowest rate among the rates used for communication with other nodes.

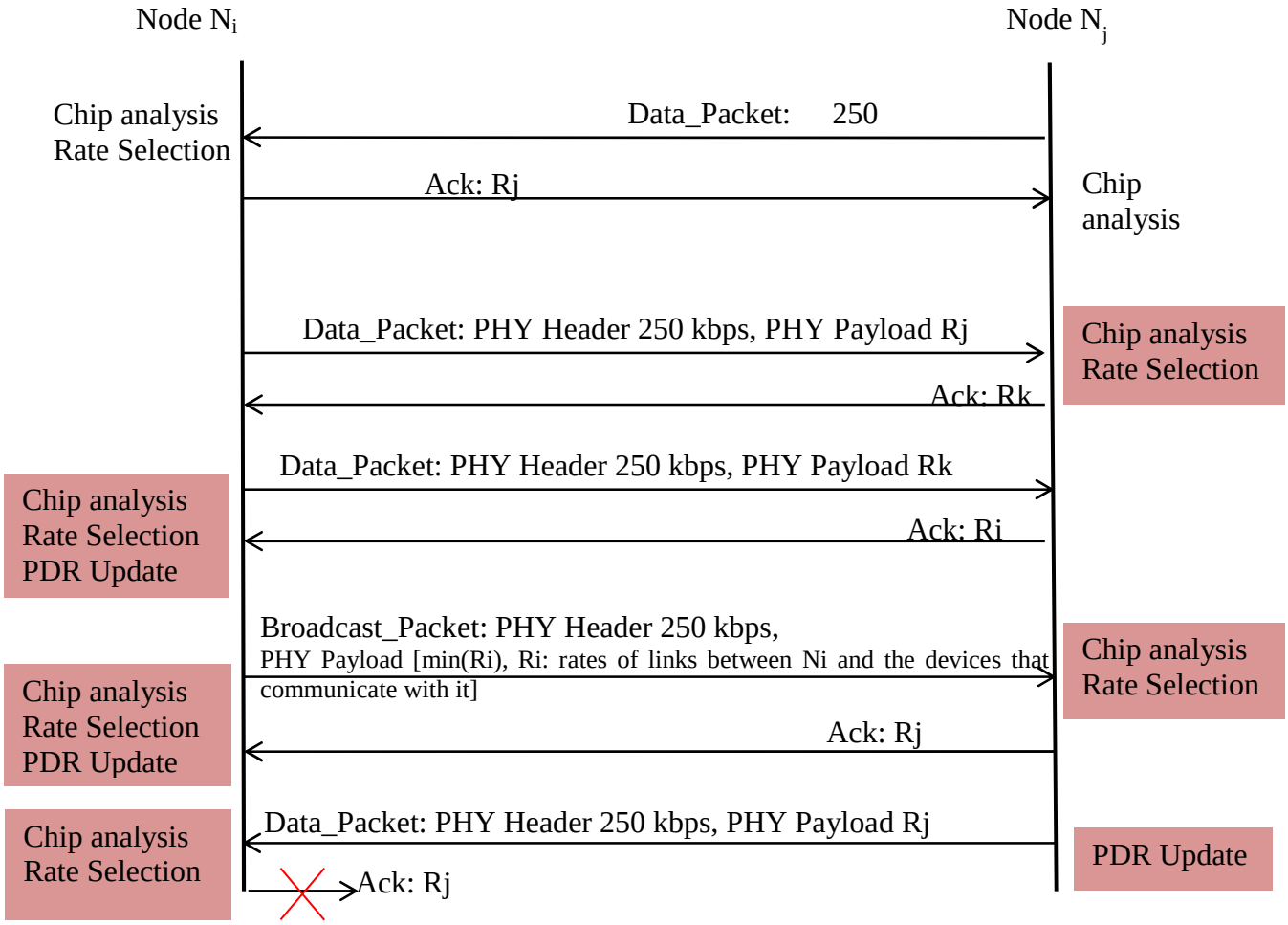

Figure 51. Data rate adaptation during packet exchange

5.3.2.1. An immediate decision to adjust data rate

The rate selection is performed thanks to *Pctg(CEPP$_{kt}$)* and *Pctg(NCP)* metrics determined from the chip errors of the last received packet. Therefore, our algorithm is responsive to the channel disruptions that may occur over time. In order to determine the appropriate rate to be used, our algorithm relies on three different thresholds. In order to introduce these thresholds, we indicate below the notations used in our algorithm.

v. Notations

- *PacketRate*: the rate at which the packet is being sent by a node N_i to a node N_j.

- *CurrentRate[i]*: the computed rate at which the node N_j sends packets to N_i.
- *CurrentRate[j]*: the computed rate at which the node N_i sends packets to N_j.
- $CEPPlw_{TH}$: lower threshold used for $Pctg(CEPP_{kt})$
- $CEPPhi_{TH}$: upper threshold for $Pctg(CEPP_{kt})$
- NCP_{TH}: threshold for *Pctg(NCP)*

vi. Choosing the appropriate data rate

The MAC sublayer uses parameters that are computed at the PHY layer in order to choose the most appropriate rate. In fact, the rate selection is updated by comparing $Pctg(CEPP_{kt})$ and *Pctg(NCP)* to the defined thresholds.

The rate selection algorithm operates as follows:

If ($Pctg(CEPP_{kt}) < CEPP_{lwTH}$ and PacketRate < 8)

    Then CurrentRate[i] = PacketRate * 2 // increase data rate

Else If (($Pctg(NCP) > NCP_{TH}$ or $Pctg(CEPP_{kt}) > CEPP_{hiTH}$) and (PacketRate > 1))

    Then CurrentRate[i] = PacketRate / 2 // decrease data rate

Else

    CurrentRate[i] = PacketRate

When node N_i receives a packet from node N_j sent at *PacketRate*, it first computes the corresponding $Pctg(CEPP_{kt})$ and *Pctg(NCP)*. Then, N_i checks if the $Pctg(CEPP_{kt})$ is lower than $CEPP_{lwTH}$. If so and if *CurrentRate[i]* is lower than the highest rate (i.e. R = 8 in Table 6), *CurrentRate[i]* is set to the next upper rate. In fact, in this case, the channel conditions are supposed to be good enough to increase the rate. However, if it is not the case, N_i checks if the $Pctg(CEPP_{kt})$ is higher than $CEPP_{hiTH}$ and if *Pctg(NCP)* is higher than NCP_{TH}. If it is the case, the channel conditions are supposed to be bad and N_i has to decrease the rate level. *CurrentRate[i]* is then set to the next lower rate if the legacy data rate (i.e. R = 1 in Table 6) has not been reached yet. Finally, if the $Pctg(CEPP_{kt})$ is between $CEPP_{lwTH}$ and $CEPP_{hiTH}$, the *PacketRate* is considered suitable to the existing channel conditions.

The combination of the $Pctg(CEPP_{kt})$ and *Pctg(NCP)* is useful in order to avoid the cases when only one part of the packet is corrupted due to an eventual exceptional event (e.g. impact of the mobility of other devices or users, collisions). In fact, using both $Pctg(CEPP_{kt})$ and *Pctg(NCP)* provides an idea of the error distribution in the packet: whether it happened

because of the bad channel conditions or because of external events. For instance, if the $Pctg(CEPP_{kt})$ is higher than $CEPP_{hiTH}$ and $Pctg(NCP)$ is lower than NCP_{TH}, the errors are distributed over a large number of PN-Codes. However, if the $Pctg(CEPP_{kt})$ is lower than $CEPP_{hiTH}$ and $Pctg(NCP)$ is higher than NCP_{TH}, the errors are distributed over a few number of PN-Codes. If the $Pctg(CEPP_{kt})$ is lower than $CEPP_{hiTH}$ and $Pctg(NCP)$ is lower than NCP_{TH}, the errors are acceptable and the channel conditions are considered good.

Of course this analysis can be more accurate if we examine the whole distribution pattern of the packet PN-Codes errors. However, this process is energy and time consuming. Therefore, our approach represents a good tradeoff between accuracy, responsiveness and energy consumption. Nonetheless, it is important to choose the appropriate thresholds for $CEPP_{lwTH}$, $CEPP_{hiTH}$ and NCP_{TH}. In the next subsection, we propose a new method to adjust these thresholds according to the channel coherence time.

5.3.2.2. Adapting the thresholds to the channel conditions

In [Heinzer 2012], authors have shown that there is a correlation between the chip error rate of a received packet and the PRR. In [Hamdi 2013], the patent proposed a method to adapt the thresholds used to change rates according to the number of success and failures of the current rate. In this patent, an additive increase multiplicative decrease (AIMD) function was incorporated in the rate adaptation algorithm for 802.11 WLAN communication systems. The AIMD rate adaptation algorithm depends on the PRR of the current rate. Thresholds of the PRR are adjusted depending on the success of transmissions.

In our approach, $CEPP_{lwTH}$ and NCP_{TH} values are adjusted every time the rate changes. Computation of these thresholds is based on the packet delivery ratio (PDR) of the current rate which is computed at MAC level. The PDR formula is given in (31). The number of received packets and the number of received ACK is reset to zero when the rate changes.

$$PDR = \frac{\text{Number of sent packets at the current rate}}{\text{number of received ACK}} * 100 \quad (31)$$

$CEPP_{lwTH}$ and NCP_{TH} thresholds computation uses two constants: α and β. In fact, they ensure the respect of the application communication requirements over time related to the PDR. When PDR is between α and β, we consider that the link between communicating nodes is

good and that the used data rate is suitable. Thus, there is no need to change the data rate thresholds. However, if PDR is lower than β (i.e. the PDR is low and the link quality is not suitable for the used data rate) or higher than α (i.e. the PDR is high and the link quality is very good for the used data rate), thresholds should be readjusted.

$$CEPP_{lwTH} = \begin{cases} CEPP_{lwTH} + A * \left(1 - \frac{PDR}{100}\right) & if\ PDR > \alpha \\ CEPP_{lwTH} - A * \frac{PDR}{100} & if\ PDR < \beta \end{cases} \quad (32)$$

$$NCP_{TH} = \begin{cases} NCP_{TH} + B * \left(1 - \frac{PDR}{100}\right) & if\ PDR > \alpha \\ NCP_{TH} - B * \frac{PDR}{100} & if\ PDR < \beta \end{cases} \quad (33)$$

The thresholds are computed according to PDR at a given data rate. Formulas are given in (32) and (33). Let us note that since PDR is a percentage, thus, we divide per 100 to obtain a value between 0 and 1. *A* and *B* are constants that are respectively used to adjust $CEPP_{lwTH}$ and NCP_{TH} thresholds. The higher A and B values, the higher the difference between the previous and the new $CEPP_{lwTH}$ and NCP_{TH} values is and vice-versa.

The aim of adjusting $CEPP_{lwTH}$ and NCP_{TH} is to ensure the stability of our algorithm as well as its responsiveness to the changes of channel conditions. In fact, nodes keep transmitting at a given data rate as long as the data rate is suitable to the channel conditions. However, if the channel conditions change, the rate has to be changed too. In our approach, when the PDR at a given data rate reaches a value which is higher than α, we consider that the channel conditions have been stable and that the $CEPP_{lwTH}$ and NCP_{TH} were suitable. In this case, the $CEPP_{lwTH}$ value is increased (i.e. the lower threshold corresponding to the percentage of the total number of chip errors per packet is increased). Therefore, data rate is more likely to be increased faster even if the channel conditions deteriorate a little (as long as $Pctg(CEPP_{kt})$ does not exceed the new value of $CEPP_{lwTH}$). At the same time, the NCP_{TH} value is increased too (i.e. the threshold corresponding to the percentage of the total number of corrupted PN-Codes per packet is increased). Thus, even when the channel conditions deteriorate a little (i.e. the percentage of the total number of corrupted PN-Codes per packet increases but does not exceed the new value of NCP_{TH}), the data rate is not decreased.

However, if the PDR is lower than β, the rate adaptation algorithm is not being efficient and thresholds are not being suitable to the current data rate. In this case, the thresholds $CEPP_{lwTH}$ and NCP_{TH} are decreased. Decreasing NCP_{TH} makes the data rate algorithm more sensitive to chip errors that may occurs. In fact, data rate is more likely to be decreased faster. At the same time, decreasing $CEPP_{lwTH}$ slows down the increase of the date rate.

Therefore, when the PDR is higher than α, increasing the algorithm encourages the increase of the data rate. However, when the PDR is lower than β, the algorithm encourages the decrease of the data rate.

5.3.3. ***Scenario description and simulation setup***

Simulations have been conducted using an ad-hoc network. Transmissions at the MAC sublayer are done according to the non-slotted IEEE 802.15.4 CSMA-CA algorithm. All nodes communicate on the same channel frequency.

Table 17. Simulation setup for the adaptive data rate adaptation algorithm

Duration of the simulation (s)	18000 (5 hours)
Routing protocol	Greedy protocol [Karp 2000]
RF transceiver	CC2420 (Table 8)
Transmission power (dBm)	0
Propagation model	Two-ray-ground
Distance between two successive nodes (m)	10
Mobility Model	Billiard
Maximum Node Speed (m/s)	3.5
CBR packet interval (s)	60
CBR packet size (Byte)	112
Hello packet interval (s)	1
Hello packet size (Byte)	80
AWGN mean (dBm)	-80
AWGN variance	3

Table 17 summarizes the parameters used in our simulations. In our scenarios, the greedy routing protocol [Karp 2000] is used: every node periodically broadcasts (P period) a NTW

HELLO message. When a node receives a HELLO message, it updates its neighbor table (i.e. which contains information about its neighbors). When an event occurs (e.g. a data message has to be sent), the data packet is forwarded to the nearest neighbor according to the neighbor table. In our simulations, the first transmission starts at a random time. Then, each second, a new HELLO message is sent. The HELLO packet size is 80 bytes at the PHY layer. A neighbor is considered lost after 2.5 seconds from the time the update occurs and if no new HELLO message has been received during this interval.

We use the constant bit rate (CBR) application to transmit data packets. In our scenarios, each node chooses a random destination and periodically sends data packets to it until the end of simulation that lasts 5 hours. The data packet size at the physical layer is 112 bytes.

We run two sets of simulations corresponding to the static use case (i.e. nodes are not moving) and to the mobility use case. In both case, at the start of the simulation, nodes are first organized in a grid network. Successive nodes are separated by 10 meters. In the mobility use case, nodes move according to the billiard mobility model. In this model, the node rebounds against the network boundaries. The maximum speed of nodes is set to 3 m/s, their initial position and the angle of their movement are random. In the mobility use case, all nodes begin to move at the start of the simulation.

The channel modeling uses the following setup:

- We use the two ray ground radio propagation model.
- We use the additive white gauss noise that is implemented according to the Box-Muller method. We set the corresponding mean to -80 dBm and the variance to 3.
- The link quality estimation is based on the CER computation. In our simulations, the BER is calculated for each PN_Code. In WSNet, the BER is equivalent to the CER. Each PN_Symbol has C chips, for instance 32 chips for the standard bit rate and 8 chips when the 1 Mb/s is used. The Hamming distance HD for each PN-code can be deduced by the following equation:

$$HD = C * BER \tag{34}$$

- The considered interferences are orthogonal interferences. In fact, since our network only uses one channel for communication, only interferences that happen within the same channel are considered.

5.3.3.1. CEPP and NCP averages

α and β parameters depend on the application requirements corresponding to PDR. Table 18 gives the values used in our adaptive data rate adaptation algorithm. We consider that the rate should be decreased when *Pctg(NCP)* of the last received packet is above 39% (i.e. $CEPP_{hiTH}$ is set to 39%) which is obviously a relatively high percentage. Therefore, there is no risk of wrongly decreasing the data rate. The constant values (A and B) used in our simulations to compute $CEPP_{lwTH}$ and NCP_{TH} thresholds are set to 5. That means that the difference between two consecutive values of $CEPP_{lwTH}$ or NCP_{TH} is in the range of [0,5] and that the maximum value is 5%. We consider that this range is suitable for the channel conditions. At the start of the simulation both $CEPP_{lwTH}$ and NCP_{TH} are set to 10%. NCP_{TH} is in the range of [5,40] and $CEPP_{lwTH}$ is in the range of [2,35].

Table 18. Parameters of the rate adaptation metrics and thresholds

A	5
B	5
A	80%
β	30%
$CEPP_{hiTH}$	39%

5.3.3.2. Battery Model

The battery model used in our simulation is a linear model: the power consumption decreases linearly with each transmission and reception. The microcontroller consumption is not taken into account. This pre-established assumption is also made considering that we use simulation-based evaluation and the microprocessor energy consumption is not known. Besides, it has been pointed out in subsection 1.2.1 that the RF transceiver is the hardware part that consumes energy the most. We consider that the processing of the channel quality estimation and the rate adaption algorithm do not require much energy compared to the RF transceiver activities. In fact, when the standard bit rate is used, the microprocessor is active during a longer time since the packets are longer. As a consequence, using the rate adaptation algorithm should even more reduce the power consumption of the microprocessor. Besides, in our study, even if a packet is corrupted, the node continues its processing; as a consequence, energy consumed at each reception concerns the whole duration of packet reception.

5.3.3.3. Implementation modifications in WSNet simulator

In order to evaluate the proposed algorithm, simulations are conducted using WSNet simulator. However, some extensions to this simulator are required in order to validate our approach. The main changes are summarized as follows:

- The acknowledgment mechanism is added to WSNet with regard to the inter-frame time intervals (subsection 2.3.5.4). Figure 52 and Figure 53 are intended to give an indication of the required modifications. The original implementation of this protocol in WSNet is given in Figure 52. The modification of the state machine that handles the unslotted CSMA-CA protocol is given in Figure 53. The retransmission of packets if the ACK is not received was not added in the state machine.
- The Box-Muller method for AWGN generation has been implemented.
- The packet processing has been modified so that BER can be computed for each received symbol and the HD can be determined according to the (34). The node also continues to process the packet until the end of the reception even if it is corrupted.
- The rate adaptation algorithm has been implemented in the simulator.

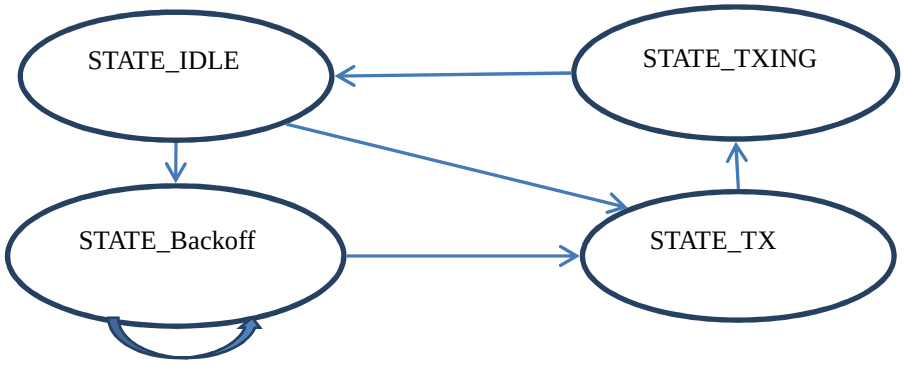

Figure 52. State machine of the unslotted CSMA-CA algorithm in WSNet simulator

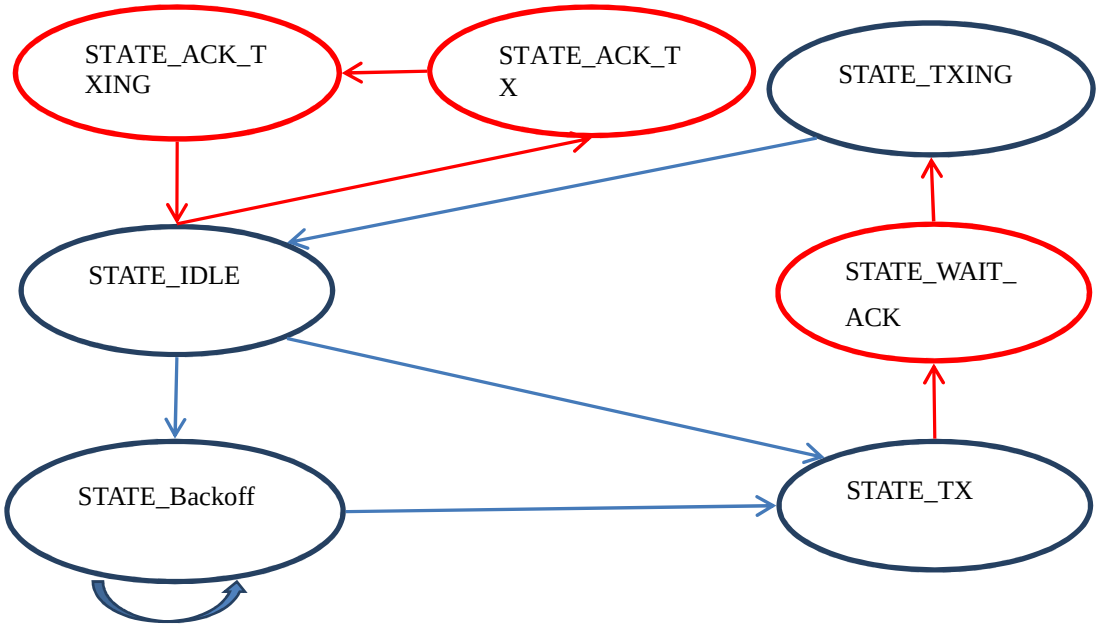

Figure 53. Modified state machine of the unslotted CSMA-CA algorithm in WSNet

*5.3.4. **PDR evaluation and mobility impact***

Figure 54 shows the PDR at the MAC sublayer obtained using our approach (named ADAPT in the Figure 54) and for the standard protocol (named STD in the same figure). This PDR includes both routing and CBR packets. It is important to take into consideration when analyzing the simulation results that the lowest data rate is the legacy rate. Increasing the rate means that channel conditions are good enough to do it without distorting the transmitted signals. The throughput (or PDR) should then be better when we do not use the rate adaptation algorithm that includes higher rates. However, we notice in Figure 54 that, except the case of only two communicating nodes, there is a very slight difference in the PDR between our approach (ADAPT) and the standard (STD). We also notice that PDR dramatically drops when the number of nodes increases. The same conclusions can be derived on the PDR of CBR packets from Figure 55 concerning the mobility use case (Mob). However, it can be noticed, in Figure 55, that in the static use case (Stc), the PDR in higher when using our data rate adaptation algorithm. This result highlights the efficiency of our approach in comparison with the standard. In fact, in our simulation scenarios, the nodes are spaced by 10 m which is a relatively high distance when using the two-ray ground propagation model. The channel coherence time is, therefore, very short. However, the packet interval is set to 60 seconds which appears to be not well adjusted regarding the channel coherence time. Using the data rate adaptation algorithm improved the PDR without changing

the packet interval. In the mobility use case scenario, this is not the case. In fact, in ad hoc networks, the mobility increases the connectivity of the mobile node, which increases the PDR.

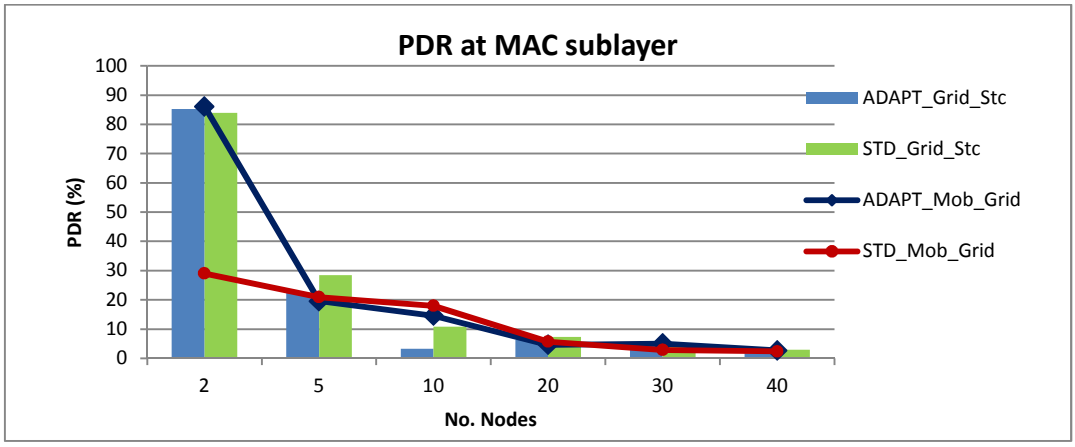

Figure 54. Packet delivery ratio (PDR) at the MAC sublayer vs. network nodes' number for static (Stc) and mobile (Mob) scenarios: The static and mobile scenarios are evaluated using respectively our rate adaptation algorithm (ADAPT) and the standard protocol (STD)

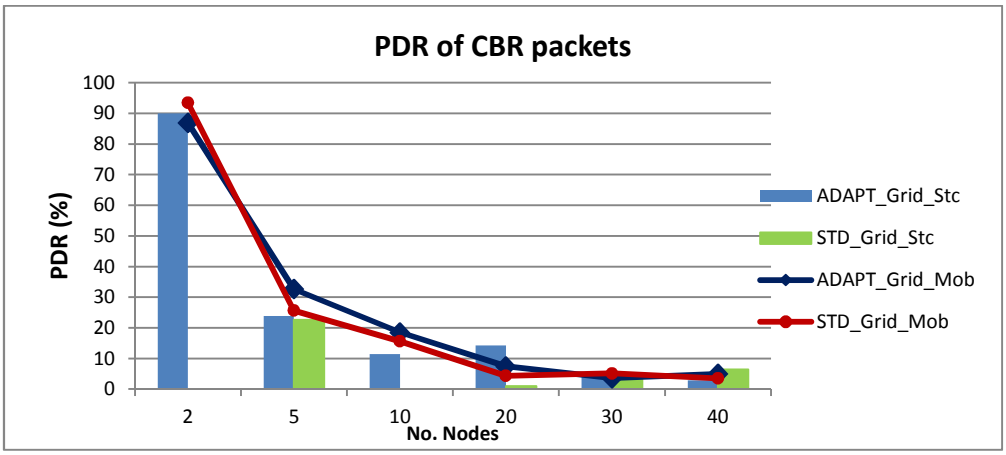

Figure 55. CBR Packet delivery ratio (PDR) vs. network nodes' number for static (Stc) and mobile (Mob) scenarios: The static and mobile scenarios are evaluated using respectively our rate adaptation algorithm (ADAPT) and the standard protocol (STD)

*5.3.5. **Energy efficiency***

Figure 56 and Figure 57 shows results corresponding respectively to the energy consumption and the gain in energy for both the mobility and the static use cases in comparison with the standard protocol. As it can be seen in Figure 56 and Figure 57, it is not possible to determine which case is more energy efficient by considering only the energy results. The results relative to the PDR must be considered in order to figure out the real energy gain. To that end, we

introduce a new metric to evaluate our approach which is the energy efficiency Eff_{Ntw} of the network. It is computed as follows:

$$Eff_{Ntw} = \frac{Average\ consumed\ energy}{Average\ number\ of\ received\ ACK\ packet} \quad (35)$$

It can be seen in Figure 58 that in all cases, our approach is more energy efficient. The gain in energy efficiency can reach up to 33%.

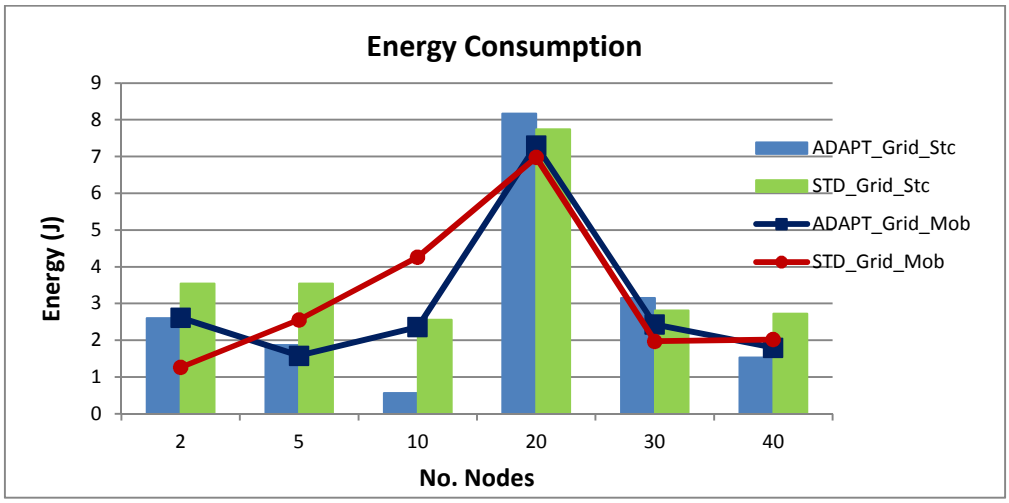

Figure 56. Energy consumption in both scenarios vs. network nodes' number for static (Stc) and mobile (Mob) scenarios

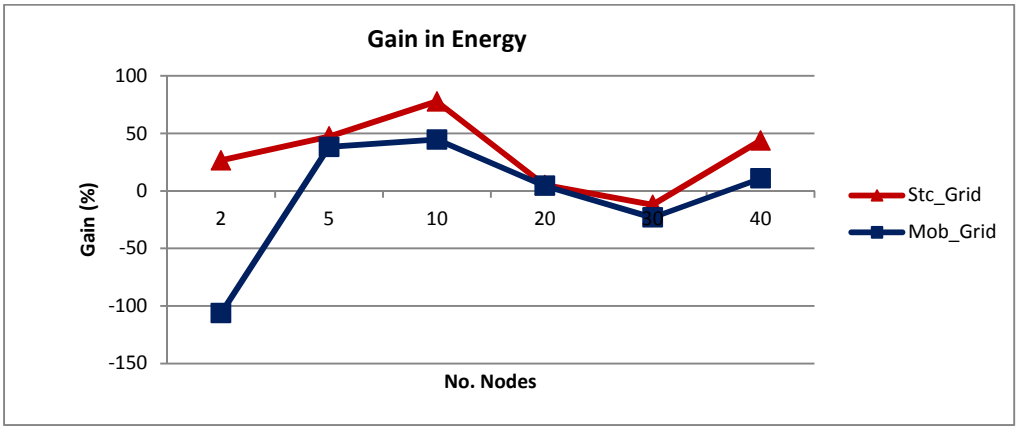

Figure 57. Gain in energy in comparison to the standard for static (Stc) and mobile (Mob) scenarios

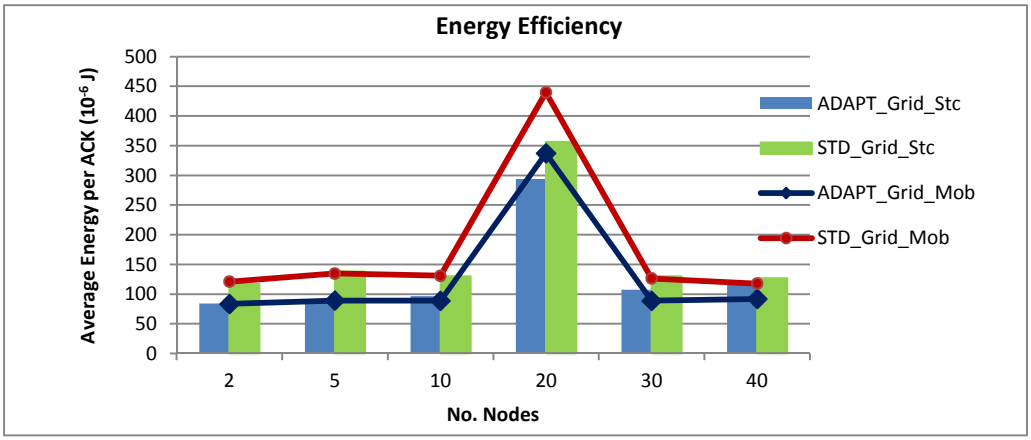

Figure 58. Network energy efficiency: ADAPT is the proposed approach, STD corresponds to standard protocol scenario, Mob and Stc respectively indicate whether nodes are mobile or static

5.4. Summary

We have first proposed a hybrid mobility-aware data rate adaptation algorithm. The joint mobility management and rate adaptation modules are based on the LQI parameter. The rate adaptation algorithm uses LQI thresholds and dynamically adjusts them according to the most recent handover procedure conduct. Although adding three additional rates to the IEEE 802.15.4 standard protocol does not require heavy changes in the hardware design, we have shown that our joint approach (RA+MM approach) is more energy efficient compared to the standard protocol and also to the case where only the mobility management approach is considered (MM approach). In fact, simulations have demonstrated that besides the considerable improvement in the average time of synchronization for both MM and RA+MM approaches compared to STD approach, the average remaining energy in RA+MM is higher. We have also analyzed the performance of communicating nodes (a sender and a receiver) and have figured out that the high remaining energy when using the standard protocol (STD) is due to long periods of synchronization loss during which nodes do not communicate. We have also demonstrated the energy efficiency of our approach compared to the mobility management (MM) approach. Communicating node analysis has also shown the efficiency of our approach in terms of synchronization time. In fact, the number of received beacons for both sender and receiver is higher than the average beacon number. Finally, we have highlighted the impact of changing the packet interval on the network performance.

After that, we have proposed a second hybrid rate adaptation approach for mobile IEEE 802.15.4 nodes based on the chip error rate (CER). This algorithm introduces the

Pctg($CEPP_{kt}$*)* and *Pctg(NCP)* percentages metrics that have been computed based on CER of both correctly received and corrupted packets. We have defined $CEPP_{lwTH}$, $CEPP_{hiTH}$ and NCP_{TH} thresholds for *Pctg(*$CEPP_{kt}$*)* and *Pctg(NCP)*. $CEPP_{lwTH}$ and NCP_{TH} thresholds are adjusted using the PDR corresponding to the current used data rate, thus ensuring responsiveness to the channel conditions variations. We have first noticed when examining the simulation result that PDR increases when the number of nodes decreases. We have also observed a slightly higher PDR using our approach even though the data rates used are higher than the legacy rate. The PDR of CBR packets can even be significantly higher in some cases. Finally, simulations have proved the energy efficiency of our method in comparison with the standard protocol. The gain in energy efficiency for both mobility and static use cases' approaches in comparison with the standard protocol can reach up to 33%.

The study conducted during the first part of this chapter (mobility-aware rate adaptation algorithm) has been published in [Chaabane 2014]. A second publication presenting the hybrid adaptive algorithm will be soon submitted in a journal.

Chapter 6. **Conclusion and perspectives**

6.1. Conclusion

An overview of the IEEE 802.15.4/ZigBee protocol and a state of the art related to its energy efficiency and to the properties that are related to the protocol specification at the PHY and MAC layers (e.g. signal strength, node active periods, CSMA-CA protocol) have been conducted. Through this study, it has been made clear that even though IEEE 802.15.4/ZigBee protocol offers mechanisms that reduce energy consumption such as the use of the idle mode and the low transmission signal power, the energy efficiency of the protocol has proven not to be optimized. Moreover, we have pointed out that unlike some other wireless protocols, IEEE 802.15.4 does not include an efficient mobility management module.

This thesis has proposed a global network organization for mobile communicating nodes and has focused on both the global organization and the node itself. The main constraint in this study is the limitation in hardware and energy budget of mobile nodes. Our proposed approaches and methods had to ensure efficiency while avoiding relatively heavy computations and changes in the standard protocol. The work has targeted the first three low layers (PHY, MAC and NWK). First, we have defined a network architecture that takes into consideration low energy budget of mobile nodes. We have proposed a cluster tree architecture where each cluster is initialized by a static coordinator that defines a unique channel frequency on which all cluster nodes have to communicate. Node synchronization is ensured using IEEE 802.15.4 beacon-enabled mode.

We investigated two main features that are the mobility management and the data rate adaptation. We highlight below the proposed approaches and the most important results.

6.1.1. ***Mobility management***

Mobility management strategy has to keep mobile nodes connected to the network when they move from one cluster to another. This is ensured thanks to the anticipation of change of cells based on the link quality between end devices and their coordinators and also thanks to the knowledge of coordinator locations. A new mobility management approach has been presented and evaluated using simulations. The proposed mobility management approach anticipates the link disruption by controlling the LQI value of each received packet and uses a speculative algorithm. An $LQI_{threshold}$ formula and two speculative algorithms have been proposed and evaluated in a grid network. The speculative algorithms are the same-road and the probabilistic algorithms. The efficiency of the mobility management approach has been demonstrated. In fact, the gains in energy and delay in comparison to the standard protocol procedure are important. Moreover, the mobility management approach has proven its efficiency even in a noisy environment. In addition to that, obtained simulations have pointed out that the mobility behavior of end devices has a great impact on network performance.

6.1.2. ***Rate adaptation***

In mobile network, there is a high fluctuation of the channel conditions that may either improve or deteriorate the link rapidly. We have used this property to adapt data rate in order to reduce energy consumption of mobile nodes while maintaining a good link quality. Therefore, this study has also focused on the data rate adaptation for IEEE 802.15.4 mobile nodes. We have first combined a mobility-aware data rate adaptation algorithm with the proposed mobility management approach. The mobility-aware rate adaptation network is also based on the LQI parameter and uses LQI thresholds that are dynamically adjusted according to the most recent handover procedure. We have shown that our mobility-aware data rate adaptation approach (RA+MM approach) is more efficient compared to the standard protocol and to the case where only the mobility management approach is used (MM approach). Its efficiency has been evaluated in terms of energy consumption and synchronization time. We have also highlighted the impact of changing the data packet transmission interval on the network performance. After that, we have proposed a hybrid rate adaptation approach for mobile IEEE 802.15.4 nodes based on the chip error rate (CER). This adaptive rate adaptation algorithm introduces the $Pctg(CEPP_{kt})$ and $Pctg(NCP)$ percentages metrics that have been computed based on CER of both correctly received and corrupted packets. We have defined

$CEPP_{lwTH}$, $CEPP_{hiTH}$ and NCP_{TH} thresholds for $Pctg(CEPP_{kt})$ and $Pctg(NCP)$. $CEPP_{lwTH}$ and NCP_{TH} thresholds are adjusted using the PDR corresponding to the current used rate, thus ensuring responsiveness to the channel conditions variations. Simulations have proved the energy efficiency of our method in comparison with the standard protocol. We have also observed a slightly higher PDR using our approach even though the rates used are higher than the legacy rate. In addition to that, we have also noticed the impact of the number of mobile nodes (the PDR decreases when the number of nodes increases). Finally, the gain in energy efficiency can reach up to 33%.

6.2. Perspectives

This thesis work opens many interesting research perspectives that are examined in the following sections.

6.2.1. ***A more efficient dynamic $LQI_{threshold}$ management***

In our work, the β parameter that has been used in $LQI_{threshold}$ computation has been set to a constant. However, it has been demonstrated in subsection 4.7.2 that the network performance changes depending on the β parameter value. Therefore, this parameter can be adjusted dynamically. The adaptive method could be based on the network conditions such as the number of end devices in the cluster, the number of transmitting nodes among them, the distance from the coordinator, the estimation of the node velocity, etc.

6.2.2. ***Enhancement of the speculative algorithm***

The proposed speculative algorithms are efficient but they are based on prediction, thus not very accurate. The probabilistic speculative algorithm itself may be evaluated using other sets of probabilities (i.e. the probabilities of selecting a coordinator on a different road). Another method for selecting next coordinator can be proposed. A model using ARIMA or another auto-regressive method [Lee 2010] can be more realistic and could be compared to our algorithm mainly in term of energy since auto-regressive algorithms are more complex than predictive algorithm. Another model based on location awareness could also be addressed. However, we should overcome the poor accuracy of the RF-based ranging method of this latter model and the high system complexity. In [Lanzisera 2009b] for instance, a roundtrip

RF time of flight ranging method for narrow-band radios was presented that successfully deals with these errors.

*6.2.3. **Accurate IEEE 802.15.4 protocol stack modeling***

It is important to mention that the lack of an accurate IEEE 802.15.4 protocol stack modeling simulator make results debatable in some use cases. In fact, methods that depend on PHY parameters (i.e. PHY-aware algorithms) have to be evaluated using a relatively accurate simulator. However, here again, a tradeoff between accuracy and complexity (e.g. development time, access to simulator modules, simulation run time) should be considered. On the other hand, algorithms that use information from upper network layers tolerate the use of less accurate simulators. In order to test a routing protocol for instance, one tolerates the inaccuracy of the channel modeling. Actually, the margin of error of the channel modeling in this case is negligible compared to the effect of errors related to the network. In our study, we had to use two different simulators, NS-2 and WSNet, in order to validate our approaches. Even though modifications have been performed on both simulators, they are still not sufficient enough to be used in comparing the two proposed data rate algorithms to each other due to implementation differences. Both simulators also do not offer the possibility to evaluate the adaptive rate adaptation algorithm when it is combined with our mobility management approach. However, it is naturally possible to add the beacon-enabled mode in WSNet [Nazim 2011][1]. At some point, experimentations using real WSN hardware platforms should be conducted in order to give a more realistic evaluation of our work in a real scenario.

*6.2.4. **Harvesting energy***

This thesis has focused on reducing energy consumption. We have considered in our simulations an initial amount of energy for each node (typically a battery). However, several

[1] In [Nazim 2011], an implementation in the WSNet simulator of the beacon enabled mode was performed. However, this new version was not available by the time this study was being conducted.

studies [Sudevalayam 2011] and some real platforms offered an energy harvesting system in order to increase node life time [CC2500]. This system can be used in designing sensor applications and algorithms. In fact, some parameters can be tuned based on the available energy budget to prevent battery full-discharge of the nodes. These parameters include packet transmission interval, signal power strength, shutting off some modules such as localization system [Castagnetti 2014]. In our case, adding an energy harvesting system can be used by the rate adaptation algorithm. Information on the battery state of charge could be considered as an additional parameter for the data rate selection.

*6.2.5. **Impact of α and β on the rate adaptation algorithm***

We have used statistics of CER distribution over packet in the adaptive rate adaptation algorithm and we have combined them to the PRR. To do so, we have used two parameters α and β that have been set to a constant value during simulations. It would be worth evaluating the impact of changing their values deeper. It is also important to notice that making decisions over several packet transmissions by analyzing successive frames (statistics) can help to identify mobility and interference-induced errors. It is for instance well established that errors over time increase in case of mobility [Wu 2010]. The coordinator should save the history of the $avg(CEPP_{kt})$ and $avg(NCP)$ of each node. Keeping track of the variation of these values may be useful to manage the mobility and control the network congestion by tuning packet transmission time.

*6.2.6. **A reverse mobility approach in order to reduce energy consumption***

In this thesis, we have focused on presenting approaches to manage the mobility of sensor end devices. The mobility of end devices was random even though we used mobility models to evaluate our approaches. The node mobility randomness deteriorates the network performance in terms of energy and synchronization time. It also has an important impact on the routing protocol. However, from another perspective and depending on the application characteristics, mobility can be investigated the other way around. That means that end devices would be static and the coordinator (i.e. the sink) would be mobile in order to optimize communication cost [Vlajic 2011] [Gomez 2012]. The mobile sink would have either an optimized mobility or a fixed (constrained) mobility. In the first case, the sink's path is a function of a particular network variable and the path is continuously adjusted to ensure optimal network

performance with regard to one or more performance metrics. On the other hand, the fixed mobility is fully deterministic. The sink follows a limited and well-defined set of path-segments inside the network field. The fixed trajectory is typically imposed by the nature of the physical terrain and/or presence of obstacles in the environment (e.g. walls, buildings, vegetation).

I think this kind of approach could be especially adapted in environments where there is a need to pick up and collect some environmental measures using mobile devices (e.g. smart phone, tablet, etc.). This is useful in home monitoring field or industrial environments.

Another way to use mobility is the use of opportunistic communication in ad hoc network [George 2010]. In this case, when two devices happen to be in the same neighborhood, they communicate to keep track of each other and/or to exchange data.

6.2.7. ***Interoperability of mobile devices and security issues***

Nowadays, users increasingly use a large number of devices that do not necessarily use the same wireless protocol. The emerging concept of the *Internet of Things* (IoT) raises new issues. In fact, the interoperability of different types of devices is increasingly required. Devices need to be connected to each other without human intervention. These countless possibilities of connecting different interfaces that use different communication protocols push the scientific community along with industrialists to think about a new standardization in order to optimize communication between different kinds of devices (e.g. smart phone, sensors, computers, etc.). There are some advances made in this area that try to propose solutions for the IoT. In that spirit, the 6LowPAN protocol is proposed in order to connect via internet sensor devices to other type of devices. However, this protocol has proven to be heavy considering the hardware limitation of sensor nodes. Another basic solution is the use of several protocol interfaces at some devices that will handle the packet adaptation and the routing. However, switching between protocols has to ensure the maintaining of the communication. One can also develop new methods that dynamically change the communication interface according to the available link quality on each interface or according to the application requirements. For instance, in our proposed architecture, coordinators may have different interfaces in order to allow other devices using different protocols to connect.

The variety of protocols and the mobility of nodes also require security cautions. The 802.15.4 MAC layer proposes security options. However, despite the fact that the

specification includes a number of security provisions and options, it was highlighted in [Sastry 2004] that the security issue was not well handled. This feature is even more important when dealing with mobile nodes that need to be able to synchronize with different types of devices in different types of networks. Controlling the access to these networks and some confidential information within mobile nodes is a crucial issue.

A possible extension of this work would be to study the possibilities to connect different types of devices in a global network architecture that is service-oriented. However, it should not change the habits of people but adapt the services and the deployment to user's expectations. Therefore, mobility management and data rate adaptation should be handled according to the link quality, but regardless of the used protocol.

References

[Abbagnale 2009] A. Abbagnale, E. Cipollone, and F. Cuomo, “A Case Study for Evaluating IEEE 802.15.4 Wireless Sensor Network Formation with Mobile Sinks,” ICC’09, pp.1-5, 14-18 June 2009.

[Akyildiz 2005] I. F. Akyildiz, and W. Xudong, "A survey on wireless mesh networks," Communications Magazine, IEEE 43.9 (2005): S23-S30. 2005.

[Anastasi 2009] G. Anastasi, M. Conti, M. Di Francesco, et al, “Energy conservation in wireless sensor networks: A survey,” Ad Hoc Networks, 2009, vol. 7, no 3, p. 537-568.

[Anastasi 2010] G. Anastasi, M. Conti, M. Di Francesco, and V. Neri, "Reliability and energy efficiency in multi-hop IEEE 802.15.4/ZigBee Wireless Sensor Networks," Computers and Communications (ISCC), 2010 IEEE Symposium on , vol., no., pp.336,341, 22-25 June 2010.

[Anastasi 2011] G. Anastasi, M. Conti, and M. Di Francesco, “A Comprehensive Analysis of the MAC Unreliability Problem in IEEE 802.15.4 Wireless Sensor Networks,” IEEE TRANSACTIONS ON INDUSTRIAL INFORMATICS, VOL. 7, NO. 1, 2011.

[Aschenbruck 2010] N. Aschenbruck, R. Ernst, E. Gerhards-Padilla, and M. Schwamborn, “BonnMotion: a mobility scenario generation and analysis tool,” the 3rd International ICST Conference on Simulation Tools and Techniques (SIMUTools '10), pp. 51:1—51, 2010.

[Bharathidasan 2002] A. Bharathidasan, and A. Vijay, "Sensor networks: An overview." paper, University of California, Davis, CA (August 2002) (2002).

[Biaz 2008] S. Biaz, and W. Shaoen, “Rate adaptation algorithms for IEEE 802.11 networks: A survey and comparison,” Computers and Communications, 2008. ISCC 2008. IEEE Symposium on. IEEE, 2008.

[Bluetooth] Bluetooth SIG - www.Bluetooth.com

[Bougard 2005] B. Bougard, F. Catthoor, D. C. Daly, A. Chandrakasan, and W. Dehaene, “Energy Efficiency of the IEEE 802.15.4 Standard in Dense Wireless Microsensor Networks: Modeling and Improvement Perspectives,” In Proceedings of the conference on Design, Automation and Test in Europe - Volume 1 (DATE '05), Vol. 1. IEEE Computer Society, Washington, DC, USA, 196-201.

[Box 1958] G. Box, and M. Muller, “A Note on the Generation of Random Normal Deviates,” Annals Math. Statistics, vol. 29, pp. 610-611, 1958.

[Braem 2010] B. Braem, and C. Blondia, “Supporting mobility in Wireless Body Area Networks: An analysis,” Body Sensor Networks (BSN), pp 52–55, 7-9 June 2010.

[Camp 2002] T. Camp, J. Boleng, and V. Davies, “A Survey of Mobility Models for Ad Hoc Network Research,” Wireless Communication and Mobile Computing (WCMC), Special issue on Mobile Ad Hoc Networking: Research, Trends and Applications, vol. 2, no. 5, pp. 483–502, September 2002.

[Cao 2009] H. Cao, V. Leung, C. Chow, and H. Chan, “Enabling technologies for wireless body area networks: A survey and outlook,” Communications Magazine, IEEE, 47(12), 84-93. 2009.

[CarbonRoom] Carbon War Room Main Page - http://www.carbonwarroom.com/

[Cassandras 2005] C. G. Cassandras, and Wei Li, "Sensor networks and cooperative control," European Journal of Control 11.4 (2005): 436-463.

[Castagnetti 2014] A. Castagnetti, A. Pegatoquet, T. Le, and M. Auguin, “A Joint Duty-Cycle and Transmission Power Management for Energy Harvesting WSN,” to appear in IEEE Transactions on Industrial Informatics Journal, Special section on “Industrial Wireless Sensor Networks”, 2014.

[CC2420] CC2420 Single Chip Low Cost Low Power RF Transceiver - http://www.chipcon.com/files/ CC2420 data sheet 1

[CC2500] CC2500 Single Chip Low Cost Low Power RF Transceiver - http://www.chipcon.com/files/ CC2500 data sheet 1.

[Chandrakasan 1999] A. Chandrakasan, R. Amirtharajah, C. SeongHwan, K. J. Goodman, G. Konduri, J. Kulik, W. Rabiner, and A. Wang, "Design considerations for distributed microsensor systems," Custom Integrated Circuits, 1999. Proceedings of the IEEE 1999, vol., no., pp.279,286, 1999.

[Crossbow] Crossbow - http://www.xbow.com

[Dessales 2010] D. Dessales, A. Poussard, R. Vauzelle, N. Richard, F. Gaudaire, and C. Martinsons, "Physical layer study in a goal of robustness and energy efficiency for wireless sensor networks," Design and Architectures for Signal and Image Processing (DASIP), 2010 Conference on , vol., no., pp.214,221, 26-28 Oct. 2010.

[Dutta 2013] D. Dutta, D. Saikia, A. Karmakar, “Analysis of IEEE 802.15.4 MAC under low duty cycle,” In: CoRR, abs/1301.6532 (2013).

[Ekici 2006] E. EKICI, Y. GU, and D. BOZDAG, “Mobility-based communication in wireless sensor networks,” IEEE Communications Magazine, 2006, vol. 44, no 7, p. 56.

[ETSI 1998] European Telecommunications Standards Institute (ETSI): Universal Mobile Telecommunications System (UMTS) - Selection procedures for the choice of radio transmission technologies of the UMTS, UMTS 30.03 version 3.2.0, TR 101 112. 1998.

[Faridi 2010] A. Faridi, M.R. Palattella, A. Lozano, M. Dohler, G. Boggia, L.A. Grieco, and P. Camarda, "Comprehensive Evaluation of the IEEE 802.15.4 MAC Layer Performance With Retransmissions," Vehicular Technology, IEEE Transactions on , vol.59, no.8, pp.3917,3932, Oct. 2010.

[Ferreira 2007] L. Ferreira, and R. Rocha, "Multi-Channel Clustering Algorithm to Improve Performance of WSNs," proceedings of CONFTELE 2007, 6th Conf. on Telecommunications, May 2007.

[Fonseca 1996] R. Fonseca, O. Gnawali, K. Jamieson, and P. Levis, “Four bit wireless link estimation,” in HotNets VI, 2007. "Wireless Communications: Principles and Practice", Theodore Rappaport, 1996.

[Francesco 2011] M. Di Francesco, G. Anastasi, M. Conti, M.; S.K. Das, and V. Neri, "Reliability and Energy-Efficiency inIEEE 802.15.4/ZigBee Sensor Networks:An Adaptive and Cross-Layer Approach," Selected Areas in Communications, IEEE Journal on , vol.29, no.8, pp.1508,1524, September 2011.

[Freescale] Zigbee/IEEE 802.15.4 Standards and Architecture Overview.

http://www.freescale.com/files/training_pdf/28081_ZIGBEE_OVERVIEW_WBT.pdf?lang_cd=en

[Ganeriwal 2005] S. Ganeriwal, D. Ganesan, H. Shim, V. Tsiatsis, and M. B. Srivastava, “Estimating Clock Uncertainty for Efficient Duty-cycling in Sensor Networks,” in Proc. Third ACM Conference on Sensor Networking Systems, Nov. 2005, pp. 130–141.

[Garcia 2007] C. F. Garcia-Hernandez, P. H. Ibraguengoytia-Gonzalez, J. Garcia-Hernandez et al, "Wireless sensor networks and applications: a survey," IJCSNS International Journal of Computer Science and Network Security, 2007, vol. 7, no 3, p. 264-273.

[George 2010] S.M. George, Wei Zhou, H. Chenji, Myounggyu Won, Yong Oh Lee, A. Pazarloglou, R. Stoleru, and P. Barooah, "DistressNet: a

wireless ad hoc and sensor network architecture for situation management in disaster response," Communications Magazine, IEEE , vol.48, no.3, pp.128,136, March 2010.

[Gomez 2012] C. Gomez, J. Oller, and J. Paradells, “Overview and evaluation of bluetooth low energy: An emerging low-power wireless technology,” Sensors, 2012, vol. 12, no 9, p. 11734-11753.

[Papadimitratos 2005] P. Papadimitratos, A. Mishra, and D. Rosenburgh, “A cross-layer design approach to enhance 802.15.4,” In Military Communications Conference, MILCOM, 2005, p. 1719-1726, October, 2005

[Guglielmo 2012] D. De Guglielmo, G. Anastasi, and M. Conti, "A localized de-synchronization algorithm for periodic data reporting in IEEE 802.15.4 WSNs," Computers and Communications (ISCC), 2012 IEEE Symposium on , vol., no., pp.000605,000610, 1-4 July 2012.

[Hamdi 2013] M. Hamdi, “WIRELESS LAN DATA RATE ADAPTATION,” STMicroelectronic Ltd. (Hong Kong), Patent number: 8547841, October 1, 2013.

[Hanzalek 2010] Z. Hanzalek, and P. Jurčík, "Energy Efficient Scheduling for Cluster-Tree Wireless Sensor Networks With Time-Bounded Data Flows: Application to IEEE 802.15.4/ZigBee," Industrial Informatics, IEEE Transactions on , vol.6, no.3, pp.438,450, Aug. 2010.

[Heinzer 2012] P. Heinzer, V. Lenders and F. Legendre, “Fast and Accurate Packet Delivery Estimation based on DSSS Chip Errors,” INFOCOM 2012, Proceedings, pp. 2916-2920. IEEE, Orlando, Florida, USA, March 2012.

[Holland 2001] G. Holland, N. Vaidya, and P. Bahl, “A rate adaptive mac protocol for multi-hop wireless networks,” Proceedings of the ACM MobiCom, 2001.

[IEEE TG 15.4 2006] IEEE TG 15.4, `Part 15.4: Wireless Medium Access Control (MAC) and Physical Layer (PHY) Specifications for Low-Rate Wireless Personal Area Networks (WPANs)', IEEE Std., New York, 2006.

[IEEE 802.11f 2003] WG802.11 - Wireless LAN Working Group, LAN/MAN Standards.
Linkhttp://standards.ieee.org/findstds/standard/802.11F-2003.html

[Jamieson 2007] K. Jamieson, and H. Balakrishnan, “PPR: partial packet recovery for wireless networks,” SIGCOMM Comput. Commun. Rev. 37, 4 (August 2007), 409-420. DOI=10.1145/1282427.1282426 http://doi.acm.org/10.1145/1282427.1282426

[Jung 2009] C. Y. Jung, H. Y. Hwang, D. K. Sung, and G. U. Hwang, "Enhanced Markov Chain Model and Throughput Analysis of the Slotted CSMA/CA for IEEE 802.15.4 Under Unsaturated Traffic Conditions", IEEE Transactions on Vehicular Technology, Jan. 2009, vol. 58, no. 1.

[Karp 2000] B. Karp, and H. T. Kung, "GPSR: Greedy perimeter stateless routing for wireless networks," In Proceedings of the 6th annual international conference on Mobile computing and networking, pp. 243-254, August, 2000.

[Kouyoumdjieva 2012] S.T. Kouyoumdjieva, O. Helgason, E.A. Yavuz, and G. Karlsson, "Evaluating an energy-efficient radio architecture for opportunistic communication," Communications (ICC), 2012 IEEE International Conference on , vol., no., pp.5751,5756, 10-15 June 2012.

[Kohvakka 2006] M. Kohvakka, M. Kuorilehto, M. Hännikäinen, and T. D. Hämäläinen, “Performance analysis of IEEE 802.15.4 and ZigBee for large-scale wireless sensor network applications,” In Proceedings of the 3rd ACM international workshop on Performance evaluation of wireless ad hoc, sensor and ubiquitous networks (PE-WASUN '06), ACM, New York, NY, USA, 48-57, 2006.

[Koubaa 2008] A. Koubaa, A. Cunha, M. Alves, and E. Tovar, “TDBS: a time division beacon scheduling mechanism for ZigBee cluster-tree wireless sensor networks,” Real-Time Systems 40(3), pp. 321-354, 2008.

[Krief 2008] F. Krief, "Les systèmes embarqués communicants : Mobilité, sécurité, autonomie," Hermes Science Publications, 2008 - 312 pages.

[Lacage 2004] M. Lacage, M. H. Manshaei, T. Turletti, “IEEE 802.11 rate adaptation: a practical approach,” ACM MSWiM ’04.

[Lanzisera 2009a] S. Lanzisera, A. M. Mehta, and K. S. J. Pister, “Reducing average power in wireless sensor networks through data rate adaptation,” In Proceedings of the 2009 IEEE international conference on Communications (ICC'09). IEEE Press, Piscataway, NJ, USA, 480-485.

[Lanzisera 2009b] S. M. Lanzisera, and K. Pister, “RF Ranging for Location Awareness,” Thesis, EECS Department, University of California, Berkeley, May 19, 2009 - http://www.eecs.berkeley.edu/Pubs/TechRpts/2009/EECS-2009-69.html

[Lee 2006] T. Lee, H. R. Lee, and M. Y. Chung, `MAC throughput limit analysis of slotted CSMA/CA in IEEE 802.15.4 WPAN', IEEE Commun. Lett., Jul. 2006, vol. 10, no. 7, pp. 561-563.

[Lee 2007] J. Lee, S. Yu-Wei, and S. Chung-Chou, "A comparative study of wireless protocols: Bluetooth, UWB, ZigBee, and Wi-Fi," Industrial Electronics Society, 2007. IECON 2007. 33rd Annual Conference of the IEEE. IEEE, 2007.

[Lee 2010] J. Lee, H. Kim, Y. Choi, Y. Chung, S. Rhee, “IP Mobility Performance Enhancement Using Link-Layer Prediction,” FGIT, pp. 171-179, 2010.

[Lu 2004] G. Lu et al., “Performance Evaluation of the IEEE 802.15.4 MAC for Low-Rate Low-Power Wireless Networks”, in Proc. EWCN’04, April 2004.

[Mangharam 2007] R. Mangharam, A. Rowe, and R. Rajkumar, "FireFly: a cross-layer platform for real-time embedded wireless networks," Real-Time Systems, vol. 37, issue, pp. 183-231, December 2007.

[Martelli 2011] F. Martelli, R. Verdone, C. Buratti, "Link Adaptation in Wireless Body Area Networks," Proc. of IEEE VTC Spring, Budapest, May 15-18, 2011.

[Mehta 2012] A. M. Mehta, “Mobility in Wireless Sensor Networks,” Thesis, EECS Department, University of California, Berkeley, December 8, 2012.

http://www.eecs.berkeley.edu/Pubs/TechRpts/2012/EECS-2012-270.html

[Miluzzo 2008] Miluzzo, E., Zheng, X., Fodor, K., & Campbell, A. T. (2008). Radio characterization of 802.15. 4 and its impact on the design of mobile sensor networks. In Wireless Sensor Networks (pp. 171-188). Springer Berlin Heidelberg.

[Mirza 2005] D. Mirza, M. Owrang, and C. Schurgers, “Energy-Efficient Wakeup Scheduling for Maximizing Lifetime of IEEE 802.15.4 Networks,” In Proceedings of the First International Conference on Wireless Internet (WICON '05). IEEE Computer Society, Washington, DC, USA, 130-137. 2005.

[Mouly 1992] M. Mouly, M. B. Pautet, and T. Foreword By-Haug, "The GSM system for mobile communications," Telecom Publishing, 1992.

[Nazim 2011] A. Nazim, and F. Theoleyre, "Implementation of a wsnet module to simulate the IEEE 802.15. 4 beacon-enabled mode in multihop topologies," (2011).

[Neugebauer 2005] M. Neugebauer, J. Ploennigs, K. Kabitzsch, "A new beacon order adaptation algorithm for IEEE 802.15.4 networks," Wireless

Sensor Networks, Proceeedings of the Second European Workshop on , vol., no., pp.302,311, 2005.

[Nia-Chiang 2006] L. Nia-Chiang, C. Ping-Chieh, S. Tony, Y. Guang, C. LingJyh, and G. Mario, “Impact of Node Heterogeneity in ZigBee Mesh Network Routing,” Systems, Man and Cybernetics (ICSMC '06), vol. 1, pp. 187–191, 8-11 October 2006.

[Norouzi 2012] A. Norouzi, and A. H Zaim, "An Integrative Comparison of Energy Efficient Routing Protocols in Wireless Sensor Network," Wireless Sensor Network, 2012, vol. 4, no 3, p. 65-75.

[NS-2] NS-2 Simulator - http://nsnam.isi.edu/nsnam/index.php/main page.

[NS-3] NS-3 Simulator - https://www.nsnam.org/

[OMNET] OMNET++ Simulator - http://www.omnetpp.org/documentation.

[Österlind 2008] F. Österlind,and A. Dunkels, "Approaching the maximum 802.15.4 multihop throughput," In Proceedings of the Fifth ACM Workshop on Embedded Networked Sensors (HotEmNets 2008), June 2008. Paper presented at Fifth ACM Workshop on Embedded Networked Sensors (HotEmNets 2008), June 2008.

[Petrova 2006] M. Petrova, J. Riihijarvi, P. Mahonen, S. Labella, "Performance study of IEEE 802.15.4 using measurements and simulations," Wireless Communications and Networking Conference, 2006. WCNC 2006. IEEE , vol.1, no., pp.487,492, 3-6 April 2006.

[Polastre 2004] J. Polastre, J. Hill, and D. Culler, “Versatile Low Power Media Access for Wireless Sensor Networks,” in Proc. 2nd International Conference on Embedded Networked Sensor Systems. ACM, pp. 95–107, 2004.

[Raghunathan 2002] V. Raghunathan, C. Schurghers, S. Park, M. Srivastava, “Energy-aware Wireless Microsensor Networks”, IEEE Signal Processing Magazine, pp. 40-50, March 2002.

[Ramakrishnan 2009] S. Ramakrishnan, and T. Thyagarajan, "Energy Efficient Medium Access Control for Wireless Sensor Networks", Journal of

Computer Science & Network Security,IJCSNS – Korea,Vol. 9 No. 6 pp. 273-279, June 2009.

[Ramakrishnan 2004] S. Ramakrishnan, Hong Huang, M. Balakrishnan, and J. Mullen, "Impact of sleep in a wireless sensor MAC protocol," Vehicular Technology Conference, 2004. VTC2004-Fall. 2004 IEEE 60th , vol.7, no., pp.4621,4624 Vol. 7, 26-29 Sept. 2004.

[Reijers 2004] N. Reijers, G. Halkes, and K. Langendoen, "Link layer measurements in sensor networks," In Proceedings of the 1st IEEE International Conference on Mobile Ad-hoc and Sensor Systems (MASS ’04). IEEE Computer Society, pp. 24–27, 2004.

[RFX] RFX 2400 daughterboard - https://www.ettus.com/product/details/RFX2400.

[Sastry 2004] N. Sastry, and D. Wagner, “Security considerations for IEEE 802.15.4 networks,” In Proceedings of the 3rd ACM workshop on Wireless security (WiSe '04). ACM, New York, NY, USA, 32-42. DOI=10.1145/1023646.1023654 http://doi.acm.org/10.1145/1023646.1023654.

[Shah 2002] R.C. SHAH, and J.M. RABAEY, "Energy aware routing for low energy ad hoc sensor networks," In proceedings of Wireless Communications and Networking Conference, 2002. WCNC2002. 2002 IEEE. IEEE, 2002. p. 350-355.

[Shih 2010] Bih-Yaw Shih, Chin-Jui Chang, Ai-Wei Chen and Chen-Yuan Chen1. Enhanced MAC channel selection to improve performance of IEEE 802.15. 4. International Journal of Innovative Computing, Information and Control ICIC International, Vol.6, no.12, pp. 5511–5526, December 2010.

[Singh 1998] Singh, Suresh, Mike Woo, and Cauligi S. Raghavendra. "Power-aware routing in mobile ad hoc networks." Proceedings of the 4th annual ACM/IEEE international conference on Mobile computing and networking. ACM, 1998.

[Srinivasan 2006] K. Srinivasan and P. Levis. RSSI is under appreciated. In Proceedings of the Third Workshop on Embedded Networked Sensors (EmNets 2006) (2006).

[Srinivasan 2008] K. Srinivasan, M. A. Kazandjieva, S. Agarwal, and P. Levis, "The β-factor: measuring wireless link burstiness," In Proceedings of the 6th ACM conference on Embedded network sensor systems (SenSys '08). ACM, New York, NY, USA, pp. 29-42, 2008. DOI=10.1145/1460412.1460416 http://doi.acm.org/10.1145/1460412.1460416.

[Srinivasan 2010] K. Srinivasan, P. Dutta, A. Tavakoli, and P. Levis, "An empirical study of low-power wireless," ACM Transaction Sen. Netw. 6, 1–49. 2010.

[Sudevalayam 2011] S. Sudevalayam, and P. Kulkarni, "Energy Harvesting Sensor Nodes: Survey and Implications," IEEE Communications Surveys and Tutorials - COMSUR, vol. 13, no. 3, pp. 443-461, 2011.

[Sun 2007] T. Sun, N. Liang, L. Chen, P. Chen, and M. Gerla, "Evaluating mobility support in ZigBee networks," Embedded and Ubiquitous Computing, Springer Berlin Heidelberg, Vol. 4808, pp. 87-100, 2007.

[Taha 2013] M. H. Taha, N. M. Khalifa, H. N. Elmahdy and I. A. Saroit, “Energy Based Scheduling Scheme for Wireless Sensor Networks,” CiiT International Journal of Wireless Communication, Vol 4, No 16, pp. 973-978, December 2013.

[Tang 2011] Lei Tang, Yanjun Sun, Omer Gurewitz, and David B. Johnson. 2011. EM-MAC: a dynamic multichannel energy-efficient MAC protocol for wireless sensor networks. In *Proceedings of the Twelfth ACM International Symposium on Mobile Ad Hoc Networking and Computing* (MobiHoc '11). ACM, New York, NY, USA, Article 23, 11 pages.

[TinyOS] TinyOS - http://www.tinyos.net/.

[Tse 2005] D. Tse, and P. Viswanath, Textbook: “Fundamentals of Wireless Communication”, Cambridge University Press, May 2005.

[Tmote] Tmote Sky Datasheet, http://www.moteiv.com/products/docs/tmote-sky-datasheet.pdf.

[USRP] USRP 2 Board - http://www.analog.com/en/rfif-components/rfif-transceivers/ad9361/products/product.html.

[Vermesan 2011] O. Vermesan and P. Friess, “Internet of Things - Global Technological and Societal Trends From Smart Environments and Spaces to Green ICT,” River Publishers' Series in Communications, 2011.

[Vlajic 2011] N. Vlajic, D. Stevanovic,and G.Spanogiannopoulos, “Strategies for improving performance of IEEE 802.15.4/ZigBee WSNs with path-constrained mobile sink(s),” Elsevier Computer Communications Journal, pp. 743-757, vol. 34, issue 6, May 2011.

[Vutukuru 2009] Mythili Vutukuru, Hari Balakrishnan, and Kyle Jamieson. 2009. Cross-layer wireless bit rate adaptation. In Proceedings of the ACM SIGCOMM 2009 conference on Data communication (SIGCOMM '09). ACM, New York, NY, USA, 3-14. DOI=10.1145/1592568.1592571 http://doi.acm.org/10.1145/1592568.1592571

[Wang 2009] K. C. Wang, J. Jacob, L. Tang, and Y. Huang, Y, “Transmission error analysis and avoidance for IEEE 802.15. 4 wireless sensors on rotating structures,” International Journal of Sensor Networks, 6(3), 224-233, 2009.

[Wimax] WiMAX Forum: Mobile WiMAX – Part I: A Technical Overview and Performance Evaluation, February 2006.

[WSNet] WSNet Simulator - http://wsnet.gforge.inria.fr/overview.html

[Wu 2010a] Kaishun Wu, Haoyu Tan, Hoi-Lun Ngan, and Lionel M. Ni. 2010. Chip error pattern analysis in IEEE 802.15.4. In Proceedings of

the 29th conference on Information communications (INFOCOM'10). IEEE Press, Piscataway, NJ, USA, 466-470.

[Wu 2010b] K. Wu, H. Tan, H. Ngan, Y. Liu, and L.M. Ni, "Measurement Study of Mobility-Induced Losses in IEEE 802.15.4," In Proceedings of ICC, pp. 1-5, 2010.

[Xiao 2010] Z. Xiao, C. He and L. Jiang, "Slot-Based Model for IEEE 802.15.4 MAC with Sleep Mechanism," IEEE Commun.Lett., vol. 14, no. 2, Feb 2010.

[Xing 2009] Xing, G., Sha, M., Hackmann, G., Klues, K., Chipara, O., and Lu, C. (2009). Towards unified radio power management for wireless sensor networks. Wireless Communications and Mobile Computing, 9(3), pp. 313-323.

[Zhang 2008] F. Zhang, F. Wang, B. Dai, Y. Li: "Performance Evaluation of IEEE 802.15.4 Beacon-Enabled Association Process," ainaw, pp. 541-546, 22nd International Conference on Advanced Information Networking and Applications - Workshops, 2008.

[Zhao 2003] ZHAO, J. AND GOVINDAN, R. 2003. Understanding packet delivery performance in dense wireless sensor networks. In Proc. of the 1st Int. Conf. on Embedded Networked Sensor Systems (SenSys ’03). ACM, 1–13.

[Zhou 2006] Gang Zhou, Tian He, Sudha Krishnamurthy, and John A. Stankovic. "Models and solutions for radio irregularity in wireless sensor networks," ACM Trans. Sen. Netw. 2, pp. 221-262, 2 May 2006.

[ZigBee] Zigbee alliance homepage - http://www.zigbee.org.

[Zbr Routing] Zbr Hierarchical Routing - http://www.loria.fr/~nefzi/downloads.html#HTR

[802.11] IEEE 802.11 WLAN specification - http://standards.ieee.org/about/get/802/802.11.html.

Personal Publications

[Chaabane 2014] **C. Chaabane**, A. Pegatoquet, M. Auguin, M. Ben Jemaa, “A Joint Mobility Management Approach and Data Rate Adaptation Algorithm for IEEE 802.15.4/ZigBee Nodes,” Wireless Sensor Network, Vol. 6 No. 2, 2014, pp. 27-34. doi: 10.4236/wsn.2014.62004.

[Chaabane 2013] **C. Chaabane**, A. Pegatoquet, M. Auguin, M. Ben Jemaa, “Mobility Management Approach for IEEE802.15.4/ZigBee Nodes in a Noisy Environment,” 26th International Conference on Architecture of Computing Systems - 3rd Workshop on Ultra-Low Power Sensor Networks (WUPS 2013), February 20th 2013, Prague, Czech Republic.

[Chaabane 2012b] **C. Chaabane**, A. Pegatoquet, M. Auguin, M. Ben Jemaa, “Efficient Mobility Management Approach For IEEE 802.15.4/ZigBee Nodes,” 14th IEEE International Conference on High Performance Computing and Communications (HPCC-2012) – Third International Workshop on Wireless Networks and Multimedia (WNM-2012), Liverpool, UK, 25-27 June, 2012.

[Chaabane 2012a] **C. Chaabane**, A. Pegatoquet, M. Auguin, M. Ben Jemaa, “Energy Optimization For Mobile Nodes in a Cluster Tree IEEE802.15.4/ZigBee Network,” Computing Communications and Applications Conference (ComComAp 2012), 11-13 janvier 2012, Hong Kong, Chine.

[Chaabane 2011] **C. Chaabane**, A. Pegatoquet, M. Auguin, M. Ben Jemaa, “An approach for mobility management of end devices in a cluster tree

zigBee Network," (Poster) JournéeTechnologies émergentes et Green Soc-Sip, 27-28 octobre 2011, Montpellier, France.

[Courtay 2010] A. Courtay, A. Pegatoquet, M. Auguin, **C. Chaabane**, "Wireless Sensor Network Node Global Energy Consumption Modelization," Conference on Design and Architectures for Signal and Image Processing, 26-28 octobre 2010, Edinburgh, Scotland, UK.

Annex A. Some MAC attributes and constants [IEEE TG 15.4 2006]

Note that MAC PIB attributes always begins with "*mac*" and MAC constants always begins with *"a"*.

MAC PIB Constant

- aUnitBackoffPeriod is equal to 20 symbols.
- aMaxSIFSFrameSize: 18 Bytes
- aBaseSuperframeDuration
- aTurnaroundTime: 12 symbols
- aUnitBackoffPeriod: 20 symbols
- *aMinCAPLength* 440 symbol periods.

MAC PIB Attributes

- macBeaconOrder
- macSuperframeOrder
- macMinSIFSPeriod
- macMinLIFSPeriod
- macMinBE is between 0 and macMaxBE. It is equal to 3 by default.
- macMaxBE is from 3 to 8. It is set to 5 by default.
- macLIFSPeriod: 40 symbols (2.4 GHz frequency band)
- macSIFSPeriod: 12 symbols (2.4 GHz frequency band)
- macMaxCSMABackoff is the maximum number of backoffs the CSMA-CA algorithm will attempt before declaring a channel access failure. It is between 0 and 5. The default value is 4.

- macMaxFrameRetries: Range 0-7; default 3
- macResponseWaitTime
- macMinBE is between 0 and macMaxBE. It is equal to 3 by default
- macMaxBE is from 3 to 8. It is set to 5 by default
- The first tentative: BE = macMinBE
- macMinBE <= BE <= macMaxBE

Annex B. CSMA-CA algorithm

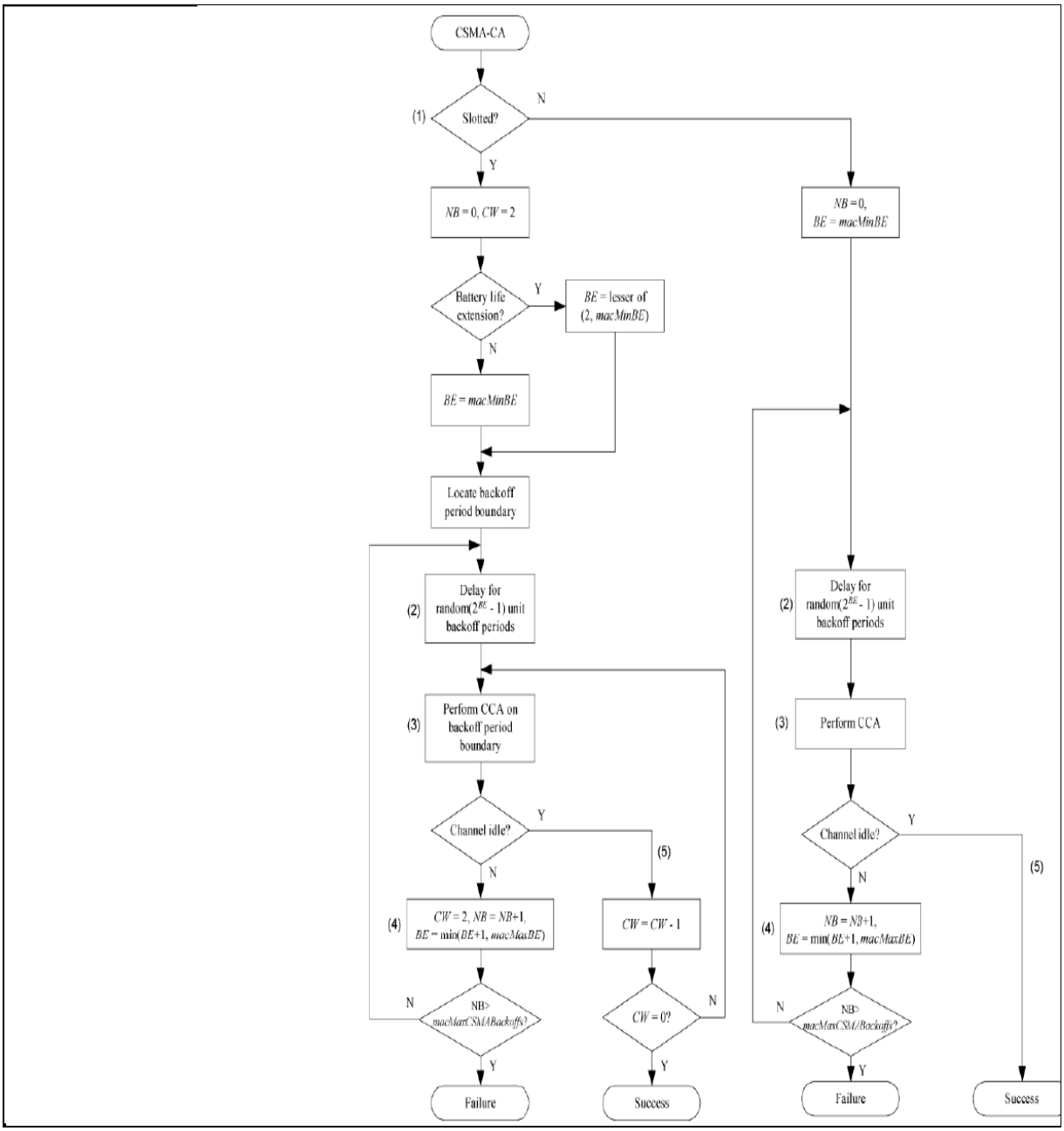

Figure 59 CSMA-CA Algorithm [IEEE TG 15.4 2006]

Annex C. Box-Muller Method [Box 1958]

The Box-Muller method is widely used in simulation software to generate a random variable. This method includes three steps: the first two ones generate independent values x_1 and x_2 of a random variable uniformly distributed over [0,1]. In the third step, the functions $f(x_1)$ and $g(x_2)$ are derived from x_1 and x_2 by:

$$f(x_1) = \sqrt{-\ln(x_1)}$$

$$g(x_2) = \sqrt{2}\ \cos(2\pi\ x_2)$$

Finally,

$$n = f(x_1)g(x_2)$$

gives a sample of the $N(0,1)$ distribution.

The code implemented in NS-2 and WSNet simulators is as follows:

```
double gaussrand()
{
    static double V1,V2,S ;
    static int phase = 0;
    double X;
    if (phase== 0){
        do {//Scale two random integers to doubles between -1 and 1
            double U1 = (double) rand()/RAND_MAX;
            double U2 = (double) rand()/RAND_MAX;
            V1 = 2 * U1 – 1; //Scale number to numbers between -1 and 1
```

```
                    V2 = 2 * U2 – 1;
                    S = V1 * V1 + V2 * V2;
            } while(S >= 1 || S == 0)
            X = V1 * sqrt(-2 * log(S)/S)
        }
        else{
            X = V2 * sqrt(-2 * log(S)/S);
        }
        phase = phase – 1;
        return X;
}
X = mean + sqrt (variance) * X
```

Annex D. Frames Fields [IEEE TG 15.4 2006] [ZigBee]

PPDU frame format

4 Bytes	1 Byte	7 bits	1 bit	N ≤ 127 Bytes
Preamble	SDF	Frame Length	Reserved	MPDU

Acknowledgment Frame format

2 Bytes	1 Byte	2 Bytes
Frame Control	Sequence Number	FCS
MHR		MFR

Frame Control field of the Acknowledgment frame

Bit0-2	3	4	5	6	7-9	10-11	12-13	14-15
Frame type	Security Enabled	Frame pending	Ack request	PAN Id compressing	Reserved	Destination addressing mode	Frame version	Source addressing mode
			SET TO ZERO					

ZigBee packet at the network layer

Bit 0-15	Variable	Variable
Frame Control	Routing Fields	Data Payload
NHR		NTW Payloyd